



ALLEGATO A

Al Direttore Istituto Scienze dell'Atmosfera e del Clima

Il sottoscritto Pappaccogli Gianluca
(COGNOME – per le donne indicare il cognome da nubile) (Nome)

Codice Fiscale

Nato a Prov. il

Attualmente residente a Prov.

Indirizzo

CAP Telefono

Indirizzo PEC:.....

chiede, ai sensi dell'art. 22 della L. 240 del 30/12/2010 di essere ammesso a sostenere la selezione pubblica, per titoli e colloquio, per il conferimento di n° 1... assegno/i per lo svolgimento di attività di ricerca nell'ambito del programma di ricerca:

JRA ENI-CNR – Artico – sotto progetto 1

sotto la responsabilità scientifica del Prof./Dott. Antonio Donadeo e del Dott. Stefano DECESARI

da svolgersi presso la sede dell'Istituto: Scienze dell'Atmosfera e del Clima Sede Secondaria di Lecce

A tal fine, il sottoscritto dichiara sotto la propria responsabilità:

- 1) di essere cittadino ...Italiano..... Valutazione d'Impatto e
- 2) di aver conseguito il diploma di laurea (o titolo estero equivalente *) in Certificazione Ambientale il 27 / 03 /2015 presso l'Università Università del Salento con votazione 108/110 ;
- 3) di aver conseguito il titolo di dottore di ricerca (o titolo estero equivalente) in Sustainable Energy and Technologies il 08/ 07 /2015 presso l'Università Libera Università di Bolzano-Bozen
- 4) di non aver riportato condanne penali e di non avere procedimenti penali pendenti a proprio carico (in caso contrario, indicare quali).
- 5) di aver/~~non aver~~-usufruito di altri assegni di ricerca dal 01/05/2011 al 12/08/2019 e di aver/non aver usufruito delle tipologie di rapporti di lavoro di cui all'art. 2 dell'avviso di selezione, intercorsi con Libera Università di Bolzano-Bozen

Il sottoscritto allega alla presente domanda:

- 1) dichiarazione sostitutiva di certificazione e dell'atto di notorietà ai sensi degli art. 46 e 47 del DPR 445/2000 e s.m.i. da compilarsi mediante l'utilizzo del modulo (allegato B) attestante la veridicità del contenuto del Curriculum vitae et studiorum;
- 2) elenco dei lavori trasmessi dal candidato per via telematica di cui all'art. 4 del bando.

Andrano, 12/08/2019



Consiglio Nazionale delle Ricerche
Istituto di Scienze dell'Atmosfera e del Clima
Sede Secondaria di Lecce



Luogo e data [Andrano, 12/08/2019](#)

FIRMA _____



*** - Qualora il titolo di studio sia stato conseguito all'estero, dovrà essere presentata idonea documentazione attestante l'equipollenza con un titolo rilasciato in Italia, secondo quanto previsto dall'art. 3, punto d) del presente avviso.**



FAC-SIMILE

ALLEGATO B


DICHIARAZIONI SOSTITUTIVE DI CERTIFICAZIONI


(art. 46 D.P.R. n. 445/2000)

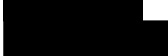
DICHIARAZIONI SOSTITUTIVE DELL'ATTO DI NOTORIETÀ

(art. 47 D.P.R. n. 445/2000)

Il... sottoscritt. 

COGNOME 
(per le donne indicare il cognome da nubile)


NOME 

NATO A:  PROV. 

IL 

ATTUALMENTE RESIDENTE A: 
PROV. 

INDIRIZZO  C.A.P. 

TELEFONO 

Visto il D.P.R. 28 dicembre 2000, n. 445 concernente "T.U. delle disposizioni legislative e regolamentari in materia di documentazione amministrativa" e successive modifiche ed integrazioni;

Vista la Legge 12 novembre 2011, n. 183 ed in particolare l'art. 15 concernente le nuove disposizioni in materia di certificati e dichiarazioni sostitutive (*);

Consapevole che, ai sensi dell'art.76 del DPR 445/2000, le dichiarazioni mendaci, la falsità negli atti e l'uso di atti falsi sono punite ai sensi del Codice penale e delle leggi speciali vigenti in materia, dichiara sotto la propria responsabilità:

che quanto dichiarato nel seguente curriculum vitae et studiorum
comprensivo delle informazioni sulla produzione scientifica
corrisponde a verità

Curriculum vitae et studiorum

Andrano, 12/08/2019





studi compiuti, i titoli conseguiti, le pubblicazioni e/o i rapporti tecnici e/o i brevetti, i servizi prestati, le funzioni svolte, gli incarichi ricoperti ed ogni altra attività scientifica, professionale e didattica eventualmente esercitata **(in ordine cronologico iniziando dal titolo più recente)**

Es: descrizione del titolo

data protocollo

rilasciato da

periodo di attività dal al

FIRMA(**)

Andrano, 12/08/2019

.....

(*) ai sensi dell'art. 15, comma 1 della Legge 12/11/2011, n. 183 le certificazioni rilasciate dalla P.A. in ordine a stati, qualità personali e fatti sono valide e utilizzabili solo nei rapporti tra privati; nei rapporti con gli Organi della Pubblica Amministrazione e i gestori di pubblici servizi, i certificati sono sempre sostituiti dalle dichiarazioni sostitutive di certificazione o dall'atto di notorietà di cui agli artt. 46 e 47 del DPR 445/2000

N.B:

- 1) Datare e sottoscrivere tutte le pagine che compongono la dichiarazione.
- 2) Allegare alla dichiarazione la fotocopia di un documento di identità personale, in corso di validità.
- 3) Le informazioni fornite con la dichiarazione sostitutiva devono essere identificate correttamente con i singoli elementi di riferimento (esempio: data, protocollo, titolo pubblicazione ecc...).
- 4) Il CNR, ai sensi dell'art. 71 e per gli effetti degli artt. 75 e 76 del D.P.R. 445 del 28/12/2000 e successive modifiche ed integrazioni, effettua il controllo sulla veridicità delle dichiarazioni sostitutive.
- 5) La normativa sulle dichiarazioni sostitutive si applica ai cittadini italiani e dell'Unione Europea.
- 6) I cittadini di Stati non appartenenti all'Unione, regolarmente soggiornanti in Italia, possono utilizzare le dichiarazioni sostitutive di cui agli artt. 46 e 47 del D.P.R. 445 del 28.12.2000 limitatamente agli stati, alla qualità personali e ai fatti certificabili o attestabili da parte di soggetti pubblici italiani, fatte salve le speciali disposizioni contenute nelle leggi e nei regolamenti concernenti la disciplina dell'immigrazione e la condizione dello straniero. Al di fuori dei casi sopradetti, i cittadini di Stati non appartenenti all'Unione autorizzati a soggiornare nel territorio dello Stato possono utilizzare le dichiarazioni sostitutive nei casi in cui la produzione delle stesse avvenga in applicazione di convenzioni internazionali fra l'Italia e il Paese di provenienza del dichiarante.

Informazioni personali

Nome Gianluca Pappaccogli
Data di nascita
Indirizzo
Mobile
Email
Researchgate



Istruzione e formazione

- Nov 2015 – Nov 2018 **Ph.D. in Sustainable Energy and Technologies**, *Libera Università di Bolzano-Bozen*, Modellazione dei processi atmosferici ed energetici in ambito urbano, presso il gruppo di Fisica dell'Atmosfera dell' Università di Trento.
- Titolo Tesi: *Numerical modelling of urban of urban atmospheric processes and energetics from city to building scale: case study in Bolzano.*
 - Attività principali: Utilizzo del modello a mesoscala Weather Research and Forecasting (WRF) per lo studio dell'ambiente urbano e delle sue interazioni con l'atmosfera.
- Feb 2018 – Lug 2018 **Ph.D Visiting**, *CIEMAT - Research Center for Energy, Environment and Technology, Avenida Complutense 40, Madrid*, presso Atmospheric Pollution Modelling Group - Environmental Impact of Energy Department.
- Utilizzo del modello BEP+BEM al fine di simulare i consumi termici per la città di Bolzano durante specifiche condizioni climatiche.
 - Analisi di sensitività del modello BEP+BEM attraverso simulazioni idealizzate per lo studio dell'impatto delle forzanti meteorologiche e delle proprietà costruttive sui consumi energetici degli edifici.
- Apr 2012 – Mar 2015 **Laurea Magistrale (LM-75) in Valutazione d'Impatto e Certificazione Ambientale** **Voto:108/110**, *Università del Salento*, Tesi di Laurea in Fisica dell'Atmosfera e Oceanografia Fisica.
- Titolo Tesi: The effects of urban trees on micrometeorology of south (Lecce) and north (Helsinki) European cities.
 - Realizzazione di due campagne sperimentali per lo studio delle aree verdi nelle città di Lecce ed Helsinki.
 - Corsi di studio:Chimica ambientale, fisica dell'atmosfera, Geomorfologia applicata, Idrogeofisica.
- Apr 2014 – Lug 2014 **Erasmus Placement**, *University of Lahti (Faculty of Applied Sciences)*, Campagna sperimentale svolta in collaborazione con il Finnish Meteorological Institute (FMI), ed University of Helsinki.
- Svolgimento di una campagna sperimentale nella città di Helsinki, per comprendere gli effetti della vegetazione (alberi) sulla ventilazione e la temperatura in street canyon.
 - Installazione e settaggio della strumentazione anemometrica.
 - Svolgimento della campagna termografica per lo studio delle temperature superficiali.

- Analisi dei dati

- Gen 2014 – Apr 2014 **Erasmus**, *University of Lahti (Faculty of Applied Sciences)*, Ricerca tesi ed attività di laboratorio per lo studio dell' ambiente urbano.
- International Winter School 2014 – Responsible Business Life Cycle and Environmental Management.
- Ott 2008 – Apr 2012 **Laurea Triennale (L32), Scienze e Tecnologie per l'Ambiente Voto:106/110**, *Università del Salento*, Principali tematiche: Chimica Generale ed Inorganica, Chimica Organica, Geologia, Ecologia del paesaggio, Botanica, Fisica, Matematica, Meteorologia e Climatologia.
- Set 2003 – Giu 2008 **Diploma di maturità scientifico sperimentale**, *Istituto Superiore Scientifico Cavazzi Sorbelli*, Pavullo nel Frignano, Modena.

Esperienza Professionale

- Nov 2018 – oggi **Assegnista di ricerca Libera Università di Bolzano-Bozen**
Laboratory of Building Physics, Progetto: Bolzano Solar Irradiance Monitoring Network (SOMNE).
- Il progetto si focalizza sulla modellazione della radiazione solare in ambiente urbano attraverso l'utilizzo del modello microclimatico SEBE. Al fine di testare la sensibilità dello stesso, si utilizzando diversi input meteorologici come: misure da stazione meteo convenzionali, stazioni meteo-radiometriche e dati da satellite (Meteosat).
 - Utilizzo dei dati da satellite Meteosat per ricavare informazioni sullo stato dell'atmosfera e sui processi di estinzione della radiazione in essa (clearness index, sky-types classification).
 - Misure meteo-radiometriche attraverso l'utilizzo di piranometri, pireliometro, sky-scanner e sky-camera
- Feb 2018 11-17 **Visiting su invito CIEMAT - Research Center for Energy, Environment and Technology**, *Avenida Complutense 40, Madrid, presso Atmospheric Pollution Modelling Group - Environmental Impact of Energy Department*
Calcolo dei parametri morfometrici per la descrizione della geometria urbana delle città di Madrid e Barcellona attraverso il processamento di dati LIDAR.
- Set 2015 – Nov 2015 **Borsa di studio CNR-ISAFOM, Ercolano via Patacca, 85**
Progetto AriaSaNa - Rilevamento e analisi dati ambientali in atmosfera.
- Gestione ed analisi dei dati provenienti da sensori low-cost mobili AirQuino, per lo studio della qualità dell'aria in ambiente urbano.
 - Manutenzione e analisi dei dati dal Supersito di San Marcellino provvisto di torre eddy covariance ed analizzatori ad alta risoluzione per la qualità dell'aria.
 - Campagna di misure all' interno del progetto BioQuAr (terra dei fuochi).
 - Presentazione finale progetto AriaSaNA: "Qualità dell' aria nei canyon urbani della città di Napoli e ruolo della vegetazione".

Corsi di formazione

- 8-12 luglio 2019 **Summer school: statistics for engineers**
Statistica descrittiva e test di ipotesi, ANOVA, Design and analysis of experiments (DOE), Analisi multivariate e regressione lineare, Minitab tutorial
- 6-10 marzo 2017 **Environmental data management and analysis with GIS**
GRASS GIS: features, logical structure and usage, Cartographic projections, reference systems and their transformations, GIS and geostatistics. Digital geographic data sources, QGIS, Geoprocessing, Geoservices, Image analysis for environmental applications, Landsat image analysis.
- Oct 2016 – Dec 2016 **Introduction to Programming with MATLAB**
Lezioni teoriche ed esercitazioni pratiche sull' utilizzo del software Matlab Principali tematiche del corso: Introduzione al programma, Operatori e matrici, Funzioni, Programmer Toolbox, cicli for/while, data type, file di input/output, interfaccia grafica.
- 24-29 Luglio 2016 **Weather Research and Forecasting (WRF) model - Basic Tutorial Course**
Lezioni teoriche sull' utilizzo del modello meteorologico a mesoscala WRF.
- Impostazioni di base per eseguire i moduli WPS e ARW.
- Esercitazioni pratiche con l'utilizzo di differenti met data, nesting, restart, and grid nudging.
NCAR Institute – Boulder (CO)
- Febbraio 2016 - 16ore **Corso di Formazione in sicurezza sul Lavoro**
Il rischio negli ambienti di lavoro, il rischio nel laboratorio Chimico-Biologico, Dispositivi di protezione, prevenzione incendi.
- Credito formativo permanente di formazione generale (4 ore).
- Credito formativo ordinario di formazione specifica (12 ore): settore ATECO 2007 Sanità e Assistenza Sociale Q 86.90.12.

Competenze personali

Competenze tecniche

MATLAB, *Eccellente*

QGIS, GRASS *Eccellente*

Weather Research and Forecasting (WRF) model, *Eccellente*

Latex, *Eccellente*

Fortran, Ncl, Ferret *Buono*

R, *Discreto*

Python, *Discreto*

SketchUp, *Discreto*

Competenze professionali

Conoscenza degli strumenti principali per lo studio dell'atmosfera, e relativa gestione degli stessi. Eccellente capacità nella raccolta ed analisi dei dati provenienti da strumentazione e dati meteo provenienti dal web (rete stazioni meteo gestite dagli enti preposti, stazioni meteo amatoriali, dati da satellite e provenienti da modelli), utilizzati anche per la validazione dei modelli. Conoscenza nel processamento di dati provenienti da telerilevamento, come immagini LIDAR e satellitari.

Competenze organizzative e gestionali

Capacità di organizzare il lavoro rispettando le tempistiche ed adempiendo a quelle che sono le richieste del lavoro di ricerca. Capacità di coordinamento di un gruppo di persone all'interno di un progetto di ricerca. Queste conoscenze sono maturate durante la preparazione e l'esecuzione di progetti di ricerca eseguiti durante la laurea magistrale il seguente periodo del dottorato di ricerca.

Competenze comunicative

L'esperienza interculturale scaturita prima dall'esperienza dell' Erasmus e poi dal periodo all'estero condotto durante il dottorato, ha dimostrato la mia capacità di adeguamento ed adattamento ad ambienti multiculturali. Ho acquisito ottime capacità di comunicazione e cooperazione grazie alla collaborazione con i diversi enti di ricerca presso i quali ho svolto il mio periodo di visiting. Ottime capacità interpersonali e buona dialettica, spirito di gruppo e predisposizione a lavorare in team.

Lingue straniere

Inglese, *Avanzato*

Spagnolo, *Scolastico*

Pubblicazioni

Pappacogli, G., Giovannini, L., Cappelletti, F. and Zardi, D., 2018. Challenges in the application of a WRF/Urban-TRNSYS model chain for estimating the cooling demand of buildings: A case study in Bolzano (Italy)', Science and Technology for the Built Environment 24(5), 529- 544. URL: <https://doi.org/10.1080/23744731.2018.1447214>.

Pappacogli, G., Giovannini, L., Cappelletti, F. and Zardi, D., 2018. Sensitivity of WRF/Urban simulations to urban morphology parameters: a case study in the city of Bolzano. Building Simulation Applications BSA 201 - 3rd IBPSA Italy Conference, Bozen-Bolzano 8th – 10th February 2017.

Di Sabatino S., Buccolieri R., Pappacogli G., Leo L.S., 2015. The effects of trees on micrometeorology in a real street canyon: consequences for local air quality. International Journal of Environment and Pollution, vol.58 (1-2), pp. 100-111. DOI: 10.1504/IJEP.2015.076587.

Di Sabatino S., Buccolieri R., Leo L.S., Pappacogli G., 2015. On the exchange velocity in street canyons with tree planting. Accepted to ICUC9 – 9th International Conference on Urban Climates, Toulouse (France), 20-24 July.

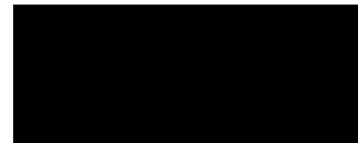
Di Sabatino S., Buccolieri R., Leo L.S., Pappacogli G., 2014. On thermal stratification in real street canyons with trees: consequences for local air quality. Proc. 16th Int. Conf. on Harmonisation within Atmospheric Dispersion Modelling for Regulatory Purposes, Varna (Bulgaria), 8-11 September.

Pappaccogli G., Buccolieri R., Maggiotto G., Leo L.S., Rispoli G., Micocci F., Di Sabatino S. 2014. The effects of trees on micrometeorology in a medium size Mediterranean city: in situ experiments and numerical simulations. Proc. 91 ASME 2014 4th Joint US-European Fluids Engineering Division Summer Meeting and 11th International Conference on Nanochannels, Microchannels, and Minichannels, Chicago (Illinois, USA), 3-7 August.

Dati personali

"Autorizzo il trattamento dei miei dati personali ai sensi del D. Lgs. 196/2003""Consa-pevole della sanzioni penali previste dall'Art. 76 del D.P.R. 28 dicembre 2000 n. 445, per le ipotesi di falsità in atti e dichiarazioni mendaci, dichiaro sotto la mia responsabilità e ai sensi degli Artt. 46 e 47 dello stesso D.P.R. n. 445/2000, che quanto riportato nel presente Curriculum Vitae corrisponde a verità"

Andrano, 12/08/2019





Challenges in the application of a WRF/Urban-TRNSYS model chain for estimating the cooling demand of buildings: A case study in Bolzano (Italy)

GIANLUCA PAPPACCOGLI^{1,*}, LORENZO GIOVANNINI², FRANCESCA CAPPELLETTI ³,
and DINO ZARDI²

¹*Faculty of Science and Technology, Piazza Università, 5 Bolzano 39100, Italy*

²*Atmospheric Physics Group, Department of Civil, Environmental and Mechanical Engineering, University of Trento, Trento, Italy*

³*Department of Design and Planning in Complex Environments, University Iuav of Venice, Venezia, Italy*

In the present study, a WRF/Urban-TRNSYS model chain is proposed to evaluate the cooling demand of buildings located in an urban area. A case study is proposed to show the applicability of the method for a hypothetical residential building located in the city of Bolzano (Italy) on a clear-sky hot day in summer. WRF/Urban results were first validated against measurements from permanent weather stations located both in the urban area and in the surrounding countryside. Then, several TRNSYS simulations were performed, in order to assess the impact of the gridded input from WRF/Urban against both measurements from a weather station located close to the sample building and to standard data from the Test Reference Year (TRY). Compared with estimates using input data from the weather station, the daily cooling demand of the sample building estimated by WRF/Urban-TRNSYS differed by only 6% to 8%, while differences of 60% were found when using standard TRY data. Moreover, results show that energy estimates obtained by means of WRF/Urban-TRNSYS model chain satisfy the standard requirement suggested by Ashrae Guidelines 14–2002, suggesting that this model chain is a useful tool for the estimation of real buildings energy consumption.

Introduction

The number and extent of urbanized areas is constantly increasing throughout the world. This fact, combined with a constant growth of population living in cities, makes the issue of urban environment a key topic, especially in view of planning a sustainable development and an efficient use of environmental resources, including energy. Indeed, this growing inflow of people into cities from the countryside is associated with a significant change in land use, which, in turn, may cause a reduced livability of urban and suburban areas, contributing to human discomfort, health threat

problems (especially from increasing pollution), and higher energy costs (Oke 1987). Many of these problems are associated with higher air temperatures, led by the current urban architecture trend toward high buildings and reduced density of green areas: such a policy contributes to the modification of the surface energy budget and to the intensive use of energy sources (for transport, buildings heating/cooling, etc.).

In this context, buildings and their layout represent the most important factor controlling energy, mass, and momentum exchanges between the earth surface and the atmosphere. This interaction has a close influence on the Urban Heat Island (UHI) phenomenon, which consists in a significant increase of air temperature in the city center compared to the surrounding areas, affecting not only local climatic conditions but also mesoscale atmospheric processes (e.g., slope and valley winds: Rotach and Zardi 2007; Giovannini et al. 2017). The urban overheating is associated with an alteration of the surface energy balance, due to a combination of factors such as street canyon geometry, artificial surfaces with increased thermal capacity, reduced vegetation, and anthropogenic heat production (Oke 1987). The UHI phenomenon is well documented in Europe

Received October 9, 2017; accepted February 18, 2018

Gianluca Pappacogli, is a PhD Student. **Lorenzo Giovannini**, PhD, is an Assistant Professor. **Francesca Cappelletti**, PhD, is an Associate Professor. **Dino Zardi**, PhD, is an Associate Professor.

*Corresponding author e-mail: gianluca.pappacogli@natec.unibz.it

Color versions of one or more of the figures in the article can be found online at www.tandfonline.com/uhvc.

(Santamouris 2007) and is common to all urban areas, regardless of size and climate where cities are located (Stewart and Oke 2012). Conversely, the microclimate variability occurring inside the urban area affects local flow characteristics, which strongly regulate the buildings energy loads (Bouyer et al. 2011). Indeed, despite the UHI intensity represents a critical variable for the assessment of buildings energy performance, the phenomenon is still neglected in most applications, even in practical assessments. The same gap also affects the climatic datasets typically used by numerical models applied to simulate buildings energy performance, which do not describe in a proper way the UHI phenomenon (Guattari et al. 2018).

On the other hand, recent progress in numerical weather prediction modelling and well-known environmental databases, along with increasing availability of high-power computational resources, allow for reaching much higher spatial resolutions, even in operational model runs for routine weather forecasting. This progress allows for a collaborative research into buildings-atmosphere interactions, which is an important effort, as buildings account for 40% of the total energy use in Europe (European Parliament and Council 2010; Directive 2010/31/EU). Accordingly, in numerical weather prediction models more detailed parameterisations of these processes can be included, reproducing building-atmosphere interactions in a more precise and realistic way, especially in urban areas. On the other hand, Building Energy Simulations (BES) often focus on single buildings without considering the urban context and the surrounding buildings effects on both radiative and convective surface

exchanges over the external envelope. Furthermore, providing appropriate initial conditions for these models remains a critical issue; they are usually derived from observations mostly taken within the rural environment and limited to a single-point measurement. On the contrary, the output from meteorological models can provide information about the distribution of micrometeorological variables at the urban scale, which are not typically available from conventional climate data, for example, Typical Meteorological Year, leading to a more robust basis for initial conditions than local observations. This approach may improve BES, especially when the impact of urbanization effects (UHI) on building energy performance is investigated.

In this study, the Weather Research and Forecasting (WRF) model, coupled with the Building Effect Parameterization (BEP) urban scheme (WRF/Urban), is used to provide an accurate description of the meteorological field at the urban scale, which will be used as input data for the building energy model implemented with TRNSYS 17 (Solar Energy Laboratory 2012), in order to assess the impact of WRF/Urban output on the dynamic energy consumption of a sample building in a well-described urban context. The city taken as case study is Bolzano, located in the northeastern Italian Alps, in a basin where three valleys join as it can be seen in the map of Domain 4 in Figure 1. Many studies investigated the interaction between an urban area and local circulation phenomena, emphasizing the important influence of local winds on the urban environment (Kuttler et al. 1996; Piringer and Baumann 1999; Giovannini et al. 2011). The

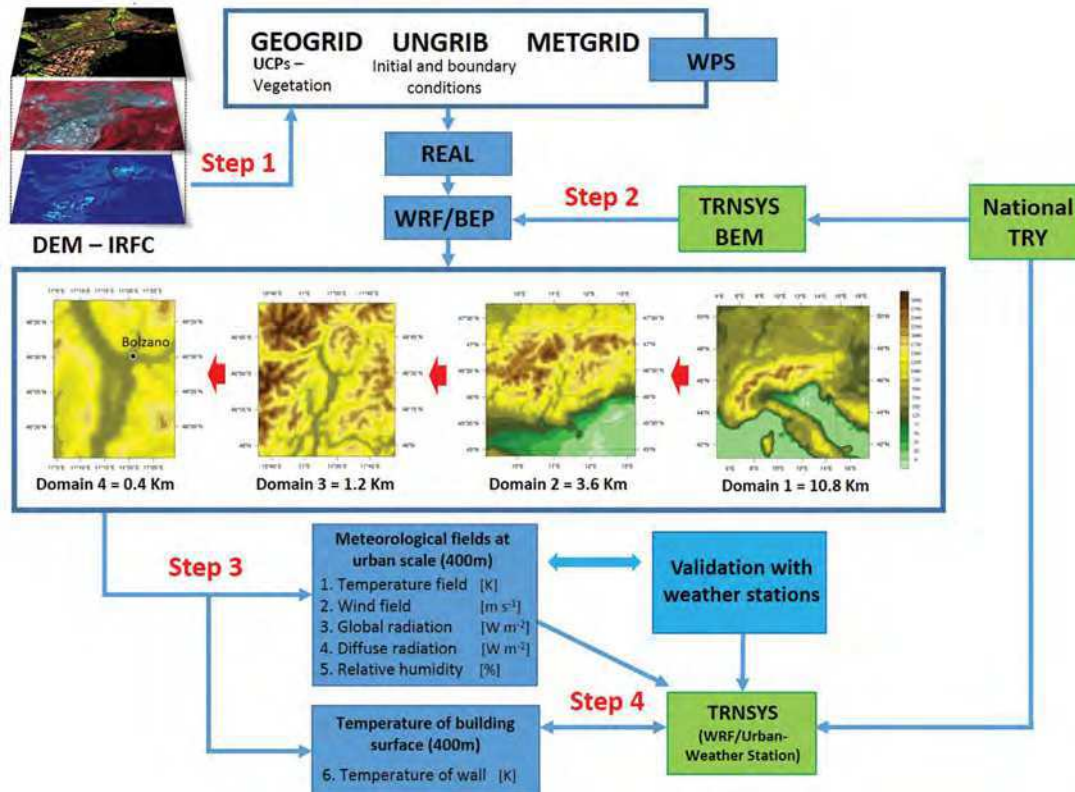


Fig. 1. Flowchart of the model chain WRF/Urban-TRNSYS. In red the main steps described in detail in the Flowchart of the WRF/Urban-TRNSYS model chain section.

typical weather conditions in this area are characterized by ground-based persistent thermal inversions (facilitated by the calm condition) during wintertime, and by a well-defined valley wind system during summertime, which is composed by a light down-valley wind at night, and by a stronger up-valley wind during daytime (Laiti et al. 2013, 2014; Giovannini et al. 2017).

A sensitivity analysis of TRNSYS output was carried out through the assessment of the daily cooling demand of the sample building, along with a comparison of external and internal wall surface temperatures obtained by means of the two models (WRF/Urban and TRNSYS fed by different inputs). The possible advantages from the use of WRF/Urban output in building energy simulations are shortly recalled in the following list:

1. A better knowledge of micrometeorological conditions representative of specific urban areas free from potential bias due to instrument location.
2. A more precise evaluation of temperatures on impervious urban surfaces, upper soil layers, and overlying urban canopy layer.
3. A better prediction of future scenarios assessing the feedback between buildings and surrounding microclimate, which are directly affected by climate change and mitigation strategies (e.g., green roof, trees, and vegetation).

This work is organized as follows. The second section introduces WRF/Urban and TRNSYS models, providing detailed information regarding the datasets and the methodologies used to obtain Urban Canopy Parameters (UCPs). The third section describes the WRF/Urban-TRNSYS model chain, along with the modelling set-up of both models. The fourth section first describes the validation of the WRF/Urban output, by means of a comparison with data from a network of weather stations, and then the sensitivity tests carried out to assess the impact of different input data on TRNSYS model results. Finally, in the fifth section, strengths and limitations of the model chain are discussed.

Modelling chain description

Mesoscale meteorological model WRF

WRF is a state-of-the-art numerical weather prediction (NWP) model, developed by the collaborative effort between the National Center for Atmospheric Research (NCAR) and several international institutes (such as NCEP, NOAA, ESRL). The WRF system was developed for both research and operational tasks, to simulate atmospheric phenomena across horizontal scales ranging from 10^1 m to 10^6 m and vertical grid spacing of 10^1 to 10^3 m (Skamarock et al. 2008). Specific land surface parameterizations recently incorporated into WRF to account for the effects of urban areas on local climatic conditions significantly improved the capability of modeling the mesoscale impact of cities. In particular, such urban parameterization schemes include the single-layer model (Kusaka et al. 2001) and the multi-layer building-effect parameterization (BEP) model (Martilli et al. 2002), which

have been applied to major metropolitan regions in the world. Several studies have shown that the WRF model, coupled with an urban parameterization, is a valuable tool to resolve wide-ranging problems about the urban environment, such as the UHI intensity variability (Miao et al. 2009), urbanization growing, anthropogenic emissions and air quality (Papangelis et al. 2012; Wang et al. 2009). Similarly, in the present study WRF is coupled with the BEP scheme (WRF/Urban), in order to provide a fine and accurate meteorological field of the urban area of Bolzano (Italy). BEP is fully coupled within the WRF infrastructure and represents the built elements as distribute sources and sinks of momentum, heat, and moisture throughout the urban canopy layer, affecting the thermodynamic structure of the lower part of the urban boundary layer. Furthermore, the effects of the street geometry on the surface energy balance and on the incoming and outgoing radiation are taken into account, including shadowing, reflection, and trapping of shortwave and long-wave radiation in the urban canyons (cf. Giovannini et al. 2013).

Input datasets – UCPs

High-resolution meteorological simulations in complex terrain require an adequately high-resolution topography dataset. Here the topography dataset has a horizontal original spatial resolution of ~ 30 m. Figure 1 (middle) shows the topography of the inner domain, highlighting the urban area of Bolzano. For the land cover parameters, the dataset Corine was used, reclassifying the 44 Corine categories into the 20 (+3 special classes for urban land use) Modis categories, in order to fit the WRF look-up tables (cf. Giovannini et al. 2014). The land cover dataset is shown in Figure 2. In particular, throughout the urban area of Bolzano, 52% of the model cells are defined as low-intensity residential (referred to as LI-R), 23% as high-intensity residential (referred to as HI-R), and the remaining 25% as industrial/commercial (named I/C) (distribution details in Figure 2b). As the goal of the present work concerns the urban environment, detailed maps of urban morphology were developed. Indeed, implementing urban schemes with detailed morphological parameters can provide better tools for evaluating the urban morphology impacts on urban microclimate and surrounding buildings, as highlighted by the National Urban Database and Access Portal Tool (NUDAPT) initiative, which was designed to provide gridded datasets of urban canopy parameters for 44 U.S. cities. Moreover, many recent studies highlighted the importance of using fine-resolution input datasets of urban morphology parameters to keep pace with the increasingly high resolution of operational model runs, in order to improve the accuracy of the results (Solazzo et al. 2010; Salamanca et al. 2011; Giovannini et al. 2014).

In this work digital surface and terrain models (0.5 m resolution) from the GeoCatalogo of the Autonomous Province of Bolzano (<http://geocatalogo.retecivica.bz.it/geocatalog>) were used to calculate fine resolution maps of urban morphology parameters by means of the QGIS + Matlab® software. Collected data and maps were processed, in order

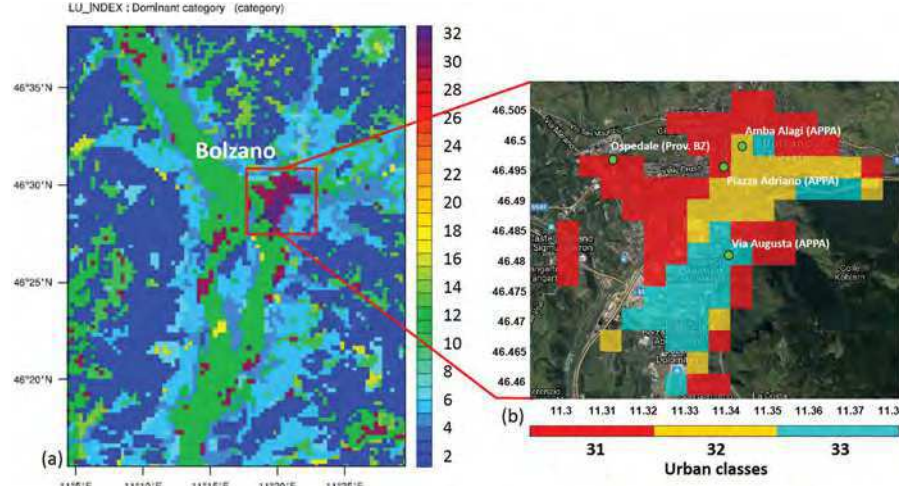


Fig. 2. (a) Modis land use categories in the inner model domain. (b) Categories 31–33 indicate urban land use (resolution 400 m x 400 m) namely 31: Low intensity residential, 32: High intensity residential, 33: Industrial or commercial.

to obtain gridded urban canopy parameters (UCPs) with a horizontal spatial resolution of 400 m, which were directly used as input for the BEP scheme. The structure of the city of Bolzano was carefully reproduced using a set of seven morphometric parameters: the average and the standard deviation of the buildings height, named, respectively h_m and h_s , the building plan area fraction $\lambda_p = A_p / A_{tot}$ (where A_p is the plan area of buildings and A_{tot} is the total area of the cell) and plan-area-weighted mean building height $h_{aw} = (A_p * h_m) / A_{tot}$; the building envelope area to plan area ratio $\lambda_b = (A_p + A_w) / A_{tot}$ (where A_w is the wall surface area); the frontal area index $\lambda_f = A_{proj} / A_{tot}$ (where A_{proj} is the total area of buildings projected into the plane normal to the approaching wind direction at 0° – 45° – 90° – 135°); the urban fraction λ_u (percentage of the cell covered by urban land use). Moreover, in this study, through the analysis of InfraRed False Colour (IRFC) images referring to 2011, green spaces (such as small parks and domestic gardens) were considered in the urban context, with the exception of street trees, which require a more complex parameterization in order to account for their effects on buildings (shadowing)

and dynamical processes (turbulence dissipation, drag, and sheltering) (Krayenhoff et al. 2015). Figure 3 shows the urban fraction λ_u obtained with (left) and without (middle) considering the information of vegetation distribution from IRFC images. As shown in Figure 3c, significant differences in land use fraction are present especially in the northern part of the city, which is characterized by scattered vineyards and several domestic gardens, where a maximum percentage in land cover change $\sim 60\%$ between the two patterns is found. Finally, the distribution of buildings heights h_i at 5 m vertical intervals was calculated on fifteen vertical urban levels. The methodology used to calculate the main urban morphological parameters is reported in Burian et al. (2008). The gridded urban morphology data used as input in the BEP scheme prevent the potential limitations of considering only three different urban classes to characterize the city, which is the standard approach of WRF/Urban simulations. Indeed, the aforementioned urban canopy parameters were set for each model grid cell, instead of using the standard approach with WRF/Urban's look-up table of standard values given to each urban class (e.g., low intensity residential, high intensity

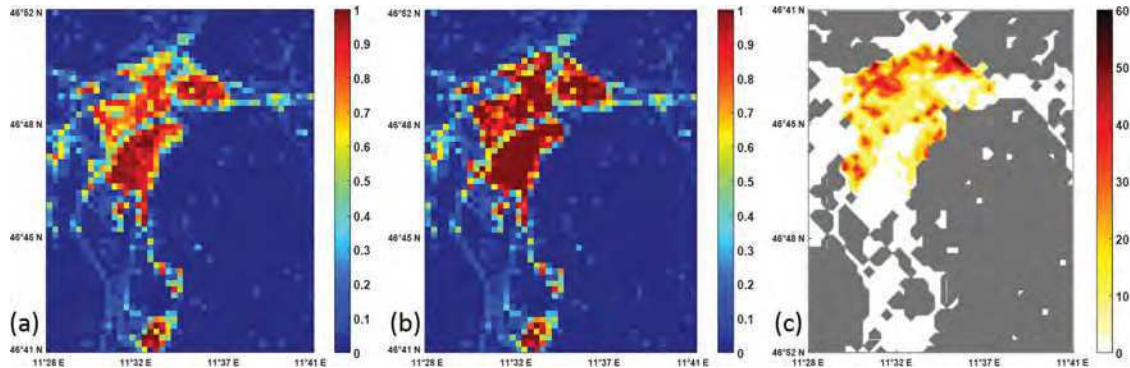


Fig. 3. (a) Urban fraction λ_u parameter calculated by means of MATLAB-QGIS software from digital surfaces and terrain model for urban area of Bolzano (fine resolution-400 m) with vegetation from IRFC. (b) without vegetation from IRFC. (c) percentage rate of land use changes between the two patterns.

residential, industrial, and commercial area). Therefore, the spatial variability of the morphology of the urban area has been taken into consideration in a more appropriate way, as it is important to determine microclimatic conditions in cities.

Results are shown in Figure 4a-i and highlight, as expected, that the highest values of these urban morphology parameters are mainly located in the central part of the city, which is characterized by typical South Tyrolean architectural design, consisting of 4 to 5-storey historic buildings flanking narrow (often arcaded) street canyons. In particular, the highest values of λ_p and λ_b occur in this area, underlining the high-density urban area. Furthermore, high values occur also in the southern area of the city, corresponding to the industrial and commercial areas, (where the maximum urban fraction occurs) and in the northwestern part of the residential area, where high residential buildings are present (Figure 4b).

Building Energy Simulation – TRNSYS

The Transient Systems Simulation Program (TRNSYS) is a well known energy simulation software, developed for transient energy system simulations (Al-Saadi and Zhai 2015). The software is divided into two main parts: the first consists of the engine, which reads and processes the input file, by solving iteratively the system, determining the convergence and finally compiling the system variables; and the second one consists of an extensive library of components, which models the performance of each part of the system. A variety of several models, such as multi-zone buildings, weather data processors, economics routines, and basic air-conditioning equipment are included in the standard library. Several studies used TRNSYS in order to evaluate the impact of UHI and climate change on energy building consumption (Salvati et al. 2017; Santamouris et al. 2015). However, most of them focused only on the distribution of air temperature within urban areas, neglecting the other meteorological variables (such as solar radiation, long-wave radiation, and moisture), despite they are used as input into such model, affecting its performance. In order to carefully represent the mutual impact of a building with its surrounding area, the integration with larger scale models is mandatory, especially when the effect of UHI on building energy performance is investigated (Mirzaei 2015).

Methodology and WRF validation

Flowchart of the WRF/Urban-TRNSYS model chain

In order to summarize the methodology used in the WRF/Urban-TRNSYS model chain, the flowchart is schematically reported in Figure 1 and described as follows:

1. Urban Canopy Parameters (UCPs) are calculated according to Burian et al. (2008) methods, in order to describe in detail the geometry and morphology of the city of Bolzano, and use these data as input in the Building Effect Parameterization (BEP) urban scheme.

Table 1. Internal gains according to the occupancy schedule.

	Schedule	Kitchen [W m ⁻²]	Bedrooms [W m ⁻²]	Total gains [W]
Week days	7–17	8	1	450
	17–23	20	1	1050
	23–7	2	6	400
Weekend	7–17	8	2	500
	17–23	20	4	1200
	23–7	2	6	400

2. An annual simulation is carried out by means of TRNSYS using standard TRY weather data file in order to provide the average daily internal temperature of the reference building, which is further used as initialization temperature in WRF/Urban parameterization scheme. The annual simulation was implemented setting controlled internal temperature between 20°C and 26°C only during the standard occupancy period for residential buildings (Table 1).
3. Numerical simulations are carried out with WRF/Urban, in order to provide fine and accurate meteorological fields at the urban scale and temperature of the external building envelope (400 m spatial resolution). The WRF/Urban output is provided according to the height and orientation (exclusively for façade) of the simulated building, (i.e., at ~10 m a.g.l.) in the TRNSYS model, with the exception of both direct and diffuse solar radiation, which are provided at ground level.
4. The weather parameters (i.e., beam and diffuse irradiation on a horizontal surface, air temperature and humidity, wind velocity) calculated by WRF/Urban are then used in a daily TRNSYS simulation. In some simulations, surface temperature of building façade calculated by WRF/Urban has been used directly as input to TRNSYS simulation instead of air temperature.

It is worth remarking that, differently to the standard practices in BES, which are usually based on long-term meteorological observations such as the TRY, the present work focuses only on a single day. However, a typical summertime day (July 19, 2015) was selected for the simulations, characterized by maximum temperatures ~36°C–38°C and minimum temperatures ~22°C–24°C inside the urban area, allowing us to estimate the energy peak demand due to space cooling in summer.

WRF simulations

In order to evaluate the meteorological field at the urban scale, the non-hydrostatic version of the WRF model (version 3.8) coupled with the Building Effect Parameterization BEP scheme (Martilli et al. 2002) was used (Skamarock et al. 2008). Simulations start at 1800 UTC (LST = UTC + 1 h) July 18, 2015 and end at 0000 UTC July 20, 2015, neglecting the results in the first 6 h, being spuriously affected by the model initialization. The interval time for the inner domain

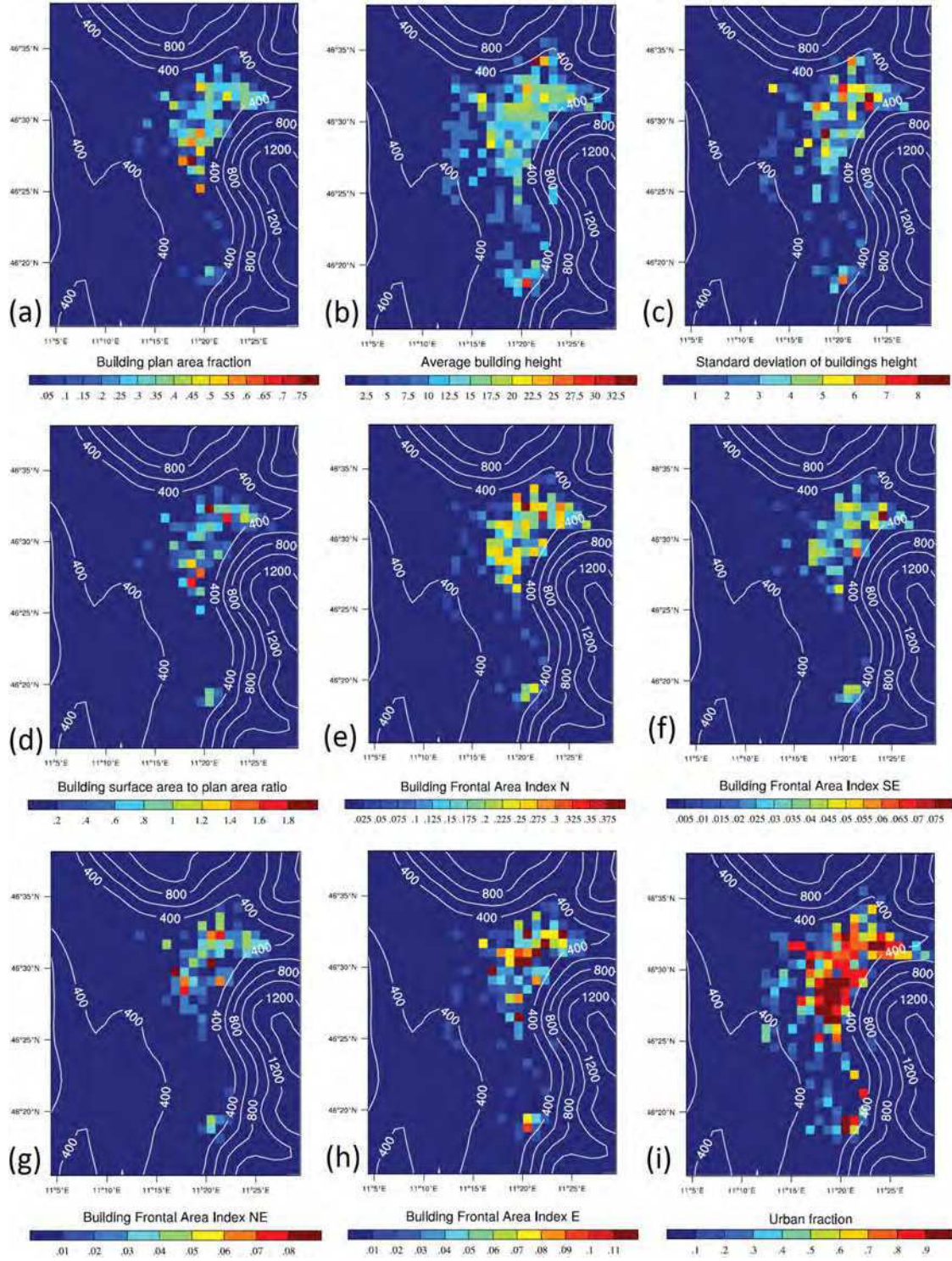


Fig. 4. Urban morphology parameters at 400-m resolution in the urban area of Bolzano. (a) Building plan area fraction λ_p . (b) average building height h_m . (c) standard deviation of building height h_s . (d) building surface area to plan area ratio λ_b . (e-h) building frontal area index to the approaching wind direction at 0° - 135° - 45° - 90° . (i) urban fraction λ_u . Detailed explanation of the parameters are in the Mesoscale meteorological model WRF section. Height contours (above sea level) are also presented.

Table 2. Thermal properties and layer thickness of the building's components used in WRF and TRN simulations.

	THP-a		THP-b		THP-c	
	L/H-IR	I/C	L/H-IR	I/C	L/H-IR	I/C
Roof heat capacity [J m ⁻³ K ⁻¹]	1.32 × 10 ⁶	1.32 × 10 ⁶	1.57 × 10 ⁶	1.40 × 10 ⁶	1.77 × 10 ⁶	1.73 × 10 ⁶
Roof thermal conductivity [J m ⁻¹ s ⁻¹ K ⁻¹]	1.54	1.54	0.263	0.621 ^a	0.669	0.502 ^a
Roof emissivity	0.90	0.90	0.90	0.90	0.90	0.90
Roof albedo	0.30	0.30	0.30	0.30	0.30	0.30
Roof thickness [m]	0.1575	0.1575	0.27	0.27	0.24	0.32
Wall heat capacity [J m ⁻³ K ⁻¹]	1.54 × 10 ⁶	1.54 × 10 ⁶	1.61 × 10 ⁶	1.73 × 10 ⁶	1.78 × 10 ⁶	1.40 × 10 ⁶
Wall thermal conductivity [J m ⁻¹ s ⁻¹ K ⁻¹]	1.51	1.51	0.279	0.856 ^a	0.726	1.32 ^a
Wall emissivity	0.90	0.90	0.90	0.90	0.90	0.90
Wall albedo	0.35	0.35	0.35	0.35	0.35	0.35
Wall thickness [m]	0.1575	0.1575	0.32	0.32	0.40	0.22

^arefers to equivalent value obtained from Equation 1.

output was set to 30 min. Simulations were carried out using four nested domains (nesting ratio = 3) with grid resolution of 10.8–3.6–1.2–0.4 km (Figure 1). Initial and boundary conditions derived from the National Center for Environmental Prediction (NCEP) Final Model Analyses, in which meteorological data have 1-deg grid resolution (about 120 km) and 6 h time resolution. The 44 eta levels (terrain-following hydrostatic-pressure vertical coordinate) were used, with the first model level at ~10 m, and 10 model levels in the first 1000 m a.g.l. The simulations were run with the Bougeault and Lacarrère (1989) scheme for the Planetary Boundary Layer (PBL) parameterization, while the Noah land surface model (Chen and Dudhia 2001) was used for the land surface processes parameterization. In order to match the two models (i.e., WRF/Urban-TRNSYS) and evaluate the impact of using different properties of building components on WRF/Urban output, two different simulations were carried out. The first simulation uses the typical urban surface thicknesses (reported in BEP) and thermal properties (THP-a) obtained by model calibration in the nearby city of Trento and is referred to as WRF-a, while the second considers the building thermal properties typical of the period from 1976 to 2005 (THP-b) according to UNI/TR 11552:2014 (UNI 2014a) and is referred to as WRF-b (Table 2). In particular, the regulation UNI/TR 11552:2014 (UNI 2014a) provides the characteristics of the building envelope (e.g., constructions materials, thermal properties, and layer thickness of the building's components) for different historical periods and different Italian regions.

Since the urban area of Bolzano includes a great variety of building ages, the envelope materials and thermal characteristics typical for the period from 1976 to 2005 provide an average representation of the buildings built in the urban area from the past up to the recent years. Therefore, an average value of thermal resistance and thickness for external walls and roof representative of that historical period was calculated for the two WRF building categories, that is, residential and industrial/commercial. The same

values were used for both low and high intensity residential (L/H-IR) class, as reported in Table 2. However, since in the WRF/Urban model only a single thickness value can be set for walls and roofs for the three urban categories, an equivalent heat conductivity was estimated and applied for industrial and commercial buildings, in order to reproduce the thermal characteristics of building components (e.g., wall and roof) as if the thickness was that derived from UNI/TR 11552:2014 (UNI 2014a). The equivalent heat conductivity was calculated as follow:

$$\lambda_{e,ic} = (\lambda_{ic} * Lres_{r,w}) / Lic_{r,w} \quad (1)$$

where $\lambda_{e,ic}$ is the heat conductivity of industrial/commercial, while $Lres_{r,w}$ and $Lic_{r,w}$ represent the thickness of roofs and walls of residential and industrial/commercial, respectively, as reported in the aforementioned regulation.

Six weather stations (four urban and two rural) were selected in order to validate WRF/Urban output. The two rural weather stations (referred to as Bronzolo and Laimburg) are located both south of the city (~8 km from the urban area) and on the floor of the Adige valley (respectively at 226 m and 224 m MSL), which is covered by cultivated land, in particular apple orchards and vineyards. On the contrary, the urban weather stations are located within the urban area of Bolzano (Figure 2b): two of them in the dense neighborhood of the city center (referred to as “Via Amba Alagi” and “Piazza Adriano”), one in the industrial and commercial area (referred to as “Via Augusta”), and one in the suburban area close to the hospital of the city (referred to as “Ospedale”). In particular, Via Amba Alagi and Piazza Adriano are both located in the urban core of the city, mainly characterized by midrise buildings (average height respectively of 13.6 m and 12.9 m), separated by nonextensive and scattered green areas ($\lambda_u \sim 70\%$). Except for the eastern part of the city, where some university facilities and museums are located, the intended use is primarily residential. On the contrary, Via Augusta is located in the southern part of the

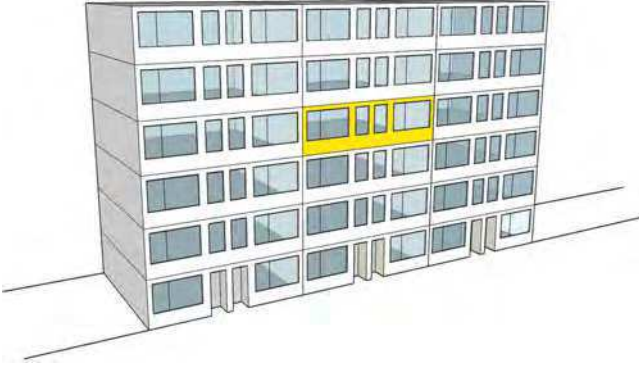


Fig. 5. Building used as case-study. The residential unit on the third floor simulated in TRNSYS is highlighted with a yellow façade.

city, at the edge of the industrial and commercial area, which is characterized by large low-rise building (average height of 9 m) and wide impervious surfaces ($\lambda_u \sim 80\%$). Finally, the suburban weather station named “Ospedale” is located in the western part of the city, where apple orchards and vineyards are contiguous to the urban area ($\lambda_u = 20\%$), and just fragmented by sparsely single-low buildings (average height 7 m).

Building Simulation: Case-study and settings

In order to simulate a representative residential building typical of the analyzed urban area of Bolzano, a single story residential unit with a floor area of 100 m² and an internal height of 3 m is considered (Figure 5). The unit is placed on the third floor of a multistorey building, close to Via Amba Alagi weather station, and it has a single external wall oriented towards South. The window surface extent is 14.4 m². The window system is a single pane glass ($U_{gl} = 5.7 \text{ W m}^{-2} \text{ K}^{-1}$) with a standard timber frame ($U_{fr} = 3.2 \text{ W m}^{-2} \text{ K}^{-1}$). Concerning the envelope structure, different thermal properties for wall materials are considered, according to the ones used in the WRF/Urban model and according to two different historical periods that the standard UNI/TR 11552:2014 (UNI 2014a) considers as a reference for different levels of envelope insulation: the period between 1976 and 2005, referred to as THP-b, and the period before 1978,

referred to as THP-c, (UNI 2014a). Detailed information on the thermal properties used are reported in Table 2. All the simulations consider an infiltration rate equal to 0.062 h⁻¹, according to the Standards EN 12207 (CEN 1999) and the EN 15242 (CEN 2007). The ventilation rate of 0.5 h⁻¹ and the internal gains are set according to the occupancy profile defined in the national Technical Standard UNI/TS 11300–1 (UNI 2014b) and reported in Table 1. The cooling demand is calculated setting the system set-point for air temperature equal to 26°C during occupancy hours. An ideal cooling system of infinite power is considered for the analysis.

In this work TRNSYS subroutine TYPE 16 was used for processing solar radiation in order to calculate several quantities related to the position of the sun, necessary for the building energy simulation (e.g., the solar azimuthal and zenith angles, the total and the beam solar irradiation on envelope surfaces and the incident angles of solar irradiation on the envelope surfaces). Perez et al. (1992) model was used to compute the solar irradiation on vertical surfaces. Then the building energy simulation was carried out by means of TRNBuild for the building description, coupled with TYPE56 Multi-Zone Building. External heat transfer convective coefficients, h_c , were provided as inputs to the TYPE56 and they were correlated to the wind velocity (Clarke 1985), v_w , according to Equation 2.

$$h_c = 5.678 * (1.09 + 0.23 * (v_w * 0.3048)) \quad (2)$$

Since WRF/Urban simulations give one-day results, in order to stabilize the dynamic response of the building, a 10-day period composed of identical weather boundary conditions was used and the last day outputs were considered as the final results. Moreover, in some simulations, surface temperature of building façade computed by WRF/Urban was used directly as input to TRNSYS simulation instead of air temperature (see Table 3). The aim of this effort is to test the sensitivity of the TRNSYS model to this input too, along with the direct comparison of the external façade temperature obtained by means of the two models (i.e., WRF/Urban and TRNSYS), using the same characteristics of the building envelope (e.g., constructions materials, thermal properties and layer thickness of the building’s components).

Different weather boundary conditions for July 19 were applied for the building simulations: the weather station data

Table 3. Overview of the TRNSYS simulations with the respective thermal properties used (left) and the meteorological input (top). WRF-a used thermal properties THP-a and WRF-b used the building thermal properties THP-b.

Thermal properties used in TRNSYS model	Meteorological input for TRNSYS			
	WRF-a	WRF-b	AMBA	TRY
THP-b-	WRF-a/TRN-b WRF-a/TRN-b ^a	WRF-b/TRN-b WRF-b/TRN-b ^a	AMBA/TRN-b	TRY/TRN-b
THP-c	WRF-a/TRN-c WRF-a/TRN-c ^a	WRF-b/TRN-c WRF-b/TRN-c ^a	AMBA/TRN-c	TRY/TRN-c

^arefers to external surface temperatures obtained by means of WRF/Urban.

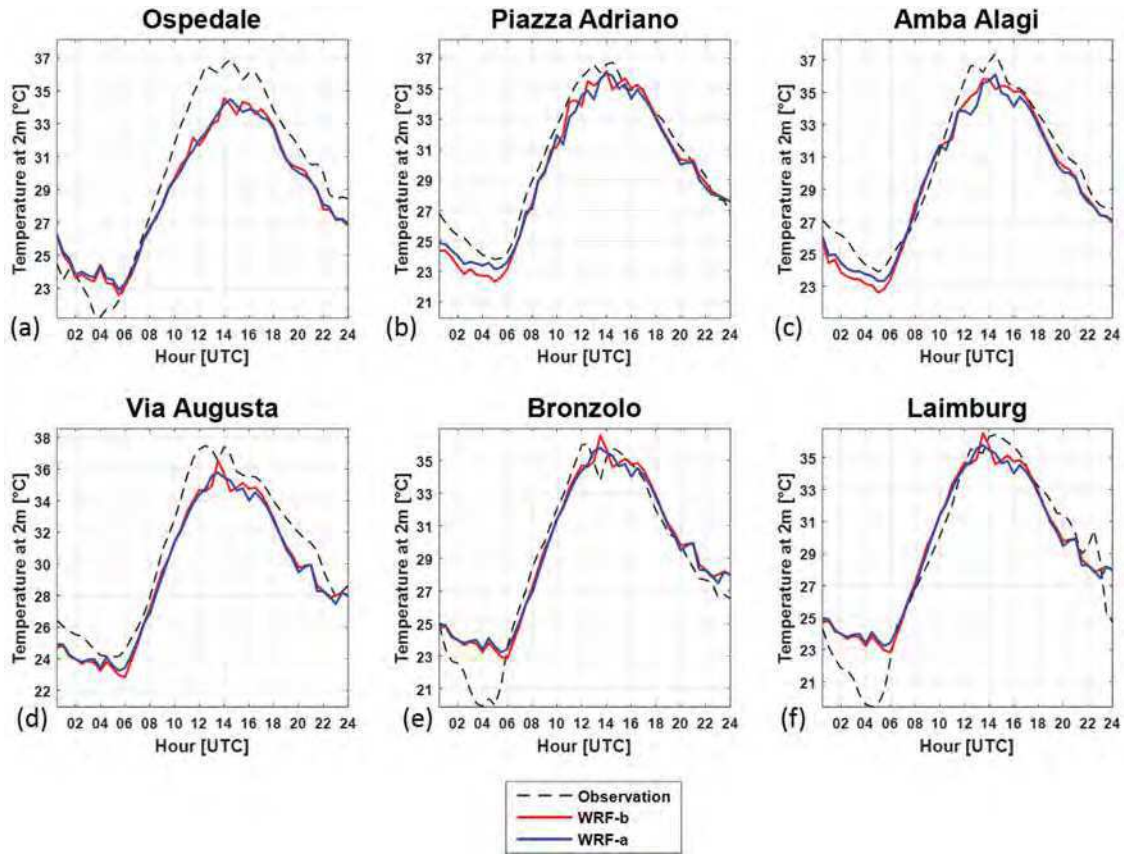


Fig. 6. Daily cycles of temperature as simulated by WRF/Urban and observed throughout the urban area of Bolzano: (a) Ospedale. (b) Piazza Adriano. (c) Amba Alagi. (d) Via Augusta, and in the rural area. (e) Bronzolo. (f) Laimburg during July 19, 2015.

collected in Via Amba Alagi station, which is close to the simulated building (referred to as AMBA), the simulated weather parameters from WRF/Urban in the model cell where the building is located (referred to as WRF-a and WRF-b) and the Test Reference Year (referred to as TRY), elaborated by the Italian Technical Committee for Energy and Environment (CTI 2016). An overview of TRNSYS simulations using the aforementioned input is reported in Table 3.

Results

WRF validation

Six weather stations were selected as reference to test the quality of WRF/Urban output, four located at different LULC classification throughout the city of Bolzano (Figure 2b), and two located in the rural area (Bronzolo and Laimburg). The Provincial Agency for Environmental Protection (APPA) and the Autonomous Province of Bolzano operate the weather stations (details in Figure 2b). Meteorological variables were measured at the acquisition frequency of 10 min; 30-min averages were calculated for comparison with WRF/Urban output. The 2-m temperature field and the 10-m wind field provided by WRF/Urban model were compared at all measurements sites, with the exception of Via Augusta

and Piazza Adriano, which do not provide anemometric data. Amba Alagi is at ~20 m a.g.l. as it is located on the APPA building rooftop and is, indeed, compared with the second level of the WRF/Urban model. In order to quantitatively validate model results, the mean error (BIAS) and the root-mean-square error (RMSE) were evaluated, quantifying the difference between simulated WRF/Urban output and observations. In particular, validation for air temperature was carried out for both WRF-a and WRF-b, while validation of wind field was carried out only for WRF-a, based on the negligible impact of building properties on the wind field. Figure 6 shows a comparison between observed and simulated 2-m temperature at all the weather stations. WRF/Urban reproduces better air temperature at Via Amba Alagi and Piazza Adriano, (representative of HI-R and LI-R respectively), while slightly greater errors are found at the remaining weather stations. In particular, stations in the core urban area (e.g., ADR, AMBA) compare well to simulation results throughout the daily cycle, while the model tends to overestimate minima and underestimate maxima in suburban (OSP) and rural areas (BRO, LAIM). This error is particularly evident at OSP station, which is probably connected to the position of the weather station, at the boundary between urban and rural areas. Overall, both WRF-a and WRF-b perform satisfactorily, with most BIAS values around or below 1°C (details in Table 4). It

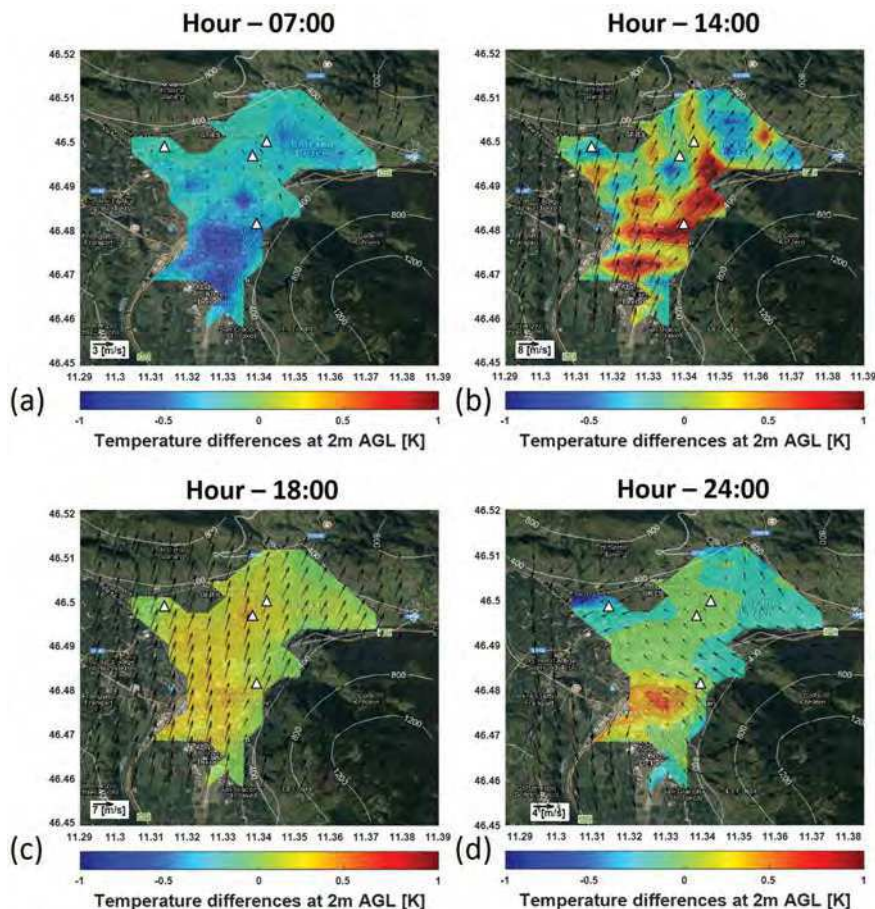
Table 4. Root-mean-square errors (RMSE) and mean errors (BIAS) for 2 m-temperature and wind speed at 10 m, compared with measurements at the six weather stations.

ID Station	Position (°N, °E)	LULC	Temperature at 2 m [°C]				Wind speed at 10 m [m s ⁻¹]	
			RMSE		BIAS		RMSE	BIAS
			WRF-a	WRF-b	WRF-a	WRF-b	WRF-a	WRF-b
OSP	46.4977 / 11.3128	LI-R	1.94	1.89	− 1.04	− 1.06	1.20	0.38
ADR	46.4954 / 11.3399	LI-R	1.04	1.15	− 0.84	− 0.87	/	/
AMBA	46.4993 / 11.3420	HI-R	1.15	1.17	− 0.85	− 0.84	1.22	− 0.42
AUGU	46.4823 / 11.3418	I/C	1.52	1.49	− 1.37	− 1.32	/	/
LAIM	46.3825 / 11.2887	RUR	1.95	1.94	− 1.00	− 1.00	1.24	0.57
BRO	46.4065 / 11.3111	RUR	1.69	1.72	− 1.00	− 1.03	1.17	− 0.11

Note: LULC urban categories are based on the 2006 NLCD: low, high intensity residential are indicated by LI-R, HI-R, while I/C and RUR represent respectively industrial-commercial and rural area.

is worth analyzing the temperature differences between the above-mentioned simulations (i.e. WRF-a and WRF-b), in order to assess the impact of different thermal and materials properties of the building envelope on the temperature field in the urban environment. Figure 7 shows the differences

between the temperature field in the urban area in the two simulations (being WRF-a the reference). The points in time were chosen being representative of the daily thermal cycle in the city. As it can be seen, thermal differences are lower than 1°C. Indeed, with the exception of the early hours

**Fig. 7.** Temperature differences at 2 m AGL in the urban area of Bolzano between WRF-b and WRF-a at (a) 07:00, (b) 14:00, (c) 18:00, and (d) 24:00 LST of July 19, 2015. Wind vectors refer to the wind field at 10 m, to get a clearer representation of the typical valley winds. The white triangles represent the urban measurement stations. Height contours are in m ASL.

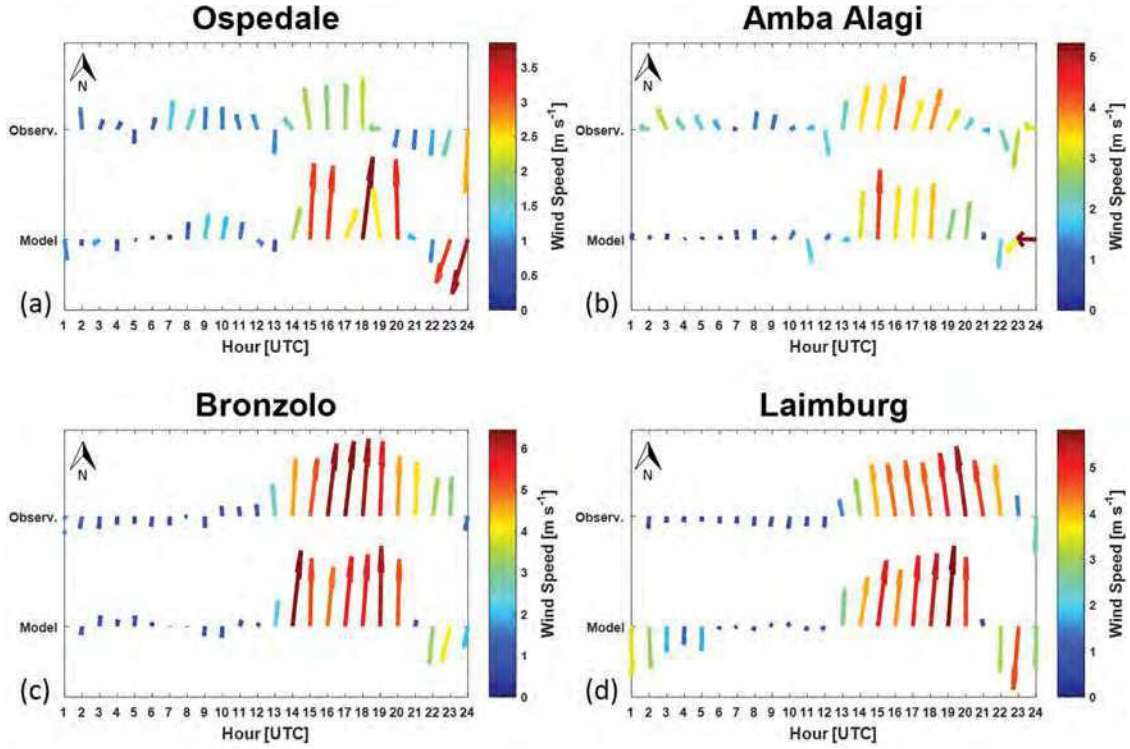


Fig. 8. Horizontal wind vectors as observed (top) and simulated by WRF/Urban (bottom) at (a) Ospedale, (b) Amba Alagi, (c) Bronzolo, (d) Laimburg, during July 19, 2015.

of the morning (7:00 LST) reported in Figure 7a, WRF-b gives higher temperatures than WRF-a, with differences growing until the nocturnal hours (24:00 LST), especially in the industrial/commercial areas (Figure 7d). This behavior is probably due to the different properties of the building envelope used in WRF-b simulation, which are not the same for all urban classes as in the WRF-a simulation (details in Table 2).

Finally, the comparison of the wind field between model results and observations at different weather stations is shown in Figure 8a–d and Table 4, which report the horizontal wind field at different hours of the day and the relative errors (RMSE and BIAS), respectively. Overall, WRF/Urban is able to predict wind field both in the Adige Valley and in the Bolzano basin, showing very low errors both in urban and rural areas, with BIAS values lower than $\sim 0.5 \text{ m s}^{-1}$. The development of the typical cycle composed of a light down-valley wind at night and a stronger up-valley wind in the afternoon in the Adige Valley is well reproduced by WRF/Urban (Figure 8c,d). The comparison at the grid point where Amba Alagi weather station lies (Figure 8b) highlights that WRF/Urban is able to reproduce satisfactorily the wind field also in the urban area (RMSE = 1.22 m s^{-1} , BIAS = -0.42 m s^{-1}).

Based on the results of the sensitivity study, both WRF-a and WRF-b simulations seem suitable to represent temperature field throughout the urban environment. It is worth highlighting that the errors obtained in this work are comparable to those reported in Conry et al. (2015), Giovannini et al. (2014), and Salamanca et al. (2011), where coupled

WRF/BEP simulations were used to reproduce meteorological fields in urban areas.

In the next section, output from the different WRF/Urban simulations will be used as input for the TRNSYS model, in order to evaluate the impact of different input data in the BES simulation.

TRNSYS analysis

As many simulations are involved in this work, adopting different methodologies and thermal properties, a general overview of the simulations carried out and of the analysis performed on them is first presented. The analysis of the model results focuses on both external and internal temperature profiles of building façade and on the cooling demand. To support the reading of the results, each TRNSYS simulation is named by means of a matrix that intersects the thermal properties used for the building envelope and the meteorological input used as boundary condition. This matrix is reported in Table 3. In particular simulations of building with thermal properties THP-b are named with the “b” letter and simulations of building with thermal properties THP-c are named with the “c” letter. The output obtained by means of TRNSYS simulations fed by observed data as weather input are taken as reference (i.e., AMBA/TRN simulations) and compared against TRNSYS simulations fed with WRF/Urban output (WRF/TRN simulations), as well as with data from the Test Reference Year (TRY/TRN simulations). Among WRF/TRN simulations, those flagged with an superscripted “a” refer to external surface

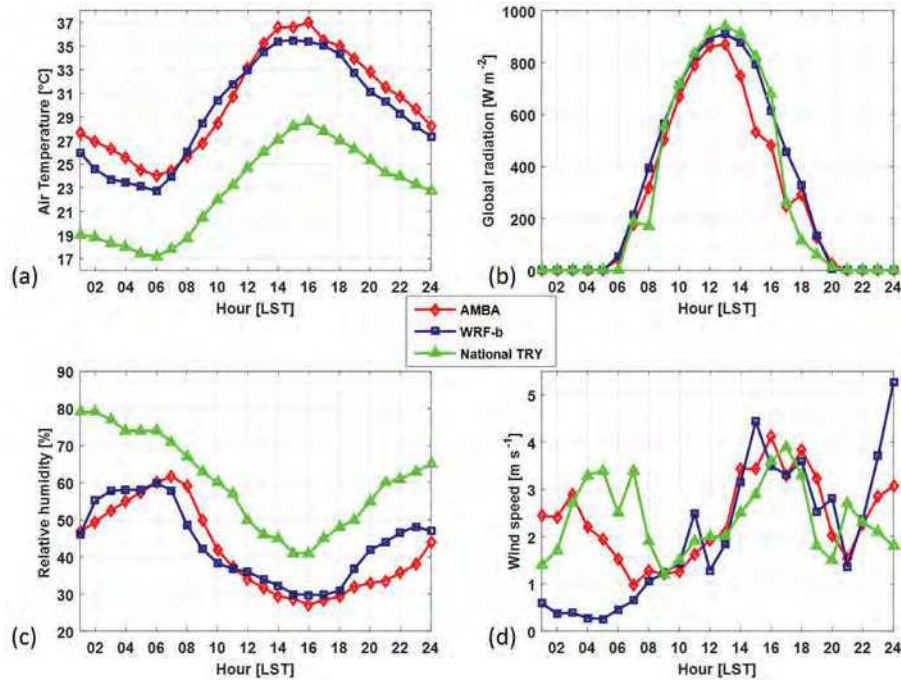


Fig. 9. (a) Air temperature. (b) global radiation. (c) relative humidity. (d) wind speed observed and simulated by WRF/Urban at the Amba Alagi site (46.49°N, 11.34°E), against the national TRY data during July 19, 2015.

temperature obtained by means of WRF/Urban and used as input in TRNSYS. Lastly, only for the external building façade analysis, both temperature profiles directly derived from WRF-a and WRF-b are analyzed and compared.

Comparison of meteorological input for TRNSYS

In order to better understand the energy assessment of the sample building, a comparison between data from Via Amba Alagi weather station, WRF/Urban simulations and the national TRY (CTI 2016) was carried out. Four different variables, for example, air temperature [°C], global solar radiation [W m⁻²], relative humidity, and wind speed [m s⁻¹] were compared. As shown in Figure 9a-d, a good correlation occurs between observed data and WRF/Urban results for all the analysed meteorological variables, while significant differences occur with national TRY data. In particular, the differences between both WRF/Urban and observations with national TRY data are around 7°C–8°C for air temperature, greater than 10% for relative humidity and a significant overestimation (max 2 ms⁻¹) of wind speed occurs during the first hours of the day.

Temperature profile of the building façade

Figure 10 presents the comparison of surface wall temperature profiles obtained with different simulations. In particular Figure 10a,b shows the simulated external and internal façade temperatures obtained directly from WRF/Urban output (WRF-a and WRF-b) and by means of TRN-b simulations using different meteorological input, while Figure 10c-d shows the temperature profiles obtained by WRF/Urban output (the same as in Figure 10a,b) and the ones calculated by TRN-c simulations. It is important to emphasize

the different source and resolution of the analyzed surface, which for TRNSYS represents a component of the simulated building, while for the WRF/Urban model is a representative surface of the 400 × 400 m grid cell. Indeed, the BEP model, along with the morphology information of the city (provided by the gridded UCPs) allows WRF/Urban to consider the shadowing and reflection effects of nearby buildings ($h_m = 13.6$ m at AMBA cell), affecting the surface temperature and consequently the resulting daily energy demand.

Overall, it can be seen that small differences occur between surface temperatures obtained using WRF/Urban as meteorological input for TRNSYS and the ones obtained using Amba Alagi measurements as input for the building energy simulations (i.e., AMBA/TRN-b and AMBA/TRN-c). Table 5 summarizes these differences in terms of RMSE. In particular, considering AMBA/TRN-b as a reference and the external surface temperature as an output, the WRF-a simulation gives the highest RMSE, excluding the TRY/TRN-b results, while WRF-b gives the best approximation and TRNSYS gives an intermediate RMSE value. In fact, for both WRF-a and WRF-b input, TRNSYS output has a RMSE equal to 1.8°C. Considering AMBA/TRN-c as a reference, although WRF-a gives the same RMSE as in the previous case, WRF-b does not provide a good estimation of the external surface temperature. However, the approximation obtained with WRF-b/TRN-c and WRF-a/TRN-c simulations is very good (<1°C), thus showing that WRF-b, coupled with BES, guarantees a good simulation of the surface temperature also in this situation.

Looking now at the indoor surface temperatures obtained by means of TRNSYS simulations fed by meteorological input from WRF/Urban and weather station data, it is

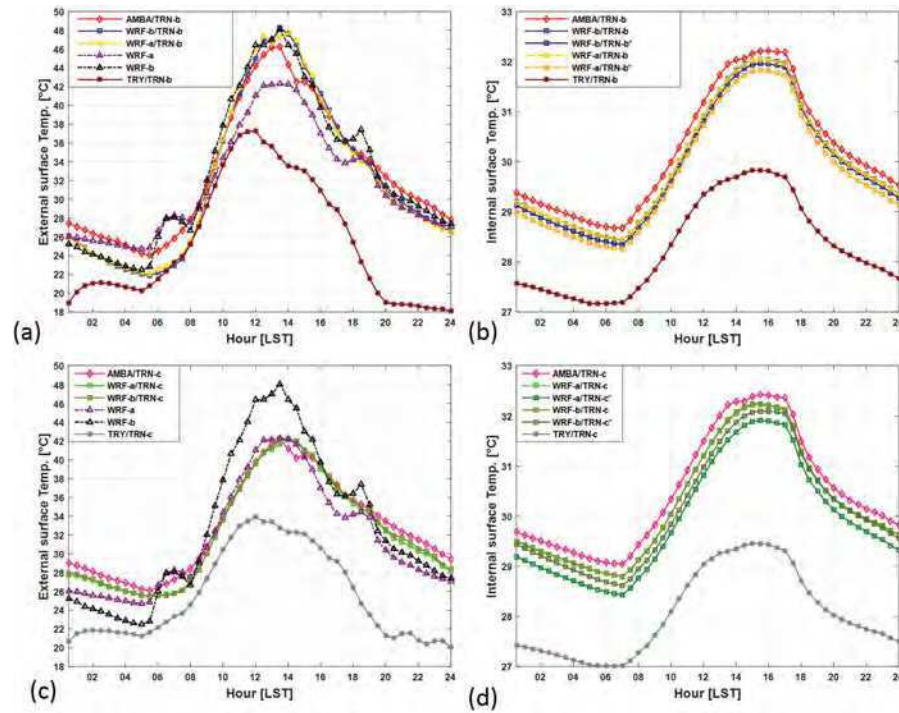


Fig. 10. (a) External (left) and internal (right) façade temperature of the analyzed building exposed to south obtained using thermal properties named WRF-b/TRN-b. a,b and c,d TRN-c.

possible to highlight the comparable trends ($RMSE < 1^{\circ}C$), regardless of type of WRF/Urban output (e.g., WRF-a, WRF-b) and the thermal properties used in TRNSYS. Furthermore, it is interesting to see that for the estimation of the indoor surface temperature the use of external air temperature as input is preferable than using directly the external

surface temperature calculated by WRF. As expected, large differences occur between the references and the surface temperature obtained using the national TRY data (referred as to TRY/TRN-b, TRY/TRN-c), especially in the second part of the day, with $RMSE > 7^{\circ}C$ on the external surface and $RMSE > 1.9^{\circ}C$ on the internal surface.

Table 5. Root-mean-square-error (RMSE) for external (left), internal (middle) façade temperature, and daily cooling demand (right) compared with references AMBA/TRN-b (top) and AMBA/TRN-c (bottom).

WRF/Urban and TRNSYS simulation	RMSE [$^{\circ}C$] – External wall surface temperature	RMSE [$^{\circ}C$] – Internal wall surface temperature	NMB – Daily cooling demand	Cv(RMSE) – Daily cooling demand (%)
Ref. AMBA/TRN-b				
WRF-a	2.00	/	/	/
WRF-b	1.60	/	/	/
WRF-b/TRN-b	1.80	0.22	-9%	11
WRF-b/TRN-b ^a	/	0.30	-6%	8
WRF-a/TRN-b	1.80	0.22	-8%	11
WRF-a/TRN-b ^a	/	0.42	-7%	9
TRY/TRN-b	8.30	1.93	/	/
Ref. AMBA/TRN-c				
WRF-a	1.99	/	/	/
WRF-b	3.35	/	/	/
WRF-b/TRN-c	0.83	0.23	-8%	11
WRF-b/TRN-c ^a	/	0.37	-5%	7
WRF-a/TRN-c	0.90	0.25	-8%	11
WRF-a/TRN-c ^a	/	0.56	-7%	9
TRY/TRN-c	7.74	2.46	/	/

^arefers to external surface temperature obtained by means of WRF/Urban and used as input in TRNSYS.

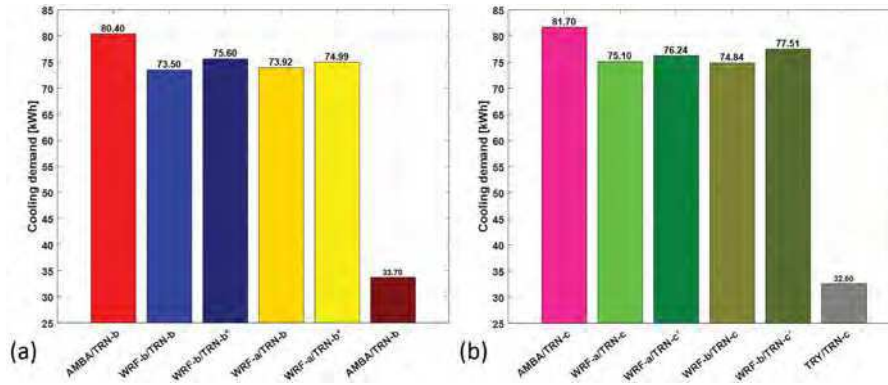


Fig. 11. Daily cooling demand for the sample building estimated by means of TRNSYS fed with different input, e.g., weather station (AMBA), WRF/Urban output (WRF-a,b) and TRY data, using thermal properties named (a) WRF-b/TRN-b and (b) TRN-c.

Cooling demand analysis

Finally, the results of the daily cooling demand obtained by means of TRNSYS simulations are shown in Figure 11a,b. The daily cooling demands calculated using meteorological data from Via Amba Alagi station (i.e., AMBA/TRN-b, AMBA/TRN-c) are higher compared to all simulations fed by WRF/Urban and national TRY data. However, slight differences occur between the estimation with input data from the weather station and WRF/Urban, while, as expected, significant differences occur when using TRY (i.e., TRY/TRN-b and TRY/TRN-c). Specifically, the daily cooling demand estimated using weather station data as input is 80.4 kWh and 81.7 kWh, respectively, using thermal properties of 1976–2005 (AMBA/TRN-b) and before 1978 (AMBA/TRN-c), which are greater of about 6% to 8% with respect to simulations fed with different WRF/Urban input. Finally, it is worth analyzing the impact of simulated external façade temperature (obtained by means of WRF/Urban) on the daily cooling demand. Indeed, cooling demand obtained by WRF-b/TRN-b^a (dark blue) is higher than WRF-a/TRN-b^a (yellow), which is consistent with the higher façade temperature ($\sim 5^{\circ}\text{C}$ during the central hours of the day) obtained with WRF-b (dashed black line), compared to that provided by WRF-a (Figure 10a,c). In order to evaluate the level of accuracy obtained by means of the modeling chain tested, two statistical indices, that is, the Normalized Mean Bias (NMB) and the Coefficient of Variation of the Root Mean Square Error (CvRMSE), were calculated and compared with acceptable calibration tolerances suggested by Ashrae Guidelines 14–2002 (ASHRAE 2002). It is worth noting that these indices have been calculated considering the cooling demand obtained by means of WRF/TRN simulations taking as a reference the cooling demand calculated by TRNSYS using monitored data as weather input and not the energy demand measured. As it can be seen in Table 5, all the indices are lower than the standard requirements both for NMB and Cv(RMSE). Both WRF-a and WRF-b, coupled with TRN models lead to a good estimation of the cooling demand with $\text{NMB} < \pm 10\%$ and Cv(RMSE) widely lower than 30%, in accord with ASHRAE recommendations (ASHRAE 2002). In particular, the best approximation is obtained when the

external surface temperature calculated by WRF is used by TRN simulation.

Discussion and conclusion

The results described in previous sections show that conventional climate data, such as Test Reference Year or weather stations data are not representative of the urban environment, commonly used as meteorological input for building energy simulations, and are not able to describe micrometeorological conditions representative of specific urban areas, due to the limitation at a single-point, which negatively affect model reliability.

However, the recent progress in numerical weather prediction modelling and, in particular, the possibility to reach increasingly finer spatial resolutions, allow researchers to reproduce building-atmosphere interactions in urban areas in a more accurate and realistic way. In this study, a model chain WRF/Urban–TRNSYS is applied as follows: based on calculated gridded Urban Canopy Parameters (UCPs), used as input for the Building Effect Parameterization (BEP) scheme, the meteorological WRF/Urban model provides fine-scale input data for Building Energy Simulation (BES) implemented by TRNSYS. Comparisons of the results obtained with TRNSYS are carried out to assess the impact of the gridded input from WRF/Urban against both weather stations measurements and Test Reference Year of Bolzano.

In order to test the quality of WRF/Urban model output, a validation with a network of permanent conventional weather stations was carried out throughout the urban environment. The results highlight that the temperature field is strongly affected by the presence of the urban area. The WRF/Urban model well describes temperature ($\text{RMSE} < 1.5^{\circ}\text{C}$, $\text{BIAS} < 1^{\circ}\text{C}$, at urban area) and wind field ($\text{RMSE} < 1.2 \text{ m s}^{-1}$, $\text{BIAS} < 0.6 \text{ m s}^{-1}$) both in the Bolzano basin and in the Adige Valley.

Results obtained show that WRF/Urban can be a reliable tool to provide meteorological input data to BES, when local measurements are not available. In fact, the comparison of external and internal building façade temperatures

simulated by WRF/Urban and by TRNSYS using different meteorological input, highlighted that the WRF/Urban-TRNSYS modeling chain is able to reproduce similar wall temperatures to those simulated using measured meteorological variables as input to TRNSYS. Differences between simulations fed by WRF/Urban and by observations are small also concerning the daily cooling demand; in particular simulations fed by WRF/Urban input give lower energy consumption of ~6% to 8% than simulations fed by local measurements.

Based on these results, we conclude that the WRF/Urban-TRNSYS model chain can provide an accurate building energy analysis especially in the urban context, based on a meteorological input, providing information which is not typically available from conventional climate data (e.g., Test Reference Year) and leading to a more robust source (spatially averaged) for initial conditions as compared to local observations. Consequently, several advantages can arise from the use of the WRF/Urban-TRNSYS method, such as: 1) a better knowledge of micrometeorological conditions representative of specific urban areas free from potential bias associated to instrument location; 2) additional information on impervious urban surfaces (e.g., wall, roof, and road), together with upper soil layers and overlying urban canopy layer; 3) a useful support to real buildings energy model calibration, giving the possibility of considering the urbanization effects, which are specifically related to the proper morphology of the urban context and taking into account the surrounding buildings effect on radiative and convective exchanges on the building envelope; and 4) a better prediction of future scenarios assessing the feedback between buildings and surrounding microclimate, which is directly affected by climate change and mitigation strategies (e.g., green roofs, trees, and vegetation). However, in this work only a basic sample residential building was simulated in order to simplify both energy and sensitivity analysis. The impact of the WRF/Urban output on the cooling demand estimation of different typical building types (e.g., single-multifamily and apartment buildings, industrial buildings), will be considered in a future research. Moreover, the availability of monitored consumption data for different building types will be a further development of the analysis, assessing the validity of the whole modeling chain. Another possible development of the present study could be represented by coupling the BEP scheme with a simple Building Energy Model (BEP+BEM) already available in WRF, which simulates in more realistic and complex way the interaction between the building and the atmosphere (Salamanca and Martilli 2010). In particular, the embedded building energy module estimates the heat diffusion through the building envelope and the radiation exchange between indoor surfaces, the heat generation of occupants and equipment, and the energy consumption of air conditioning systems and natural ventilation. Further progress may be achieved by the adoption of more precise parameterizations of turbulent exchange processes based on similarity relationships carefully separating different components in the turbulent flows, for example, low-frequency effects arising from local heterogeneities (including urban

fingerprint) from more intrinsic high-frequency components (de Franceschi and Zardi 2003; de Franceschi et al. 2009).

ORCID

Francesca Cappelletti  <http://orcid.org/0000-0003-2158-0449>

References

- Al-Saadi, S.N., and Z. Zhai. 2015. A new validated TRNSYS module for simulating latent heat storage walls. *Energy and Buildings* 109:274–90.
- ASHRAE. 2002. *Ashrae Guideline 14–2002: Measurement of Energy Demand and Savings*. Atlanta, GA: American Society of Heating, Refrigerating and Air-Conditioning Engineers.
- Bougeault, P., and P. Lacarrère. 1989. Parameterization of orography-induced turbulence in a mesobeta-scale model. *Monthly Weather Review* 117:1827–90.
- Bouyer, J., C. Inard, and M. Musy. 2011. Microclimatic coupling as a solution to improve building energy simulation in an urban context. *Energy and Buildings* 43:1549–59.
- Burian, S., N. Augustus, I. Jeyachandran, and M.J. Brown. 2008. *Final Report for the National Building Statistics Database, Version 2*.
- CEN. 1999. *EN 12207, Windows and Doors. Air Permeability – Classification*. Brussels: CEN-CENELEC.
- CEN. 2007. *EN 15242, Ventilation for Buildings – Calculation Method for the Determination of Airflow Rates in Buildings Including Infiltration*. Brussels: CEN-CENELEC.
- Chen, F., and J. Dudhia. 2001. Coupling an advances land surface-hydrology model with the Penn State-NCAR MM5 modeling system. Part I: Model implementation and sensitivity. *Monthly Weather Review* 129:569–85.
- Clarke, J.A. 1985. *Energy Simulation in Building Design*. Bristol: Adam Hilger, 362 pp.
- Conry, P., A. Sharma, M.J. Potosnak, L.S. Leo, E. Bensman, J. Hellmann, and J.H.S. Fernando. 2015. Chicago's Heat Island and climate change: Bridging the scales via dynamical downscaling. *Journal of Applied Meteorology and Climatology* 54:1430–48.
- CTI. 2016. Website of the Italian Technical Committee for Energy and Environment. <http://try.cti2000.it/>
- de Franceschi, M., and D. Zardi. 2003. Evaluation of cut-off frequency and correction of filter-induced phase lag and attenuation in eddy covariance analysis of turbulence data. *Boundary-Layer Meteorology* 108:289–303.
- de Franceschi, M., D. Zardi, M. Tagliazucca, and F. Tampieri. 2009. Analysis of second order moments in the surface layer turbulence in an Alpine valley. *Quarterly Journal of the Royal Meteorological Society* 135:1750–65.
- European Parliament and Council. 2010. Directive 2010/31/EU of the European Parliament and of the Council of 19 May 2010 on the energy performance of buildings. *Official Journal of the European Union* L153:13–35.
- Giovannini, L., L. Laiti, S. Serafin, and D. Zardi. 2017. The thermally driven diurnal wind system of the Adige Valley in the Italian Alps. *Quarterly Journal of the Royal Meteorological Society* 143:2389–402.
- Giovannini, L., D. Zardi, and M. de Franceschi. 2011. Analysis of the urban thermal fingerprint of the city of Trento in the Alps. *Journal of Applied Meteorology and Climatology* 50:1145–1162.
- Giovannini, L., D. Zardi, and M. de Franceschi. 2013. Characterization of the thermal structure inside an urban canyon: Field measurements and validation of a simple model. *Journal of Applied Meteorology and Climatology* 52:64–81.

- Giovannini, L., D. Zardi, M. de Franceschi, and F. Chen. 2014. Numerical simulations of boundary-layer processes and urban-induced alterations in an Alpine valley. *International Journal of Climatology* 34:1111–31.
- Guattari, C., L. Evangelisti, and C.A. Balaras. 2018. On the assessment of urban heat island phenomenon and its effects on building energy performance: A case study of Rome (Italy). *Energy and Buildings* 158:605–15.
- Krayenhoff, E.S., J.L. Santiago, A. Martilli, A. Christen, and T.R. Oke. 2015. Parameterization of drag and turbulence for urban neighborhoods with trees. *Boundary-Layer Meteorology* 156:157–89.
- Kusaka, H., H. Kondo, Y. Kinogawa, and F. Kimura. 2001. A simple single-layer urban canopy model for atmospheric models: Comparison with multi-layer and slab models. *Boundary-Layer Meteorology* 101:329–58.
- Kuttler, W., A.-B. Barlag, and F. Roßmann. 1996. Study of the thermal structure of a town in a narrow valley. *Atmospheric Environment* 30:365–78.
- Laiti, L., D. Zardi, M. de Franceschi, and G. Rampanelli. 2013. Atmospheric boundary layer structures associated with the Ora del Garda wind in the Alps as revealed from airborne and surface measurements. *Atmospheric Research* 132–133:473–89.
- Laiti, L., D. Zardi, M. de Franceschi, G. Rampanelli, and L. Giovannini. 2014. Analysis of the diurnal development of a lake-valley circulation in the Alps based on airborne and surface measurements. *Atmospheric Chemistry and Physics* 14:9771–86.
- Martilli, A., A. Clappier, and M.W. Rotach. 2002. An urban surface exchange parameterization for mesoscale models. *Boundary-Layer Meteorology* 104:261–304.
- Miao, S., F. Chen, M.A. LeMone, M. Tewari, Q. Li, and Y. Wang. 2009. An observational and modeling study of characteristics of urban heat island and boundary layer structures in Beijing. *Journal of Applied Meteorology and Climatology* 48:484–501.
- Mirzaei, P.A. 2015. Recent challenges in modeling of urban heat island. *Sustainable Cities and Society* 19:200–6.
- Oke, T.R. 1987. *Boundary Layer Climates*. 2nd Ed. London: Routledge.
- Papangelis, G., M. Tombrou, A. Dandou, and T. Kontos. 2012. An urban green planning approach utilizing the Weather Research and Forecasting (WRF) modeling system. A case study of Athens, Greece. *Landscape Urban Planning* 105:174–83.
- Perez, R.R., P. Ineichen, and E.L. Maxwell. 1992. Dynamic global-to-direct irradiance conversion models. *ASHRAE Transactions* 98(1):354–69.
- Piringer, M., and K. Baumann. 1999. Modifications of a valley wind system by an urban area—Experimental results. *Meteorology and Atmospheric Physics* 71:117–25.
- Rotach, M., and D. Zardi. 2007. On the boundary layer structure over highly complex terrain: key findings from MAP. *Quarterly Journal of the Royal Meteorological Society* 133:937–48.
- Salamanca, F., and A. Martilli. 2010. A new building energy model coupled with an urban canopy parameterization for urban climate simulations—Part II. Validation with one dimension off-line simulations. *Theoretical and Applied Climatology* 99: 345–56.
- Salamanca, F., A. Martilli, M. Tewari, and F. Chen. 2011. A study of the urban boundary layer using different urban parameterizations and high-resolution urban canopy parameters in WRF. *Journal of Applied Meteorology and Climatology* 50:1107–28.
- Salvati, A., H. Couch Rouna, and C. Cecere. 2017. Assessing the urban heat island and its energy impact on residential buildings in Mediterranean climate: Barcelona case study. *Energy and Buildings* 146:38–54.
- Santamouris, M. 2007. Heat island research in Europe—the state of the art. *Advances in Building Energy Research (ABER)* 1: 123–150.
- Santamouris, M., C. Cartalis, A. Synnefa, and D. Kolokotsa. 2015. On the impact of urban heat island and global warming on the power demand and electricity consumption of buildings – A review. *Energy and Buildings* 98:119–24.
- Skamarock, W.C., J.B. Klemp, J. Dudhia, D.O. Gill, D.M. Barker, M. Duda, X.-Y. Huang, W. Wang, and J.G. Powers. 2008. NCAR Technical Note 2016. A description of the Advanced Research WRF version 3. *NCAR Technical Note*. TN-475+STR, 125.
- Solar Energy Laboratory. 2012. TRNSYS 17, TRNSYS. A transient system simulation program. <http://sel.me.wisc.edu/trnsys>.
- Solazzo, E., S. Di Sabatino, N. Aquilina, A. Dudek, and R. Britter. 2010. Coupling mesoscale modelling with a simple urban model: The Lisbon case study. *Boundary-Layer Meteorology* 137: 441–57.
- Stewart, I.D., and T.R. Oke. 2012. Local climate zones for urban temperature studies. *Bulletin of the American Meteorological Society* 93:1879–900.
- UNI. 2014a. *Technical Report UNI/TR 11552 Opaque Envelope Components of Buildings. Thermo-physical Parameters*. Rome: UNI.
- UNI. 2014b. *UNI/TS 11300-1, Energy Performance of Buildings Part 1: Evaluation of Energy Need for Space Heating and Cooling*. Rome: UNI.
- Wang, X., F. Chen, Z. Wu, M. Zhang, M. Tewari, A. Guenther, and C. Wiedinmyer. 2009. Impacts of weather conditions modified by urban expansion on surface ozone: Comparison between the Pearl River Delta and Yangtze River Delta regions. *Advances in Atmospheric Science* 26:962–72.

Sensitivity of WRF/Urban simulations to urban morphology parameters: a case study in the city of Bolzano

Gianluca Pappaccogli – Faculty of Science and Technology, Free University of Bozen-Bolzano – gianluca.pappaccogli@natec.unibz.it

Lorenzo Giovannini – Atmospheric Physics Group – Department of Civil, Environmental and Mechanical Engineering – University of Trento, Trento, Italy – lorenzo.giovannini@unitn.it

Francesca Cappelletti – Department of Design and Planning in Complex Environments, University IUAV of Venezia, Venezia, Italy – francesca.cappelletti@iuav.it

Dino Zardi – Atmospheric Physics Group – Department of Civil, Environmental and Mechanical Engineering – University of Trento, Trento, Italy – dino.zardi@unitn.it

Abstract

The recent progress in numerical weather prediction modelling, and in particular the possibility to reach increasingly finer spatial resolutions, allowed researchers to reproduce building-atmosphere interactions in a more accurate and realistic way, especially in urban areas.

The present work aims at evaluating the impact of high-resolution gridded datasets of urban morphology parameters on the results of numerical simulations of atmospheric processes performed with the WRF/Urban suite in the city of Bolzano (Italy), and to analyze how they affect near-ground temperature fields.

A sensitivity test was carried out combining the WRF model with the Building Effect Parameterization (BEP) scheme to simulate two typical clear-sky summer days, respectively with and without the input gridded data of urban morphology. The structure and the morphology of the city of Bolzano were carefully reproduced through several fine-scale morphometric parameters from surface and terrain models (0.5 m resolution).

The results highlight that urban morphological parameters display a high spatial variability, moderately affecting the distribution of the temperature field near the ground.

High-resolution meteorological fields inside urban areas can be a valuable information for building energy simulations. Accordingly, a scheme of model chain coupling WRF and TRNSYS codes is proposed, in order to enhance the future assessment of urbanization effects and in the same way to provide more realistic and accurate building energy simulations.

1. Introduction

In densely urbanised areas, buildings are among the most important factors controlling energy, mass and momentum exchanges between the earth surface and the atmosphere. This interaction has close influence on the Urban Heat Island (UHI) phenomenon, which consists in a significant increase of air temperature in the city center compared to the surrounding areas. Nowadays, recent progress in numerical weather prediction modelling, along with increasing availability of high-power computational resources, allow for reaching much higher spatial resolutions, even in operational model runs for routine weather forecasting. Accordingly, a more detailed parameterisation of these processes can be included, reproducing building-atmosphere interactions in a more precise and realistic way, especially in urban areas. Numerical models involve different spatial scales. In particular, two main models can be distinguished: mesoscale models (representing the atmospheric structures and working at horizontal resolutions of 1-10 km) and microscale models (e. g. Computational Fluid-Dynamics (CFD) models, Building Energy Simulations, working at much finer resolutions). Focusing on urban areas, microscale models require detailed information about buildings

structure, while meso-scale models need a parameterization of averaged urban morphology features. In this context, mesoscale meteorological models, estimating the mean thermal and dynamical effects of the cities on the atmosphere, have been increasingly applied to urban areas (Salamanca et al., 2011). Indeed, implementing urban schemes with detailed urban morphological parameters can provide better tools for evaluating the urban morphology impacts on urban microclimate and surrounding buildings. For this reason, the National Urban Database and Access Portal Tool (NUDAPT) was designed to provide gridded datasets of urban canopy parameters for 44 US cities. Many recent studies highlighted the importance of using fine-resolution input datasets of urban morphology parameters to keep pace with the increasingly high resolution of operational model runs, in order to improve the accuracy of the results (Solazzo et al., 2010; Salamanca et al., 2011, Giovannini et al., 2014). The Weather Research and Forecasting (WRF) model can be coupled either with a single-layer urban canopy model (Kusaka et al. 2001) or with a multi-layer canopy model (Martilli et al. 2002), providing a valuable approach to represent the heterogeneities of urban morphology, considering three different urban surfaces (walls, roofs, and roads) and infinitely long street canyons (cf. Giovannini et al. 2013). Moreover, the BEP scheme can be coupled with a simple Building Energy Model (BEP+BEM), which provides a multilayer urban parameterization that accounts the exchanges of energy between building and atmosphere (Salamanca and Martilli, 2010). The embedded building energy module estimates the heat diffusion through building envelope and the radiation exchange between indoor surfaces, the heat generation of occupants and equipment, the energy consumption of air conditioning systems and natural ventilation.

The present work adopts the most advanced urban parameterization scheme coupled with the WRF model, i. e. the Building Effect Parameterization (BEP) (Martilli et al., 2002), in order to evaluate climatic conditions in the city of Bolzano. The city is located in the north-eastern Italian Alps, in a basin where three valleys join (Fig. 1). Climatic conditions in the city are tightly connected with the

complex topography of the surrounding area that influences in particular the flow field, mainly characterized by daily-periodic up- and down-valley winds from tributary valleys, especially in the warm season. Many studies investigated the interaction between urban area and these phenomena, emphasizing the important influence of local winds on urban environment (Kuttler et al., 1996, Piringer, M., and K. Baumann, 1999, Giovannini et al., 2011).

The objective of the present work is to develop a complete dataset of fine-scale urban canopy parameters (UCPs) in Bolzano, in order to assess their impact in WRF-urban canopy models. This methodology, besides providing an accurate description of the temperature field in the urban area, can be used also to evaluate the effects of particular urban heat island mitigation strategies, or to assess the energy consumption in buildings.

This work is organized as follows. The datasets and the methodologies used to obtain urban canopy parameters are described in detail in section 2. Section 3 describes the results of sensitivity tests performed by means of the WRF/urban scheme. Finally, Section 4 presents some conclusions and the proposal of a model chain including mesoscale model (nested WRF-urban from 10.8 to 0.4 km resolution) and the well-known building energy simulation code TRNSYS.

2. Input datasets and modelling set-up

2.1 Input datasets - UCPs

As reported in the study of Giovannini et al. (2014), high-resolution meteorological simulations in complex terrain require a high-resolution topography dataset. For this reason, here the topography data obtained from the Viewfinder Panoramas (original horizontal spatial resolution ~30 m) were used. Fig. 1 (right) shows the topography of the inner domain, highlighting the urban area of Bolzano. The dataset Corine was used for the land cover parameters, reclassifying the 44 Corine categories into the 20 (+3 special classes for urban land use) Modis categories, in order to fit the WRF look-up tables.

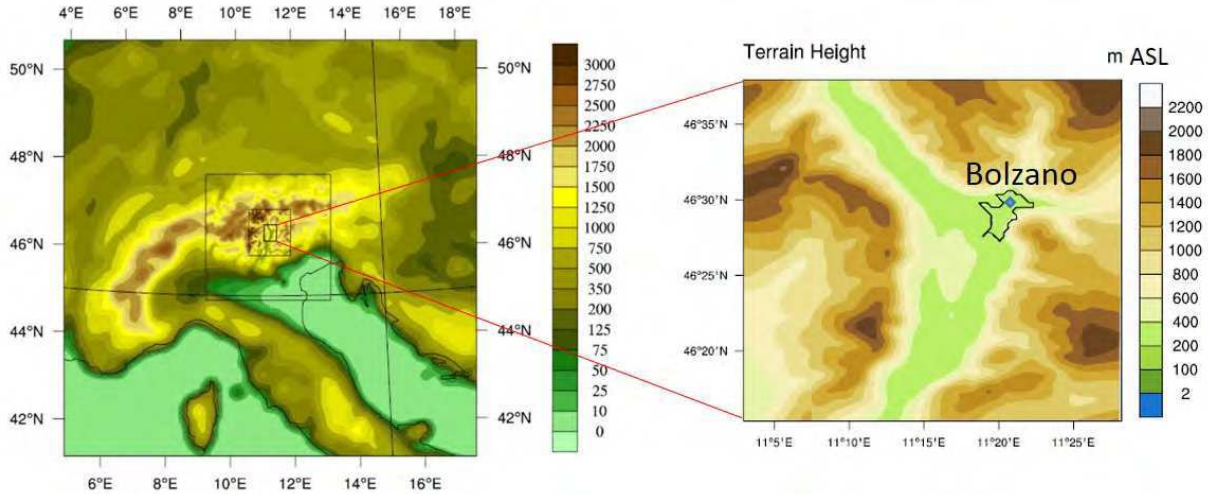


Fig. 1 The four nested domains used for the numerical simulations (left). The zoomed-in area (right) represents the inner domain and the black line contours the urban area of the city of Bolzano.

The land cover dataset is shown in Fig. 2. As the goal of this research concerns the urban environment, detailed maps of urban morphology were developed. Using digital surface and terrain models (0.5 m resolution) from the GeoCatalogo of the Autonomous Province of Bolzano (<http://geocatalogo.retecivica.bz.it/geokatalog>), fine resolution maps of urban morphology parameters were calculated by means of the QGIS + Urban Multi-scale Environmental Predictor (UMEP) and Matlab© software. Collected data and maps were processed, in order to obtain gridded urban canopy parameters (UCPs) with a horizontal spatial resolution of 100 m, which were directly used as input for the BEP scheme. The structure of the city of Bolzano was carefully reproduced using a set of seven morphometric parameters: the average and standard deviation height of the buildings named respectively h_m and h_s , the building plan area fraction $\lambda_p = A_p/A_{tot}$ (where A_p is the plan area of buildings and A_{tot} is the total area of the cell) and plan-area-weighted mean building height $h_{aw} = (A_p * h_m)/A_p$; the building envelope area to plan area ratio $\lambda_b = (A_p + A_w)/A_{tot}$ (where A_w is the wall surface area); the frontal area index $\lambda_f = A_{proj}/A_{tot}$ (where A_{proj} is the total area of buildings projected into the plane normal to the approaching wind direction at 0°-45°-90°-135°), the urban fraction λ_u (percentage of the cell covered by urban land use). Finally, the distribution of buildings heights h_i

(corresponding to the plan area fraction of buildings every five meters in each computational cell) at 5 m vertical intervals was calculated on fifteen vertical urban levels. The methodology used to calculate the main urban morphological parameters is reported in Burian et al. (2008). Fig. 3 shows respectively the distribution of λ_p (a), λ_b (b), h_m (c) and λ_u (d), on 100 m grid resolution. The same parameters have been used as input for the BEP scheme in the WRF model, averaging those previously calculated in order to adapt them to the 400 m WRF resolution. Results are shown in Fig. 4. Figs. 3 and 4a, 4b, and 4c highlight, as expected, that the highest values of these urban morphology parameters are mainly located in the central part of the city, which is characterized by typical South Tyrol architectural design, consisting of 4-5-storey historic buildings flanking narrow (often arcaded) street canyons. In particular, the highest values of λ_p and λ_b occur in this area, underlining the high density urban area. Furthermore, high values occur also in the south area of the city, corresponding to the industrial and commercial areas, and in the northwestern part of the residential area, where high residential buildings are present (Fig. 4c). Finally, in order to check the consistency of gridded morphology data, they were overlaid on Google Earth maps.

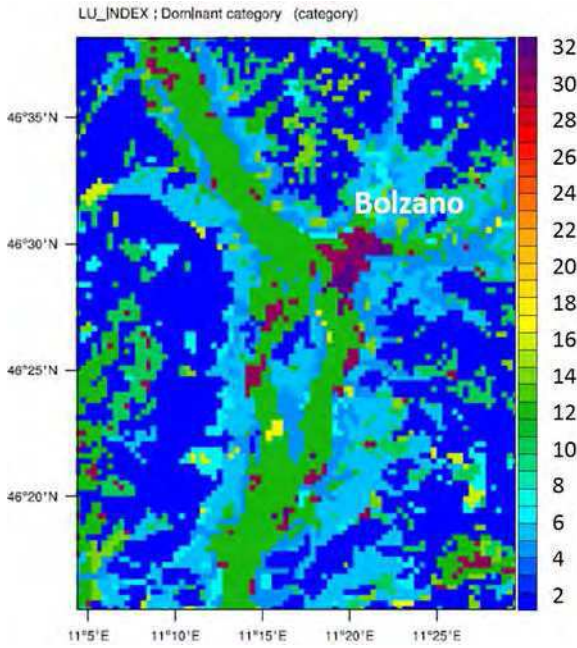


Fig. 2 – Modis land use categories in the inner model domain. Categories 31-33 indicate urban land use, namely 31: Low intensity residential, 32: High intensity residential, 33: Industrial or commercial.

2.2 WRF numerical simulation

In order to assess the impact of urban canopy parameters on WRF simulation output, the non-hydrostatic version of the WRF model (version 3.8) coupled with Building Effect Parameterization BEP scheme (Martilli et al., 2002) was used (Skamarock et al., 2016). The 54-h WRF-urban simulations start at 1800 UTC (LST=UTC+1 h) 19 July 2015 and end at 0000 UTC 21 July 2015. Simulations were carried out using four two-way nested domains (nesting ratio=3) with the grid resolution for the inner domain of 400m×400m (Fig.1 and Table 1 show details about domains dimension and resolution). Initial and boundary conditions derive from National Center for Environmental Prediction (NCEP), in which meteorological data have 1-deg grid resolution (about 120 km) and 6 h time resolution. 30 eta levels (terrain-following hydrostatic-pressure vertical coordinate) are used in the vertical. The simulations were run with the Bougeault and Lacarrère (1989) scheme for the Planetary Boundary Layer (PBL) parameterization, while the Noah land surface model (Chen and Dudhia, 2001) for the land surface processes parameterization.

Table 1 – Details of resolution of nested WRF domains.

Domain	n.points_we	n.points_sn	dx(m)	dy(m)
d01	100	100	10800	110800
d02	91	91	3600	3600
d03	91	100	1200	1200
d04	82	106	400	400

3. Sensitivity test

In order to analyze in detail the impacts of the gridded datasets of urban morphology parameters, sensitivity simulations were performed with and without these input data. The simulation considering urban morphology parameters is referred to as BEP_PAR, while the one using only standard input for the BEP scheme (i.e. without the gridded datasets of urban morphology) is referred to as BEP_NOPAR. In this case, since the grid data of urban morphology are absent, the three urban classes describe the urban settlements (Fig. 2), i.e. the ancient and high-intensity residential class (class number 31), the recent high- or low-intensity residential class (class number 32), and the industrial and commercial class (class number 33), from which the urban scheme looks up the morphology parameters.

The simulation results show that the strongest temperature differences between the two simulations occur in the central part of the city, where the influence of the morphology parameters on the performance of the urban scheme is higher. At night temperatures are slightly higher (~0.5-1°C) in BEP_PAR than in BEP_NOPAR, especially in the central part of the urban area, while in the central hours of the day the opposite occurs, mainly in the downtown area, which is characterized by densely packed buildings and narrow street canyons.

These results (obtained from BEP_PAR) are in reasonable agreement with observations performed in Trento (Giovannini et al., 2011), showing a quite strong nocturnal urban heat island (UHI), especially under low wind speed and clear sky conditions, whereas an urban cool island is likely to develop in the morning.

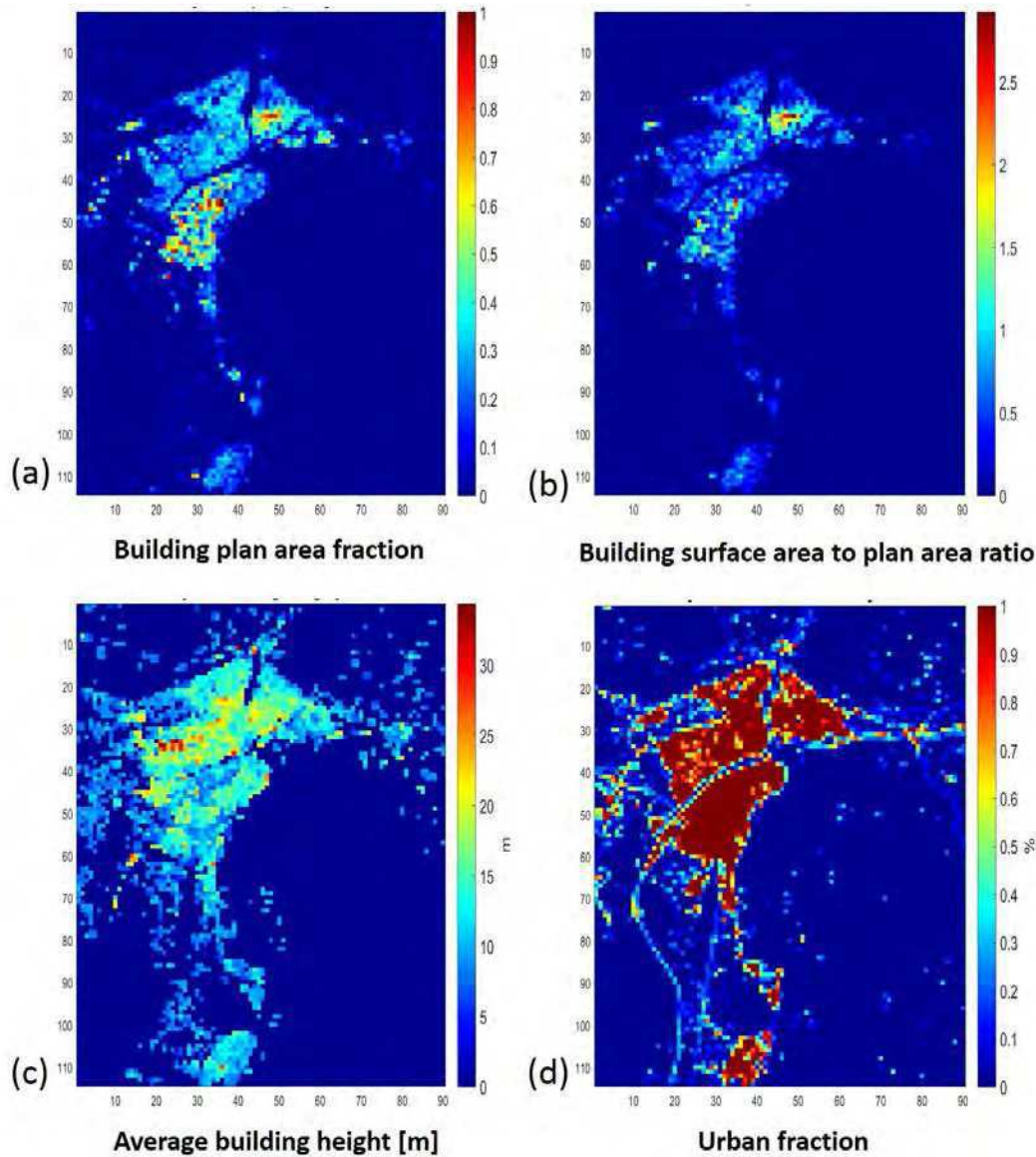


Fig. 3 - Urban morphology parameters calculated by means of MATLAB-QGIS software from digital surfaces and terrain model for urban area of Bolzano (fine resolution-100 m). (a) Building plan area fraction λ_p , (b) building surface area to plan area ratio λ_b , (c) average building height h_m , (d) urban fraction λ_u .

Focusing on Fig. 5a, referring to nighttime (2315 UTC), the highest differences occur in the central part of the urban area, in accord with the average values of the UCPs used in BEP_PAR, which, unlike the default urban classes, capture well the detail of the denser morphology and greater height of the buildings in that area. On the contrary, negative differences occur during daytime (Fig. 5b), especially in the morning, due to the density of urbanization which prevents solar radiation to penetrate inside narrow street canyons. However,

this difference decreases until the central hours of the day, when the temperature differences between the two schemes are less than 0.5°C. Summing up, as can be seen in Fig. 5a,b, areas with low positive and negative differences are present throughout the urban area, depending closely on the local values of the gridded morphology parameters. The maximum differences between the two simulations (i.e. BEP_PAR-BEP_NOPAR) are more than 1°C, both during day and night, when negative and positive differences occur respectively.

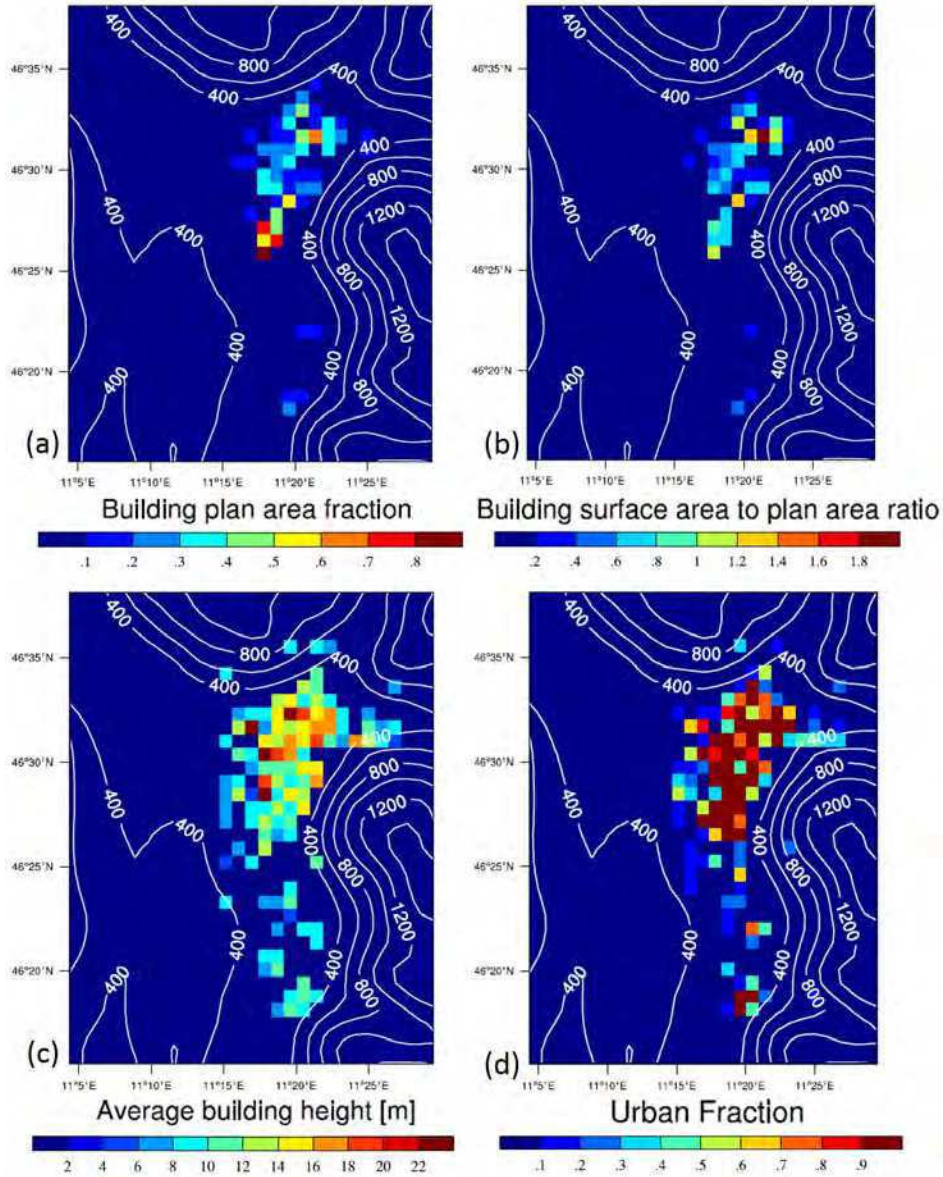


Fig. 4 - Urban morphology parameters averaging the finer-resolution ones previously calculated in Fig.3 and used in BEP scheme.

(a) Building plan area fraction λ_p , (b) building surface area to plan area ratio λ_b , (c) average building height h_m , (d) urban fraction λ_u . Detailed explanation of the parameters are in Section 2.1. Height contours are in above sea level (ASL).

4. Discussion and conclusion

The WRF/BEP coupled model was applied, with and without urban morphology parameters, to simulate atmospheric processes in the city of Bolzano during the hottest days in the summer 2015. A sensitivity test was performed to assess the impact of the gridded datasets of urban morphology in the BEP scheme. Results show that the detailed urban parameters influence significantly the spatial and temporal variability of

the urban temperatures throughout the day. In particular, the BEP_PAR simulation shows higher temperature than BEP_NOPAR in the historical city center already in the first nocturnal hours. On the contrary, temperature in the downtown tends to remain lower in BEP_PAR than in BEP_NOPAR throughout the morning ($\sim 1^\circ\text{C}$), due to a cool island effect.

Further analyses are ongoing in order to investigate the model sensitivity, with respect to fluxes and other micrometeorological variables. Based on the results of this paper, on the ongoing

research activities, and on the continuous improvement of numerical capabilities at all scales, modelling building elements in more details seems the further effort in order to represent in more accurate way the interaction between buildings and the urban atmosphere. To this regard there are some issues to overcome. On one hand resolution typically used in mesoscale model simulations is not enough to provide details about the single building in the urban context. On the other hand, building energy simulations (BES) often focus on the single building without considering the urban context and the surrounding buildings effect on radiative and convective surface exchanges on the external envelope. Furthermore, providing proper initial conditions for these models remains a difficult task, as they are usually derived from observations (mostly taken within rural environment) limited at a single-point, which negatively affect model reliability. These criticalities pose a challenge on coupling these models with mesoscale models, especially when the impact of urbanization effects (UHI) on building energy performance is investigated.

In this context, WRF/Urban output can provide information that are not typically available from conventional climate data, e.g. Typical Meteorological Year, leading to a more robust source (spatially averaged) for initial conditions as compared to local observations. The possible advantages arising from use of WRF/Urban output in building energy simulation may be shortly recalled in the following list:

- 1) a better knowledge of micrometeorological conditions representative of specific urban areas free from potential bias due to instrument location;
- 2) a more precise evaluation of temperatures on impervious urban surfaces, upper soil layers and overlying urban canopy layers;
- 3) a better prediction of future scenarios assessing the feedback between buildings and surrounding microclimate which are directly affected by climate change mitigation strategies (e.g. green roof, trees and vegetation).

A challenging opportunity that may be pursued in future developments of this research is the coupling of WRF/Urban with models dynamically reproducing building energetics (e.g. TRNSYS).

Table 2 Principal features of the simulations in this paper.

Schemes	BEP_PAR	BEP_NOPAR
Urban land use	Yes	Yes
Urban scheme	BEP	BEP
Gridded dataset of urban morphology	Yes	No

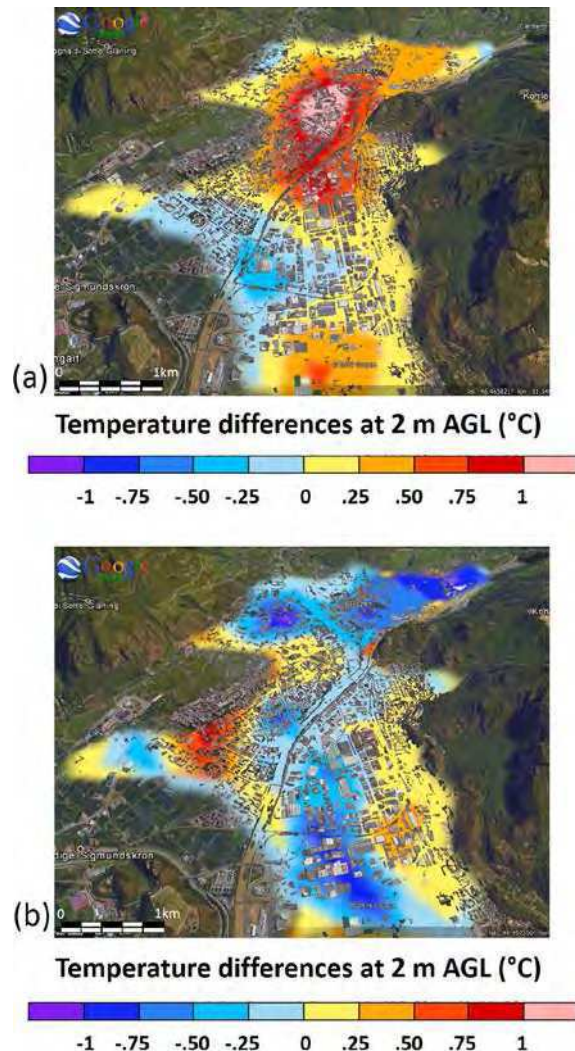


Fig. 5 - Temperature differences at 2 m AGL in the urban area of Bolzano at (a) 2315-nighttime, (b) 1200-daytime UTC respectively 19 and 20 July 2015.

5. Acknowledgement

The first author thanks the Faculty of Science and Technology of the Free University of Bolzano, and in particular the PhD Program in Sustainable Energy and Technologies, for supporting his research project.

References

- Bougeault, P. and Lacarrère, P. 1989. "Parameterization of orography-induced turbulence in a mesobeta-scale model." *Monthly Weather Review* 117: 1827-1890.
- Burian, S., Augustus, N., Jeyachandran, I., Brown, M.J. 2008. "Final Report for the National Building Statistics Database, Version 2."
- Chen, F., Dudhia, J. 2001. "Coupling an advances land surface-hydrology model with the Penn State-NCAR MM5 modeling system. Part I: model implementation and sensitivity." *Monthly Weather Review* 129: 569-585.
- Giovannini, L., Zardi, D., de Franceschi, M. 2011. "Analysis of the urban thermal fingerprint of the city of Trento in the Alps." *Journal of Applied Meteorology and Climatology* 50: 1145-1162.
- Giovannini, L., Zardi, D., de Franceschi, M., 2013. "Characterization of the Thermal Structure inside an Urban Canyon: Field Measurements and Validation of a Simple Model." *Journal of Applied Meteorology and Climatology* 52: 64-81.
- Giovannini, L., Zardi, D., de Franceschi, M., and Chen, F., 2014. "Numerical simulations of boundary-layer processes and urban-induced alterations in an Alpine valley." *International Journal of Climatology* 34: 1111-1131.
- Kusaka, H., Kondo, H., Kinogawa, Y., F. Kimura, 2001. "A simple single-layer urban canopy model for atmospheric models: comparison with multi-layer and slab models." *Boundary-Layer Meteorology* 101: 329-358.
- Kuttler, W., A.-B. Barlag, and F. Roßmann, 1996. "Study of the thermal structure of a town in a narrow valley." *Atmos. Environ.* 30: 365-378.
- Martilli, A., Clappier, A., Rotach, M.W. 2002. "An urban surface exchange parameterization for mesoscale models." *Boundary-Layer Meteorology* 104: 261-304.
- Piringer, M., and K. Baumann, 1999. "Modifications of a valley wind system by an urban area—Experimental results." *Meteor. Atmos. Phys.* 71: 117-125.
- Salamanca, F., and A. Martilli, 2010. "A new building energy model coupled with an urban canopy parameterization for urban climate simulations—Part II. Validation with one dimension off-line simulations". *Theor. Appl. Climatol.*, 99, 345-356.
- Salamanca, F., Martilli, A., Tewari, M., Chen, F. 2011. "A study of the urban boundary layer using different urban parameterizations and high-resolution urban canopy parameters in WRF". *Journal of Applied Meteorology and Climatology* 50: 1107-1128.
- Skamarock, W.C., Klemp, J.B., Dudhia, J., Gill, D.O., Barker, D.M., Duda, M., Huang, X.-Y., Wang, W., and Powers, J.G. 2016. "NCAR Technical Note 2016. A description of the Advanced Research WRF version 3." NCAR Technical Note TN-475+STR, 125.
- Solazzo, E., Di Sabatino, S., Aquilina, N., Dudek, A., Britter, R. 2010. "Coupling mesoscale modelling with a simple urban model: the Lisbon case study." *Boundary-Layer Meteorology* 137: 441-457.

The effects of trees on micrometeorology in a real street canyon: consequences for local air quality

Silvana Di Sabatino*

Department of Physics and Astronomy,
University of Bologna,
Viale Berti Pichat 6/2, 40127, Bologna, Italy
Email: silvana.disabatino@unibo.it

*Corresponding author

Riccardo Buccolieri and Gianluca Pappaccogli

Dipartimento di Scienze e Tecnologie Biologiche ed Ambientali,
University of Salento,
S.P. 6 Lecce-Monteroni,
73100 Lecce, Italy
Email: riccardo.buccolieri@unisalento.it
Email: gianluca.pappaccogli@yahoo.it

Laura S. Leo

Department of Civil and Environmental Engineering and
Earth Sciences,
Environmental Fluid Dynamics Laboratories,
University of Notre Dame,
Notre Dame, IN 46556, USA
Email: lleo1@nd.edu

Abstract: This study analyses the effects of trees on local meteorology of a Mediterranean City (Lecce, IT) using field measurements and computational fluid dynamics simulations. Measurements were collected for 51 days in a street canyon with trees to cover different meteorological and foliage conditions. Building façades and ground temperatures were estimated from infrared images, flow and turbulence measured by ultrasonic anemometers. In the case of approaching wind parallel to the street axis, trees induce large wind direction fluctuations below tree crowns and velocities up to about 80% lower than those at roof top. This, combined with the obstruction by tree crown, lead to lower ventilation in the bottom part of the street, especially during nocturnal hours, and to in-canyon volume-averaged pollutant concentration about 20% larger than in the tree-free case. Ignoring trapping effects of trees, as typically done in many air quality models, may lead to underestimation of ground level concentrations.

Keywords: urban temperature; flow and turbulence; pollutant concentration; trees; computational fluid dynamics; CFD.

Reference to this paper should be made as follows: Di Sabatino, S., Buccolieri, R., Pappacogli, G. and Leo, L.S. (2015) ‘The effects of trees on micrometeorology in a real street canyon: consequences for local air quality’, *Int. J. Environment and Pollution*, Vol. 58, Nos. 1/2, pp.100–111.

Biographical notes: Silvana Di Sabatino is an Associate Professor of Atmospheric Physics at University of Bologna, where she teaches Boundary-layer Physics and Turbulent Dispersion, Dynamic Meteorology, and Climatology. She holds a PhD from the University of Cambridge, UK in the area of environmental fluid mechanics. Her current research relates to urban microclimate and its links with climate variability, city breathability and its connections with urban planning. Among her research interests there is the development of tools to bridge basic research with applied science closely related to respond to the needs of modern society. She has co-authored more than 100 scientific publications of which over 50 in peer review journals, and several book chapters.

Riccardo Buccolieri is a Post-Doctoral researcher at the University of Salento in the Micrometeorology Laboratory. His research, both experimental and modelling, deals with the study of the urban microclimate, flow and pollutant dispersion in urban areas. He is co-author of research papers in international journals, conference proceedings as well as book chapters.

Gianluca Pappacogli is a PhD student in Sustainable Energy and Technologies at the Free University of Bozen. His research is devoted to understand how urban vegetation affects temperature, ventilation and air quality condition in street canyon. He is the co-author of three conference proceedings.

Laura S. Leo is a Research Assistant Professor in the Department of Civil and Environmental Engineering and Earth Sciences at the University of Notre Dame, IN, USA. Her research focuses on urban meteorology and atmospheric circulation in complex terrain and boundary layer data analysis from field experiments. She has published peer-reviewed manuscripts, primarily in the fields of urban and mountain meteorology, which include international journals, conference proceedings as well as book chapters.

This paper is a revised and expanded version of a paper entitled ‘On thermal stratification in real street canyons with trees: consequences for local air quality’ presented at the 16th International Conference on Harmonisation within Atmospheric Dispersion Modelling for Regulatory Purposes, Varna, Bulgaria, 8–11 September 2014.

1 Introduction

The maintenance and expansion of tree cover in urban areas has been widely recognised as a key preventive measure to mitigate the urban heat island phenomenon (Desplat et al., 2009). At the street and pedestrian scales, however, the ability of trees to provide thermal comfort by evaporative cooling and shading must be set off against its obstacle-effect to the wind, which leads to larger concentration than in the tree-free counterpart. Recent experimental and numerical studies (e.g., Gromke et al., 2008; Shashua et al., 2011; Janhäll, 2015) pointed out that the presence of trees along a street canyon can affect significantly the flow patterns and turbulent diffusion of pollutants therein. Nevertheless,

the actual quantification of such perturbations depends on the synergic effect played by the specific meteorological conditions, street canyon geometry and vegetation configuration.

In this context, effects of trees on flow and pollutant dispersion in a street canyon located in a Mediterranean City (Lecce) in south Italy are investigated here by using results from a field experiment and their interpretation assisted by computational fluid dynamics (CFD) modelling. Data were collected in a straight street canyon with deciduous trees. In order to quantify the role of trees on in-canyon air temperature, wind and pollutant dispersion, the study period includes observations prior to and after to leaf-out of trees. Building façades and ground temperatures were inferred from infrared (IR) images, while flow and turbulence were measured through ultrasonic anemometers.

Pollutant concentration patterns were analysed by simulating real conditions with and without trees (e.g., Buccolieri et al., 2009).

2 Site description

The street canyon analysed here (Redipuglia St.) is located in Lecce, a medium-size city of south Italy characterised by a Mediterranean climate and a classical Mediterranean architectural design, consisting of two to three storey buildings and narrow street canyons [Figure 1(a)]. The street canyon is on the western side of the city where buildings, despite the different heights, are distributed in a rather regular pattern [Figure 1(b)].

Figure 1 (a) Position of Lecce City in south-east Italy (b) Street neighbourhood analysed (base maps from Google Earth) (c) 3D view of Redipuglia St. with position of three GILL R3-50 sonic anemometers (green polyline) (see online version for colours)



Redipuglia St. is 100 m long and 12 m wide, running north-south, with buildings heights ranging from 13 m to 21 m [Figure 1(c)], with aspect ratio H/W (where

$H = H_{avg} = 15$ m is the average building height and $W = 12$ m is the width of the street) equal to 1.2. The street canyon is characterised by the presence of 36 deciduous trees (*Tilia Cordata* Mill.) located along both sides of the street of which 22 are along the left side and 14 along the right side. The spacing between tree trunks is approximately 4 m, so that there is a leaf crown interference. The average height of the branch-free trunk is about 5 m and the crown extends to about 8 m.

3 Measurements and numerical simulations

Flow and air temperature measurements were carried out continuously in the period 11 October–7 December 2013 (Main Campaign hereinafter). The Main Campaign included three intense measurements periods where leaf area index (LAI, m^2m^{-2}) measurements, thermal imaging measurements of building façades, air temperature and relative humidity measurements were also conducted; specifically from noon to noon of 11–12 October (Campaign 1 hereinafter), 8–9 November (Campaign 2 hereinafter) and 6–7 December 2013 (Campaign 3 hereinafter). The intense campaigns were devoted to the investigation of the influence of trees on temperature of building façades and in-canyon air to delve into the trapping mechanism of heat during a whole day under several LAI and solar radiation inclination conditions.

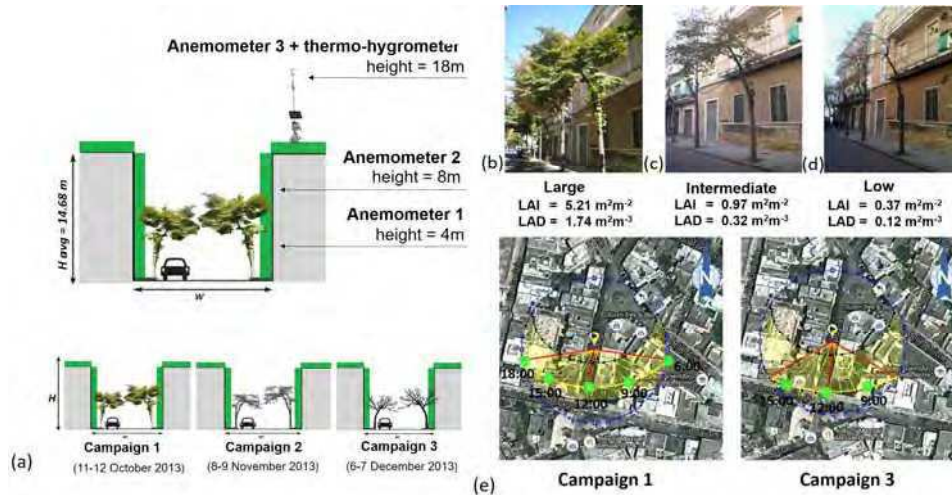
3.1 Flow and turbulence measurements

The three components of wind velocity and virtual temperature were measured at the acquisition sampling frequency of 50 Hz by three GILL R3-50 sonic anemometers [Figure 2(a)] positioned at three different heights. Two anemometers were positioned inside the street canyon: the first (Anemometer 1) was just below the tree crown at $z = 4.5$ m a.g.l. (above ground level) and the second (Anemometer 2) was just above the tree crown at $z = 8.5$ m a.g.l. The third anemometer (Anemometer 3), together with a Vaisala HMP45C thermo-hygrometer, was positioned at the roof of the same building at 18 m a.g.l. 10 min averages of wind direction and wind speed and 5 min averages of turbulent fluxes were calculated using the three-rotation method by McMillen (1988).

3.2 LAI measurements

LAI of *Tilia Cordata* tree crowns was estimated from measurements of the photo-synthetically active radiation (PAR) acquired by an Accu-PAR LP80 ceptometer. All measurements were taken parallel to the ground and perpendicular to the orientation of Redipuglia St. (281°). Five replicas were done at the same measurement point just near the crown (where the sensor measured unobstructed PAR) and at its base (where it was supposed that the LAI is maximum). The leaf area density (LAD, m^2m^{-3}) was thus estimated dividing LAI by the depth of tree crown (3 m) [Figure 2(b), Figure 2(c), Figure 2(d)]. We will refer to large LAI of trees for Campaign 1, intermediate LAI for Campaign 2 and low LAI (leafless trees) for Campaign 3. It should be noted that solar inclination and the daylight period are not the same for the three intense campaigns and this is taken into account in the discussion of results [Figure 2(e)].

Figure 2 (a) Cross-section of Redipuglia St. showing anemometers position during the Main Campaign and periods of the three intense campaigns. Texture of vegetation canopy during (b) Campaign 1 (c) Campaign 2 (d) Campaign 3 (e) sun path (yellow) indicating the hourly positional change of the sun during Campaign 1 and Campaign 3. Red lines indicate the sun position at sunrise, noon and sunset (see online version for colours)



3.3 Thermal imaging measurements

To evaluate temperature distribution within the street canyon, IR thermal images were taken every 3 hours during Campaigns 1, 2 and 3 through a high performance FLIR T620 ThermalCAM, with a 640×480 pixels resolution and an image acquisition frequency of 50/60 Hz. Two representative buildings in Redipuglia St. were selected based on the assumption of homogeneity in construction material and the absence of obstacles (balconies, eaves, etc.), metal or glass. Air temperature and humidity were recorded with an Extech Instruments MO297 moisture psychrometer. Air temperature was also measured every five minutes using a PT100 sensor assembled with Tinytag TGP-0073 by Gemini data loggers during the Main Campaign. The sensor was positioned at the roof of the same building where the anemometers were installed. Images were analysed using an emissivity value of 0.96 for asphalt and 0.94 for brick-limestone (building façade). These values are those recommended by FLIR (User's manual) and consistent with values proposed by Danov et al.'s (2007) study on limestone. Images were analysed using the FLIR QuickReport 1.2.

3.4 Numerical simulations

3D isothermal CFD simulations were performed by means of the general purpose code Fluent (at the Dipartimento di Ingegneria dell'Innovazione – University of Salento). The aim was to aid interpretation of field measurements by providing information about the flow structure in the vicinity of the measurements points and the influence of trees on pollutant dispersion. A preliminary analysis considered meteorological conditions recorded at 21:00 (when conditions inside the canyon could be assumed to be isothermal) during Campaign 1. The study area includes Redipuglia St. (with trees, large LAI). To

match recorded conditions, an approaching flow was taken to be equal to the mean hourly value ($U_{ref} = 2.3 \text{ m s}^{-1}$) observed at a meteorological station located outside the urban area (at $z = 20 \text{ m}$), with a wind direction equal to 140° (i.e., from south-south/east direction), corresponding to the mode of wind directions as it will be shown in Subsection 4.2. The same simulation was performed without trees (tree-free).

The Reynolds stress model (RSM) (Launder, 1989) was used. The domain was built using about one million elements, with a finer resolution within the entire built area. The smallest dimension of the elements in the x, y and z directions was 0.25 m, based on grid convergence analysis. Equilibrium profiles of wind speed, turbulent kinetic energy (TKE) and dissipation rate (ϵ) were specified at the inlet (Di Sabatino et al., 2007), with a friction velocity $u_* = 0.17 \text{ m s}^{-1}$ estimated from log-law curve fitting of the observed wind velocity at the meteorological station. Symmetry boundary condition was specified at the top, while at the downwind boundary a pressure-outlet condition was used. The aerodynamic characteristics of trees were modelled adding a momentum sink in the governing momentum equations, where the inertial term is parameterised using a pressure loss coefficient $\lambda = 0.35 \text{ m}^{-1}$ (Gromke et al., 2008) estimated through $C_d \times LAD$, where C_d is the leaf drag coefficient taken equal to 0.2 (Gromke and Blocken, 2015). A ground-level line source was modelled along the southern part of Redipuglia St. (that bounded by the buildings at both sides) and the advection-diffusion module was used to calculate pollutant concentration. As an example, a CO emission rate $Q = 10 \text{ g s}^{-1}$ was assumed.

4 Results

4.1 Effects of trees on temperature

Figure 3 shows profiles of ‘In-canyon Temp. – Roof-Air Temp.’ during the three intense campaigns, where In-canyon Temp. is the surface (façades or ground) or in-canyon air temperature, and Roof-Air Temp. is the air temperature recorded above roof level (i.e., at Anemometer 3 position). Façades of buildings exposed to east are denoted with E and those exposed to west are denoted with W. For example, the profile named BW in Figure 3 indicates the temperature at the bottom (B) of the building façade exposed to west (W).

Figure 3 shows that the effect of trees during Campaign 1 (large LAI) and Campaign 2 (intermediate LAI) was to lower air and ground temperatures during daytime with respect to the leafless case in Campaign 3 (low LAI), during which there were similar roof-air and ground temperatures. This is attributable to both evapotranspiration and trees shadowing thus preventing the asphalt to get lit by direct solar radiation [as also shown in Figure 4(a), Figure 4(b)]. This temperature decrease is emphasised by the change of the sun path with respect to the street, e.g., during Campaign 1 at noon sun’s ray were approximately parallel to the street axis, while during Campaign 3 sun’s rays were slightly inclined towards east. On the contrary, during the night the presence of trees in Campaigns 1 and 2 resulted in larger air and ground temperatures until sunrise with respect to Campaign 3, given that tree crowns reduced radiative cooling of the ground and trapped heat below the tree canopy.

Figure 3 Difference between in-canyon temperatures (of building façades, ground and air) and air temperature recorded at roof level during, (a) Campaign 1 (b) Campaign 2 (c) Campaign 3 (see online version for colours)

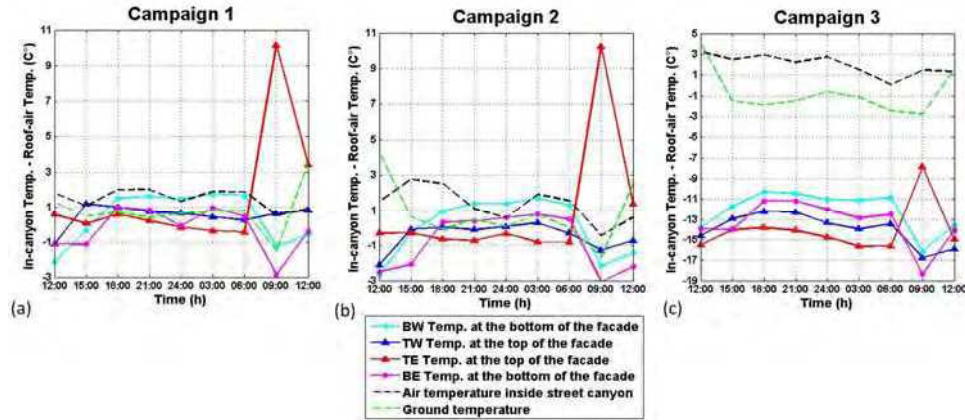
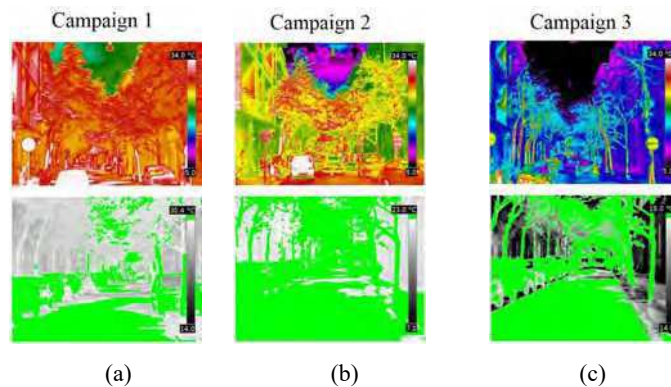


Figure 4 Example of cross-section thermal images of Redipuglia St. during, (a) Campaign 1 (b) Campaign 2 (c) Campaign 3 at noon (see online version for colours)



Notes: Images at the bottom were obtained from IR-images by applying a contrasting colour (green) to all pixels with a temperature above a threshold (taken as the air temperature recorded at roof level). These images show a decrease of shadowing (grey zone) from Campaign 1 to Campaign 3 and a different distribution of solar radiation at ground.

The analysis of temperature of building façade further highlights the influence of trees on temperature distribution within the street. Owing to the north-south orientation of the street, buildings exposed to east experienced a high mean temperature at 9am until 3pm. Surface temperature in the afternoon until sunrise was instead slightly larger in buildings exposed to west. This result confirms previous findings (e.g., Hoyano et al., 1999) that at mid latitudes in the north hemisphere surfaces directly exposed to east usually experience maximum temperature at about 9am, while surfaces exposed to west reach their maximum temperature at about 3pm. The effect of trees was clearly different at the top and bottom of the façade, being trees lower than buildings. Specifically, during Campaigns 1, 2 in daytime, the top of the façade experienced larger temperatures than the

bottom due to trees shadow [Figure 3 (a), Figure 3 (b)], while during the night the bottom became warmer than the top due to the trapping of heat by trees. As expected, during Campaign 3 [Figure 3(c), Figure 4(c)] no inversion was found in daytime being trees characterised by low LAI.

It is worth noting that façade temperatures were significantly lower than air temperatures, especially during Campaign 3. This can be attributed to several reasons. First, the in-canyon air temperature measurements were carried out at pedestrian height (1.50 m a.g.l.) and were thus affected by heat of the surfaces (especially ground) accumulated during daytime in absence of shading trees during Campaign 3. This also partially explains in-canyon air temperatures higher than those above roof level. Second, surface temperatures inferred from IR thermal images were strongly influenced by the presence of moisture, which can reach 30% especially in the oldest buildings as those investigated in the present paper. Specifically, interstitial moisture on buildings façades increases during wintertime, favoured by lower temperatures, and high precipitation, which increase the capillary constant water (Roche, 2012). From IR images one cannot isolate this effect but the result is reasonably lower surface temperatures due to evaporation cooling of the surface.

Finally, it is worth analysing differences between building façade and air temperatures, considering the difference in sun path shown in Figure 2(e). During Campaign 1 [Figure 2(c), left], sun path is intersected from 6am to 18pm, i.e., 2 hours more than in Campaign 3. The smaller incidence angle during Campaign 1 occurred during the morning on surfaces exposed to east, and in the evening on those exposed to west. This explains larger temperatures at the top of the buildings exposed to east than air temperature (up to 10°C larger), in particular at 9am. On the contrary, the larger incidence angle during Campaign 3 with respect to Campaign 1 caused a slightly smaller difference between building façade and air temperatures (7°).

4.2 Effect of trees on wind and turbulence

The analysis of high-frequency flow measurements allowed us to investigate the effects of trees on flow and turbulence within Redipuglia St. and their dependence on tree crown density. We focus on wind coming from south (in the range of wind direction 170°–225°) since it was the most prevalent wind direction during the intense campaigns. Figure 5 shows a windbreak effect in Redipuglia St. during Campaign 1 (a), Campaign 2 (b) and Campaign 3 (c). Percentage reduction of wind speed (nrU) was calculated as follows:

$$\left(1 - \frac{U_{1,2}}{U_1}\right) \times 100 = nrU_{1,2} \quad (1)$$

where U_1 is the wind speed recorded at Anemometer 1, U_2 at Anemometer 2 and U_3 at Anemometer 3. $nrU_{1,2}$ refers to the reduction of wind speed at Anemometer 1 (nrU_1) and Anemometer 2 (nrU_2).

During Campaign 1 (large LAI) an average reduction of 79% occurred just below the crown (Anemometer 1) and 59% just above the crown (Anemometer 2). During Campaigns 2 (intermediate LAI) and 3 (low LAI) the percentage reduction decreased to 44% and 39%, respectively, below the crown, and to 26% and 31%, respectively, above the crown. This indicates that the change in foliage volume strongly influence the ventilation inside the canyon.

With respect to the leafless period (Campaign 3), during Campaign 1, despite the above roof wind blew from south (i.e., almost parallel to the street canyon axis), there was no wind channelling in the street since the interaction with trees induced wind direction oscillations below crowns and this was dominant on the longitudinal component. During Campaigns 2, 3 tree's influence was smaller and the wind direction in the street was similar to that recorded above the roof (not shown here).

Figure 6 shows observed vertical profiles of TKE and momentum fluxes estimated at 15:00 and 21:00 at Anemometer 1, Anemometer 2 and Anemometer 3 during Campaigns 1 and 3. Both TKE and are normalised by calculated using data from Anemometer 3. Figure 6 also shows profiles obtained from CFD simulations (with trees) at 21:00 of Campaign 1, when the mode of wind directions was 140° (Figure 5). We remind here that a CFD simulation without trees was also performed using the same meteorological conditions of Campaign 1, thus it does not correspond to Campaign 3 condition and for this reason it has not been reported in Figure 6. Simulated vertical profiles performed considering isothermal conditions are in agreement with measurements. Both measurements and simulations show a TKE decrease with height in the canyon, while the maximum is found in the shear-layer region just above the roof-level [Figure 6(a)], in accordance with previous studies (e.g., Louka et al., 2000). It can be further noted that normalised TKE values below the tree crown are larger during Campaign 3 than those recorded during Campaign 1 an effect due to smaller values of friction velocities during those hours. Further, the analysis of momentum fluxes obtained from both measurements and simulations [Figure 6(b)] confirms the strong influence of tree crowns during Campaign 1. Similar to what found from TKE results, negative in-canyon fluxes found below tree crowns during Campaign 3 (low LAI) becomes positive in the presence of trees with large LAI (Campaign 1) probably due to flux of heat released from surfaces below crowns, as already discussed in Subsection 4.1.

Figure 5 Wind speed and direction (left) and percentage reduction of wind speed (right) during Campaigns, (a) 1 (b) 2 (c) 3 (see online version for colours)

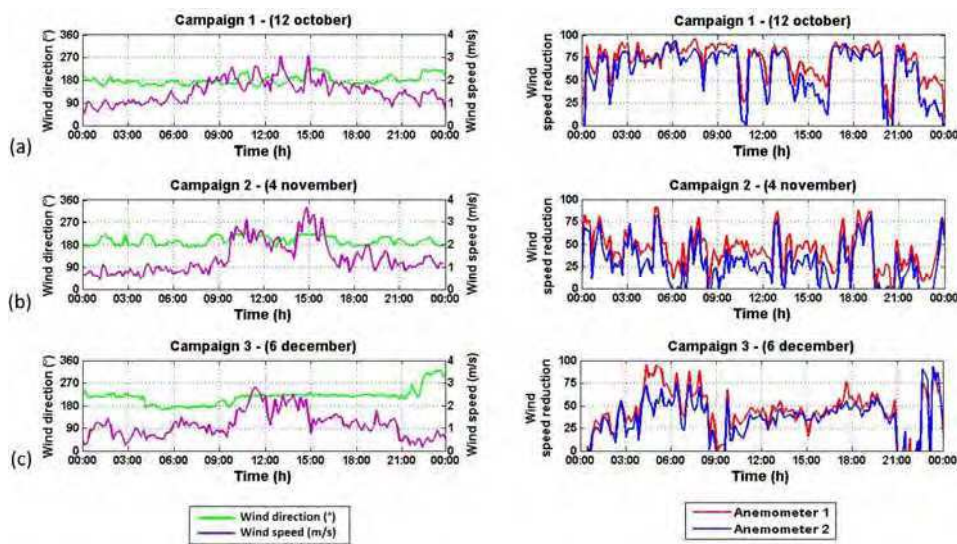
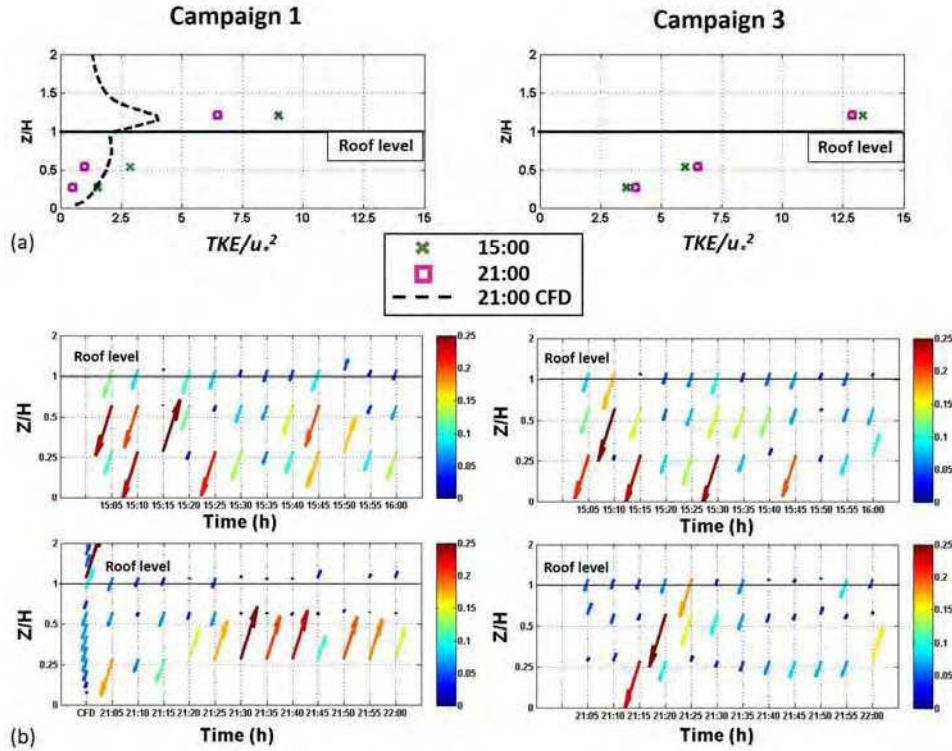


Figure 6 Profiles of, (a) TKE (b) momentum fluxes $\overline{u'w'}$ during Campaign 1 (left) and Campaign 3 (right) (see online version for colours)



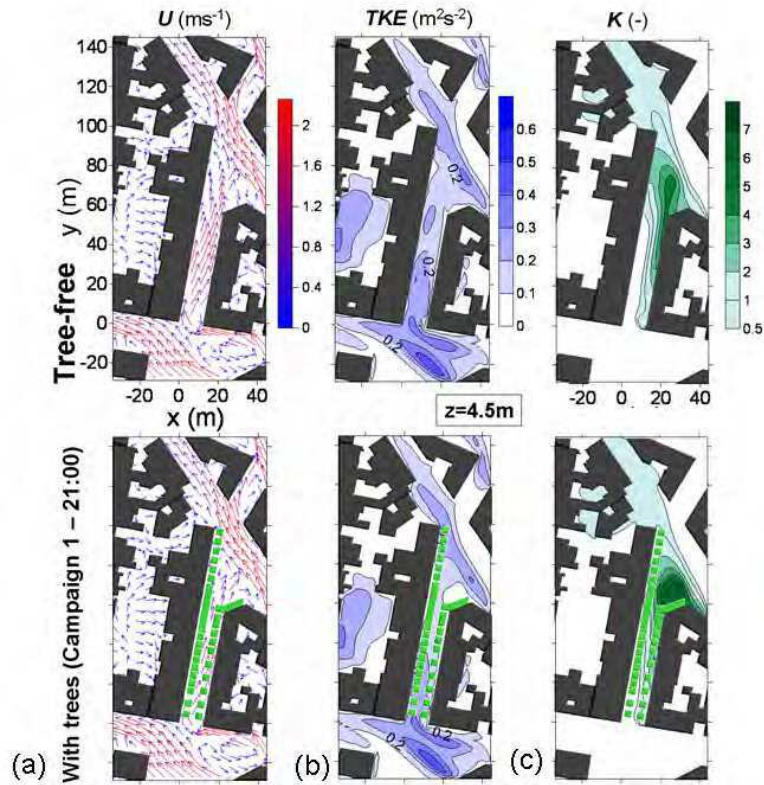
Note: Arrows indicate negative (downward) and positive (upward) fluxes.

CFD simulations performed using the meteorological conditions of Campaign 1, with and without trees, allowed us to isolate the effect of wind direction. The results show a typical wind channelling along Redipuglia St. in the tree-free case. In the presence of trees, even though the main flow pattern within the street canyon was still maintained, an average wind speed reduction [equation (1)] of 35% occurred just below the crown (Anemometer 1) and 42% just above the crown (Anemometer 2). Vortices occurred leading to reverse flow at the downstream exit and at the downstream opening of Redipuglia St. [Figure 7(a)] and TKE was also suppressed especially at the upstream entry [Figure 7(b)]. In the tree-free case, the percentage reduction decreased to 28% below the crown and to 19% above the crown. These wind speed reductions, even though in qualitative agreement, are slightly lower than the observations (see Figure 5), probably because of the effect of leaf-induced turbulence which was neglected in CFD simulations. However, they confirm what found from the field campaigns that the presence of trees strongly influenced the ventilation inside the canyon. Larger concentrations in the tree case can be understood by looking at the flow structure. The channelled flow transports pollutant towards the downstream exit where it accumulated within the vortex [Figure 7(c)]. In Figure 7, the concentration K is given by:

$$K = \frac{C_{calc} \times H_{avg}^2 \times U_{ref}}{Q} \quad (2)$$

where C_{calc} is the calculated concentration (kg/m^3). Specifically, the percentage increase of volume-averaged concentration within the street canyon in presence of trees was about 20%. Results well compare with our previous wind tunnel and CFD investigations (Buccolieri et al., 2011) which showed that trees of similar crown porosity and stand density of those considered here may reduce volume flow rate at the canyon-roof interface. This reduction in volume flow rate is one of the main mechanism of diluting pollutant concentration at the street level thus justifying the larger concentration at street level in the tree-case.

Figure 7 Vectors of, (a) wind speed (b) contours of TKE (c) contours of normalised concentrations at $z = 4.5$ m (just below the tree crown) obtained from CFD simulations (see online version for colours)



5 Conclusions

The effects of trees on local meteorological variables in the inner core of a medium-size Mediterranean city were investigated through in situ measurements and CFD simulations. The combined use of IR thermal images with classical air temperature sensors allowed us to investigate the temperature distribution within street canyons with and without trees.

The analysis has shown that presence of trees in street canyons may trap heat closer to the ground. Observations show that after sunset both temperature of façade and air temperature are larger in street canyon with trees, with respect to those without trees.

Focusing on cases with incoming wind flow parallel to the street axis, both measurements and numerical simulations show a significant windbreak effect in the street canyon with trees. The main flow pattern observed in the tree-free street canyon was still maintained in the presence of trees, but with reduced wind speed and enhanced concentrations with reverse flow within the street. Further analyses are required to quantify the trapping effects of trees on scalar variables but this work has shown that their effects are not negligible and ignoring them in dispersion model formulations may lead to underestimation of in-canyon concentrations.

References

- Buccolieri, R., Salim, S.M., Leo, L.S., Di Sabatino, S., Chan, A., Ielpo, P., de Gennaro, G. and Gromke, C. (2011) 'Analysis of local scale tree-atmosphere interaction on pollutant concentration in idealized street canyons and application to a real urban junction', *Atmospheric Environment*, Vol. 45, No. 9, pp.1702–1713.
- Danov, M., Petkov, D. and Tsanev, V. (2007) 'Investigation of thermal infrared emissivity spectra of mineral and rock samples', in Bochenek, Z. (Ed.): *New Developments and Challenges in Remote Sensing*, ISBN 978-90-5966-053-3, Mill Press, Rotterdam.
- Desplat, J., Salagnac, J-L., Kouunkou-Arnaud, R., Lemonsu, A., Colombert, M., Lauffenburger, M. and Masson, V. (2009) 'EPICEA project 2008–2010 'Multidisciplinary study of the impacts of climate change on the scale of Paris', *7th International Conference on Urban Climate*, Yokohama, Japan.
- Di Sabatino, S., Buccolieri, R., Pulvirenti, B. and Britter, R. (2007) 'Simulations of pollutant dispersion within idealised urban-type geometries with CFD and integral models', *Atmospheric Environment*, Vol. 41, No. 37, pp.8316–8329.
- Gromke, C. and Blocken, B. (2015) 'Influence of avenue-trees on air quality at the urban neighborhood scale. Part I: quality assurance studies and turbulent Schmidt number analysis for RANS CFD simulations', *Environmental Pollution*, Vol. 196, pp.214–223.
- Gromke, C., Buccolieri, R., Di Sabatino, S. and Ruck, B. (2008) 'Dispersion study in a street canyon with tree planting by means of wind tunnel and numerical investigations – evaluation of CFD data with experimental data', *Atmospheric Environment*, Vol. 42, No. 37, pp.8640–8650.
- Hoyano, A., Asano, K. and Kanamaru, T. (1999) 'Analysis of the sensible heat flux from the exterior surface of buildings using time sequential thermography', *Atmospheric Environment*, Vol. 33, Nos. 24–25, pp.3941–3951.
- Janhäll, S. (2015) 'Review on urban vegetation and particle air pollution – deposition and dispersion', *Atmospheric Environment*, Vol. 105, pp.130–137.
- Launder, B.E. (1989) 'Second-moment closure: present and future?', *International Journal of Heat Fluid Flow*, Vol. 10, No. 4, pp.282–300.
- Louka, P., Belcher, S.E. and Harrison, S.G. (2000) 'Coupling between air flow in streets and the well-developed boundary layer aloft', *Atmospheric Environment*, Vol. 34, No. 16, pp.2613–2621.
- McMillen, R.T. (1988) 'An eddy correlation technique with extended applicability to non-simple terrain', *Boundary-Layer Meteorology*, Vol. 43, No. 3, pp.231–245.
- Roche, G. (2012) *La termografia per l'edilizia e l'industria*, Maggioli, Ravenna.
- Shashua-Bar, L., Pearlmutter D., and Erell, E. (2011) 'The influence of trees and grass on outdoor thermal comfort in a hot-arid environment', *International Journal of Climatology*, Vol., 31, No. 10, pp.1498–1506.



On the exchange velocity in street canyons with tree planting

Silvana Di Sabatino^{1,4}, Riccardo Buccolieri^{2,4}, Laura S. Leo^{3,4}, Gianluca Pappaccogli²

¹*Department of Physics and Astronomy (DIFA) - ALMA MATER STUDIORUM, University of Bologna (Italy),
silvana.disabatino@unibo.it*

²*Dipartimento di Scienze e Tecnologie Biologiche ed Ambientali, University of Salento, Lecce (Italy),
riccardo.buccolieri@unisalento.it; gianluca.pappaccogli@yahoo.it*

³*Department of Civil & Environmental Engineering and Earth Sciences, Environmental Fluid Dynamics
Laboratories, University of Notre Dame, Indiana (USA), laurasandra.leo.13@nd.edu*

⁴*RESEAU S.r.l., Lecce (Italy)*

dated: 15 June 2015

1. Introduction

Tree planting has been widely recognized as a first mitigation strategy to reduce pollutant concentrations in cities. Trees (and vegetation in general) have the capability of cleaning the air by filtering out pollutants, improving the urban microclimate and reducing greenhouse gases concentrations (Litschke and Kuttler, 2008). However, recent numerical studies (e.g. Buccolieri et al., 2011; Vos et al., 2013; Abhijith and Gokhale, 2015) have shown that trees in urban street canyons also have significant effect on the street canyon breathability, impairing the air circulation and pollutant removal processes at the pedestrian zone (Janhäll, 2015). Eventually, the overall impact of trees (positive versus negative effects) at the street scale depends upon the specific synergy between meteorological conditions and both street canyon and vegetation configurations but a well-defined and universal framework is still missing; and so are field measurements needed to corroborate these theoretical and numerical results.

The goal of this paper is to investigate the effects of trees on flow and turbulence in a street canyon by means of *ad-hoc* field measurements integrated with Computational Fluid Dynamics (CFD) modelling. The field campaign was carried out prior to and after the leaf-out of trees in order to assess the effects of different tree canopy structures (i.e. with different Leaf Area Index LAI) on air circulation inside the street canyon. Results were used to estimate the exchange velocity as quantified from vertical mean and turbulent fluxes under several wind direction and different density of the canopy (with trees and tree-free).

2. Description of the study site

The investigated street canyon (namely Redipuglia St.) is located in Lecce, a medium-size city of south Italy characterized by a Mediterranean climate and a classical Mediterranean architectural design, consisting of 2-3 storey buildings and narrow street canyons (Figure 1a). Redipuglia St. is located on the western side of the city where buildings, despite the different heights, are distributed in a regular configuration (Figure 1b). The street canyon is 100m long and 12m wide, running approximately north-south (11° from North) with building heights ranging from 13m to 21m (Figure 1c). The aspect ratio H/W is ~1.2 (where H~15m is average building height and W~12m is the width of the street). Thirty-six deciduous trees (*Tilia Cordata* Mill.) are planted along both sides of the street, twenty-two of which located along the left side and fourteen along the right side. The spacing between tree trunks is approximately 4m, so that there is leaf crown interference. The average height of the branch-free trunk is about 5m and the crown extends to about 8m (Figure 1d,e,f). *Tilia Cordata* Mill. is widespread throughout Europe and is characterized by a dense pyramidal or oval crown which casts deep shade. It is commonly used in urban areas due to its predictable symmetrical shape, which makes it recommendable for shading sidewalks in residential streets.

3. Methodology

3.1 Field experiments

Flow and air temperature measurements were carried out continuously in the period 11 October - 7 December 2013 (Main Campaign hereinafter). The Main Campaign included three intense measurements periods where Leaf Area Index (LAI, m²m⁻²) were also performed; specifically on 11-12 October (Campaign 1 hereinafter), 8-9 November (Campaign 2 hereinafter) and 6-7 December 2013 (Campaign 3 hereinafter).

The three components of wind velocity and sonic temperature were measured at the acquisition sampling frequency of 50Hz by three GILL R3-50 sonic anemometers in Redipuglia St. (Figure 1c). Measurements were taken at three different heights. Two anemometers were positioned inside the street canyon: the first (Anemometer 1) was just below the tree crown at z=4.5m AGL (Above Ground Level) and the second (Anemometer 2) was just above the tree crown at z=8.5m AGL. Both anemometers were positioned on banisters

of two balconies at the first and second floors of a 15m high building. The third anemometer (Anemometer 3) and a Vaisala HMP45C thermo-hygrometer were positioned at the roof of the same building at 18m AGL. 10-mins averages of wind direction and wind speed and 5-mins averages of turbulent fluxes (for the calculation of the exchange velocity) were computed, following standard techniques for the treatment of high frequency flow data in real scenarios (McMillen, 1988).

LAI of *Tilia Cordata* tree crowns was estimated from measurements of the photosynthetically active radiation (PAR) (light in the 400-700nm waveband) acquired by an Accu-PAR LP80 ceptometer. All measurements were taken parallel to the ground and perpendicularly to the orientation of Redipuglia St. Five replicas were done at the same measurement point just near the crown (where the sensor measured unobstructed PAR) and at its base (where i LAI is assumed to be maximum). The Leaf Area Density (LAD, m^2m^{-3}) was thus estimated dividing LAI by the depth of tree crown (3m) (Figure 1d,e,f). We will refer to large LAI of trees for Campaign 1, intermediate LAI for Campaign 2 and low LAI (leafless trees) for Campaign 3.

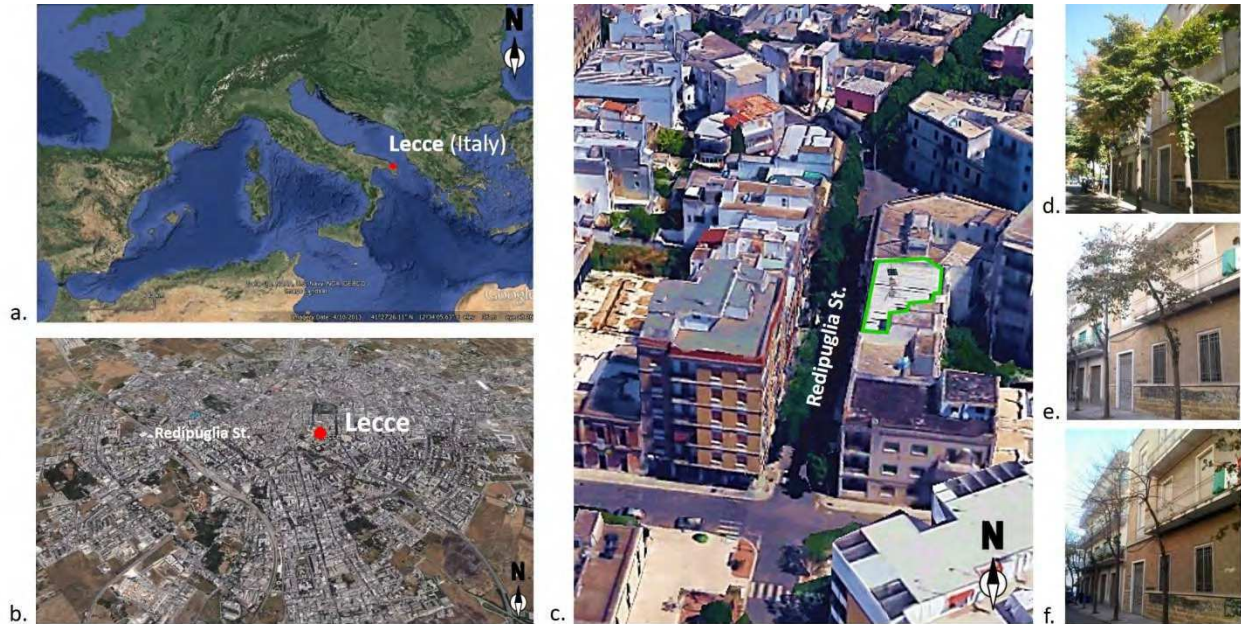


Fig. 1 (a) Position of Lecce in south-east Italy and (b) position of the street neighbourhood analysed (base maps from Google Earth). (c) View of Redipuglia St. ; the green contour indicates the building where the three sonic anemometers were located. Texture of vegetation during Campaign 1 (d), Campaign 2 (e) and Campaign 3 (f).

Note: Image (d), Campaign 1: $LAI=5.21m^2m^{-2}$, $LAD=1.74m^2m^{-3}$; Campaign 2: $LAI=0.97m^2m^{-2}$, $LAD=0.32m^2m^{-3}$; Campaign 3: $LAI=0.37m^2m^{-2}$, $LAD=0.12m^2m^{-3}$.

3.2 CFD simulations

3D isothermal CFD simulations were performed by means of the general purpose code Fluent (at the Dipartimento di Ingegneria dell'Innovazione - University of Salento). A preliminary analysis considered meteorological conditions recorded at 21:00 local time (when conditions inside the canyon could be assumed to be isothermal) during Campaign 1. The study area includes Redipuglia St. (with trees, large LAI). To match recorded conditions, an approaching flow was taken to be equal to the mean hourly value ($2.3ms^{-1}$) observed at a meteorological station located outside the urban area (at $z=20m$), with a wind direction equal to 140° (i.e. from south-south/east direction). The same simulation was performed without trees (tree-free). The Reynolds Stress Model (RSM) (Launder et al., 1989) was used. The domain was built using about one million elements, with a finer resolution within the entire building area. The smallest dimension of the elements in the x, y and z directions was 0.25m, based on grid convergence analysis. Equilibrium profiles of wind speed, turbulent kinetic energy (TKE) and dissipation rate (ϵ) were specified at the inlet (Di Sabatino et al., 2007), with a friction velocity $u^* = 0.17ms^{-1}$ estimated from log-law curve fitting of the observed wind velocity at the meteorological station. Symmetry boundary condition was specified at the top, while at the downwind boundary a pressure-outlet condition was used. The aerodynamic characteristics of trees were modelled adding a momentum sink in the governing momentum equations, where the inertial term is parameterized using a pressure loss coefficient $\lambda=0.35m^{-1}$ estimated through $C_d \times LAD$, where C_d is the leaf drag coefficient taken equal to 0.2 (Gromke and Blocken, 2015). For the purpose of estimating the exchange velocity (see next section), a ground-level line source was modelled along the southern part of Redipuglia St. (that is bounded by buildings at both sides) and the advection-diffusion module was used to calculate pollutant concentration. As an example, a CO emission rate $Q_U=10gs^{-1}$ was assumed.

3.3 Exchange velocity

A main parameter to estimate vertical fluxes between the street canyons and the overlying atmosphere is the exchange velocity U_e , originally introduced by Bentham and Britter (2003) as a measure of city ventilation. Several formulations have been proposed in the literature, mainly based on modelling simulations, and only few studies investigated the effect of street vegetation on exchange flux and pollutant dispersion (Ng and Chau, 2011). A recent review of different approaches and results obtained from different research groups in street canyons and built-up areas is given in Panagiotou et al. (2013).

Hamlyn and Britter (2005) applied the model concept of exchange velocity as a ratio of the momentum flux to the difference between the mass flux above and below the canopy top (exchange plane of the street roof A_c), which is defined as follows (Panagiotou et al., 2013):

$$U_e = \frac{\iint (\rho \overline{u'w'} + \rho uw) dS}{\rho A_c (U_{ref} - U_c)} \quad (1)$$

The momentum flux in Eq. (1) is evaluated from the Reynolds shear stresses $\overline{u'w'}$ and the average values of the x and z components of velocities (uw). U_{ref} is the reference velocity and U_c is the in-canopy velocity. Starting from the work by Hamlyn and Britter (2005), the aim here is to estimate the exchange velocity from field measurements and evaluate the influence of tree planting in a real street canyon. In this study, since flow and turbulence measurements were taken at three points (Anemometers locations), assuming the one-dimensionality of surface area of plane, and considering longitudinal wind speed recorded at Anemometer 3 as the reference velocity U_{ref} , the normalized exchange velocity was estimated as follows:

$$U_e/U_{ref} = \left| \frac{\overline{u'w'} + uw}{U_{ref}(U_{ref} - U_c)} \right| \quad (2)$$

where $\overline{u'w'}$ and uw were those recorded at Anemometer 2 (the available positions closest to the exchange interface between the canyons and the overlying atmosphere) and U_c is the averaged sum of longitudinal wind speed recorded at Anemometer 1 (below the tree canopy) and 2 (above the tree canopy). By using $\overline{u'w'}$ and uw recorded above the tree canopy and an average of velocities measured below and above, we expect to capture the influence of trees on the vertical exchange velocity and thus on the ventilation efficiency below the tree crown (i.e. at pedestrian level).

The exchange velocity was also calculated from CFD modelling results using the current formulation given by the ratio between the pollutant flux at roof level through the exchange surface and the difference between the spatially averaged pollutant concentration within the urban canopy and the background concentration (Buccolieri et al., 2015):

$$U_e = \frac{q_v}{(\langle \bar{C}_{canopy} \rangle - \langle \bar{C}_{bkg} \rangle)} \quad (3)$$

where q_v is the pollutant flux (kg/s) at roof level through the exchange surface A_{roof} , $\langle \bar{C}_{canopy} \rangle$ denotes the averaged pollutant concentration within the urban canopy and $\langle \bar{C}_{bkg} \rangle$ is the background concentration, i.e. pollutant concentration of the incoming atmospheric flow (in our case it is null). The value of U_e is calculated from q_v , that is computed as the residual of a balance of the pollutant fluxes entering and leaving the canyon (i.e. in the horizontal plane - while the faces are vertical planes) through the sections of the streets at its borders as follows:

$$q_v = \int_V Q_v dV - \int_A \bar{U}_i \cdot \bar{C}_i dA \quad (4)$$

where V is the whole volume of the canyon (i denotes the x and y horizontal directions), C the calculated concentration and A the area of the street lateral sides.

4. Results and discussion

4.1 Flow and turbulence

The analysis of anemometric measurements allowed us to investigate the effects of trees on flow and turbulence within Redipuglia St. Figure 2 shows the windbreak effect in Redipuglia St. for parallel (top) and perpendicular approaching wind (bottom) during Campaign 1 (left), Campaign 2 (middle) and Campaign 3 (right). In the figures, the normalized percentage reduction of wind speed (nrU_1) was calculated as follows:

$$\left(1 - \frac{U_1}{U_{ref}}\right) \times 100 = nrU_1 \quad (5)$$

where U_1 is the longitudinal wind speed recorded at Anemometer 1. In the figure, wind directions refer to those recorded at Anemometer 3 (roof level). During Campaign 1 (large LAI) (Figure 2a) winds speed have an average reduction of 57% for parallel (top) and 50% for perpendicular wind condition (bottom). During Campaigns 2 (intermediate LAI) (Figure 2b) and 3 (low LAI) (Figure 2c) the percentage reduction decreased to 54% and 39%, respectively, for parallel approaching conditions (top), and to 37% and 43% for perpendicular approaching conditions (bottom). A significant reduction of wind speed was found during Campaign 3 for wind coming from north. This suggests that the different structure of the canopy strongly influenced the ventilation inside the canyon and this influence was higher in the case of wind approaching parallel to the street axis.

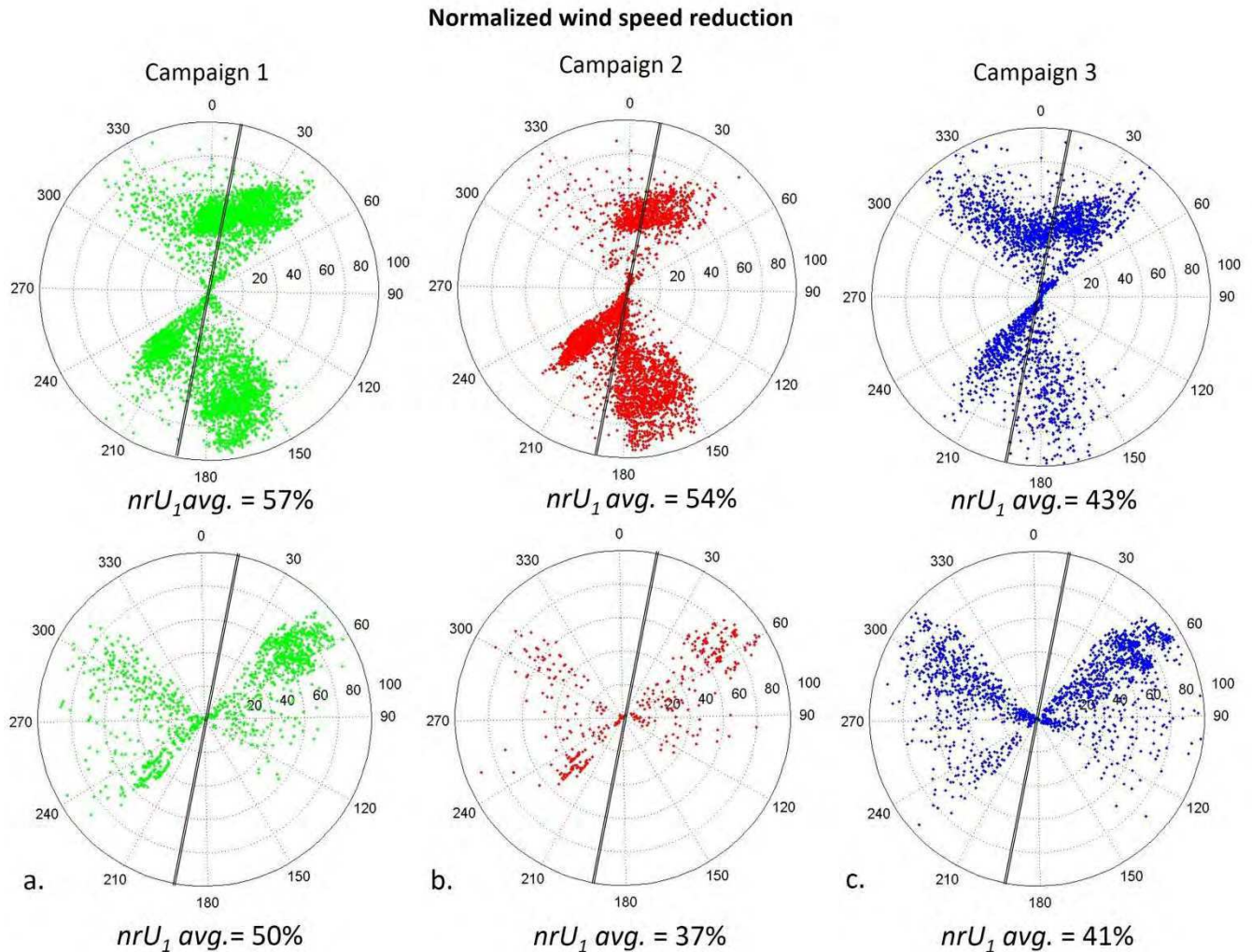


Fig. 2 Normalized percentage reduction of wind speed during Campaign 1 (a), Campaign 2 (b) and Campaign 3 (c) for parallel (top) and perpendicular (bottom) approaching wind conditions. The black line identifies the street axis direction. $nrU_1 \text{ avg.}$ refers to the average wind speed reduction.

4.2 Exchange velocity

Figure 3 shows the estimated normalized exchange velocity for parallel (top) and perpendicular approaching (bottom) conditions during Campaign 1 (left), Campaign 2 (middle) and Campaign 3 (right). During Campaign 1 (Figure 3a) the average value is 0.17ms^{-1} for parallel (top) and 0.20ms^{-1} for perpendicular wind condition (bottom). During Campaigns 2 (Figure 3b) and 3 (Figure 3c) the average values became 0.17 and 0.21, respectively, for parallel approaching condition (top), and to 0.20 and 0.25 for perpendicular approaching condition (bottom). Overall, it can be noted that the effect of trees during Campaign 1 and Campaign 2 was that of lowering the exchange velocity of about 20% with respect to Campaign 3. There was thus a general increase of the exchange velocity from Campaign 1 to Campaign 3 confirming that trees partially obstructed the exchange of air between the canyon and the overlying atmosphere.

Our estimates of the normalized exchange velocity compare relatively well with estimates from previous numerical studies (see the review by Panagiotou et al., 2013). Specifically, our values are in the range they

reported for a planar area index $\lambda_p = 0.49$ (that of our study site), i.e. between about 0.01 and 0.23.

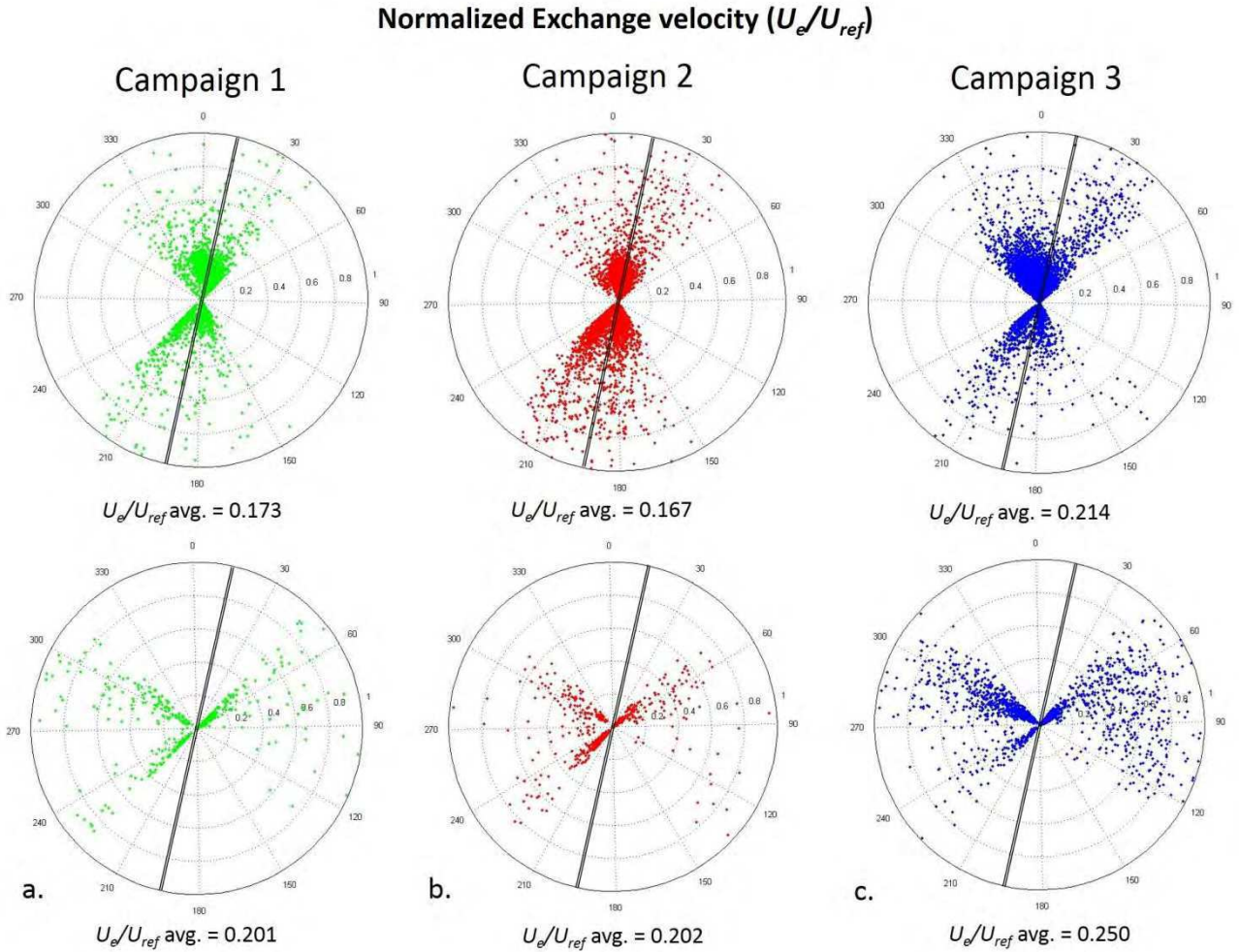


Fig. 3 Normalized exchange velocity during Campaign 1 (a), Campaign 2 (b) and Campaign 3 (c) for parallel (top) and perpendicular (bottom) wind conditions. The black line identifies the street axis direction. $U_e/U_{ref} \text{ avg.}$ refers to the average normalized exchange velocity.

Figure 4 shows the normalized exchange velocity obtained from daily averages and hourly averages (hh 14:00-15:00 and hh 21:00-22:00) over the whole Main campaign. Overall, each subfigure contains 37 values of the 51 field campaign days, since in 14 days there were missing or inaccurate data. In the figures, wind directions refer to those prevailing during the day or the investigated hours as recorded at Anemometer 3, while the circle size at each point qualitatively indicates the variability of data during the day.

From the figure, as already discussed before (Figure 4), it is evident the effect of trees in lowering the exchange velocity between the canyon and the overlying atmosphere. The figure further shows a high variability of the exchange velocity during Campaign 3, while in the presence of trees with leaves (Campaigns 1 and 2) the obstruction effect lead to lower turbulence levels and thus to lower values of the vertical exchange. This is more pronounced during isothermal conditions (Figure 4c) when the buoyancy did not increase the vertical exchange as for the convective case (Figure 4c). CFD simulations (for the case hh 21:00-22:00) confirmed what found from the field measurements, showing a lower vertical exchange ($U_e/U_{ref} = 0.05$) in the presence of trees compared to the tree-free case ($U_e/U_{ref} = 0.06$).

5. Conclusions

The effect of trees on wind speed reduction and vertical turbulent exchange between a street canyon and the overlying atmosphere was examined using high-frequency wind data measured in the city of Lecce (south Italy). It is shown that the overall effect of trees reduce street ventilation. The canyon ventilation was quantified in terms of the two adimensional variables (U_e/U_{ref}) and nrU_1 , which take into account the volume of air exchanged in-out canyon in the vertical and horizontal directions respectively. Results indicated a more pronounced reduction for the case of approaching wind perpendicular to the street axis and during the night-time (during isothermal conditions).

Although in-deeper analysis are still in progress, this preliminary investigation has provided useful insights on

the potential adverse effects of trees on street ventilation which may stimulate further research for a more effective urban planning.

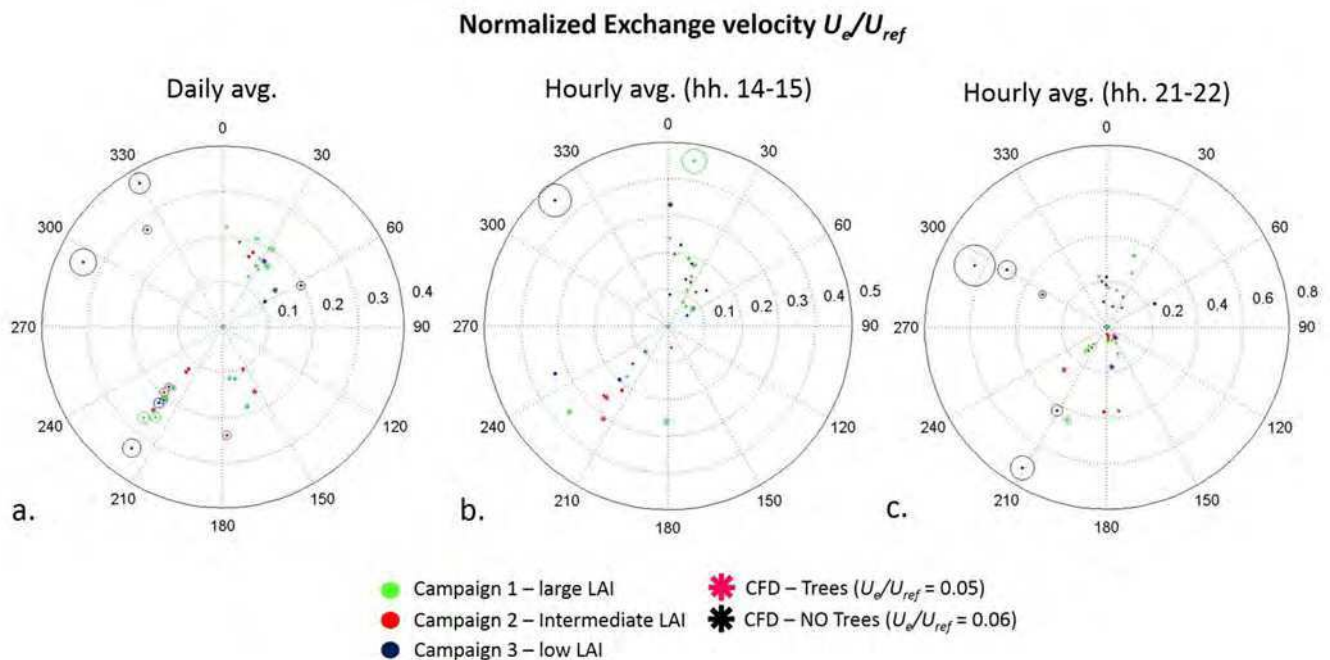


Fig. 4 Normalized exchange velocity obtained from daily averages (a), hourly averages (hh. 14:00-15:00) during light-time (b) and 1-hour averages (hh. 21:00-22:00) during night-time (c) over the whole Main campaign. The circle size at each point indicates the standard deviation. St. dev. avg. refers to the average standard deviation for each campaign.

References

- Abhijith K.V., Gokhale S., 2015: Passive control potentials of trees and on-street parked cars in reduction of air pollution exposure in urban street canyons. *Environmental Pollution*, **204**, 99-108.
- Bentham J.T., Britter R.E., 2003: Spatially averaged flow within obstacle arrays. *Atmospheric Environment*, **37**, 2037-2043.
- Buccolieri R., Sandberg M., Di Sabatino S., 2010: City breathability and its link to pollutant concentration distribution within urban-like geometries. *Atmospheric Environment*, **44**, 1984-1903.
- Buccolieri R., Salim M. S., Leo L. S., Di Sabatino S., Chan A., Ielpo P., de Gennaro G., Gromke C., 2011: Analysis of local scale tree – atmosphere interaction on pollutant concentration in idealized street canyons and application to a real urban junction. *Atmospheric Environment*, **45**, 1702-1713.
- Buccolieri R., Salizzoni P., Soulhac L., Garbero V., Di Sabatino S., 2015: Breathability of compact cities. *Accepted for publication in Urban Climate*. DOI: 10.1016/j.uclim.2015.06.002
- Di Sabatino S., Buccolieri R., Pulvirenti B., Britter R., 2007: Simulations of pollutant dispersion within idealised urban-type geometries with CFD and integral models. *Atmospheric Environment*, **41**, 37, 8316-8329.
- Gromke C., Blocken B., 2015: Influence of avenue-trees on air quality at the urban neighborhood scale. Part I: Quality assurance studies and turbulent Schmidt number analysis for RANS CFD simulations. *Environmental Pollution*, **196**, 214-223.
- Hamlyn D., Britter R., 2005: A numerical study of the flow field and exchange processes within a canopy of urban-type roughness. *Atmospheric Environment*, **39**, 3243–3254.
- Janhäll S., 2015: Review on urban vegetation and particle air pollution – Deposition and dispersion. *Atmospheric Environment*, **105**, 130-137.
- Launder B.E., 1989: Second-moment closure: present and future? *International Journal of Heat Fluid Flow*, **10**, 282-300.
- Litschke T., Kuttler W., 2008: On the reduction of urban particle concentration by vegetation e a review, *Meteorologische Zeitschrift*, **17**, 229-240.
- McMillen R.T., 1988: An Eddy Correlation Technique with Extended Applicability to Non-simple Terrain. *Boundary-Layer Meteorology*, **43**, 56-65.
- Panagiotou I., Neophytou M.K.A., Hamlyn D., Britter E.R., 2013: City breathability as quantified by the exchange velocity and its spatial variation in real inhomogeneous urban geometries: An example from central London urban area. *Science of the Total Environment*, **442**, 466–477.
- Tallis M., Taylor G., Sinnett D., Freer-Smith P., 2011: Estimating the removal of atmospheric particulate pollution by the urban tree canopy of London, under current and future environments. *Landscape and Urban Planning*, **103**, 129-138.
- Vos P.E.J., Maiheu B., Vankerkom J., Janssen S., 2013: Improving local air quality in cities: To tree or not to tree? *Environmental Pollution*, **183**, 113-122.

**16th International Conference on
Harmonisation within Atmospheric Dispersion Modelling for Regulatory Purposes
8-11 September 2014, Varna, Bulgaria**

**ON THERMAL STRATIFICATION IN REAL STREET CANYONS WITH TREES:
CONSEQUENCES FOR LOCAL AIR QUALITY**

Silvana Di Sabatino^{1,2}, Riccardo Buccolieri¹, Laura S. Leo², Gianluca Pappacogli¹

¹University of Salento, Dipartimento di Scienze e Tecnologie ed Ambientali, S.P. 6 Lecce-Monteroni,
73100 Lecce (Italy)

²University of Notre Dame, Environmental Fluid Dynamics Laboratories, Department of Civil &
Environmental Engineering and Earth Sciences, Notre Dame, IN 46556 (USA)

Abstract: This study analyses the effects of trees on local meteorology in a medium-size Mediterranean city (Lecce, IT) using field measurements and Computational Fluid Dynamics (CFD) simulations. Measurements were taken in two parallel street canyons with and without trees. Building façades and ground temperatures were estimated from infrared (IR) images, while flow and turbulence were measured by three ultrasonic anemometers. CFD simulations were performed by employing the Reynolds Stress Model (RSM). Overall the analysis shows that trees reduce the wind speed and alter the typical diurnal cycle of surface and air temperature within the canyon. In particular, the flow interaction with trees induces wind direction fluctuations below tree crowns and lower velocities which are expected to lead to larger pollutant and heat trapping in the lower part of the street canyon, especially in nocturnal hours.

Key words: *urban temperature, flow and turbulence, pollutant concentration, trees, Computational Fluid Dynamics.*

INTRODUCTION

Quantification of thermal stratification in street canyons is very important in the modelling of urban air quality as well as for mitigation strategies. Thermal stratification may change dramatically during the day as a function of local temperature differences, street canyon aspect ratio H/W (where H is the average building height and W is the street canyon width) and building materials. The change in thermal structure is further exacerbated by the presence of trees. Urban vegetation is a primary preventive measure to mitigate the Urban Heat Island phenomenon by shading of buildings and ambient cooling. However, at street scale the capability of mitigating high temperatures must be set off against the obstruction effect to the wind, which reduces pollutant dispersion (Gromke, C. et al., 2008). Despite the large number of laboratory and numerical investigations, field studies are less numerous and conclusions about the effect of trees on local air quality are still controversial within the research community.

Within this context, here we investigate some of these issues by using temperature, flow and turbulence data integrated with Computational Fluid Dynamics (CFD) modelling. Data were collected in a Mediterranean city (Lecce) in south Italy, in two parallel street canyons with and without trees.

THE STUDY AREA

The study area is located in Lecce, a medium-size city characterized by a Mediterranean climate and a classical Mediterranean architectural design, consisting of 2-3 storey buildings and narrow street canyons (Figure 1a). The study area is on the western side of the city where buildings despite the different heights are distributed in a rather regular configuration (Figure 1b).

The area size is 130m x 200m and comprises two main parallel street canyons (namely Redipuglia St. and Gorizia St.) running north-south with buildings heights ranging from 5m to 25m (Figure 1c). Gorizia St. is a tree-free street canyon with aspect ratio H/W equal to 1.1, while Redipulia St. aspect ratio is equal to 1.2 and is characterized by the presence of deciduous trees. A total of 36 trees (*Tilia Cordata* Mill.) are located along both sides of the street. The spacing between tree trunks is approximately 4m. The average height of the branch-free trunk is about 5m and the crown extends to about 8m in height (Figure 1d).

MEASUREMENTS AND NUMERICAL SIMULATIONS

Flow and air temperature measurements were carried out in Redipuglia St. in the period 11 October-7 December 2013 (Main Campaign hereinafter). The Main Campaign included three intense measurements periods where Leaf Area Index (LAI) measurements, thermal imaging measurements of building façades, air temperature and relative humidity measurements were also conducted in Redipuglia St. and Gorizia St.; specifically from noon to noon of 11-12 October (Campaign 1 hereinafter), 8-9 November (Campaign 2 hereinafter) and 6-7 December 2013 (Campaign 3 hereinafter).

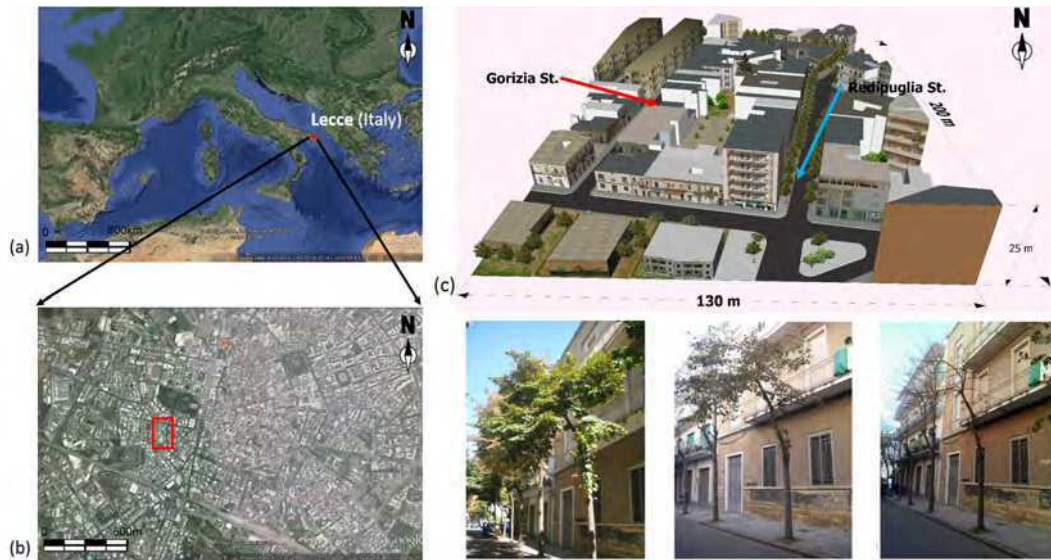


Figure 1. Position of Lecce city in south-east Italy (a) and study area (b) (base maps from Google Earth). 3D view of the study area (c). Texture of vegetation canopy (d) at Campaign 1 on the left (LAI, LAD = 5.21, 1.74), Campaign 2 in the middle (LAI, LAD = 0.97, 0.32) and Campaign 3 on the right (LAI, LAD = 0.37, 0.12)

Flow and turbulence measurements

The three components of wind velocity and sonic temperature were measured at the acquisition sampling frequency of 50Hz by three GILL R3-50 sonic anemometers installed in Redipuglia St. (Figure 2). Two anemometers were positioned inside the street canyon: the first (Anemometer 1) was just below the tree crown at $z=4.5\text{m}$ a.g.l. (above ground level) and the second (Anemometer 2) was just above the tree crown at $z=8.5\text{m}$ a.g.l. The third anemometer (Anemometer 3), together with a Vaisala HMP45C thermo-hygrometer, were positioned on the roof of the same building at 18m a.g.l. 10mins averages of wind direction and wind speed and 5mins averages of turbulent fluxes were calculated (McMillen, R.T., 1988).

Leaf area index (LAI) measurements

LAI (m^2m^{-2}) of tree crowns was estimated from measurements of the photo-synthetically active radiation (PAR) acquired by an Accu-PAR LP80 ceptometer. The Leaf Area Density (LAD, m^2m^{-3}) was thus roughly estimated dividing LAI by the depth of tree crown (3m) (Figure 1d). We will refer to large LAI for trees for Campaign 1, intermediate LAI for Campaign 2 and low LAI (leafless trees) for Campaign 3.

Thermal imaging measurements

To analyze temperature distribution of building façades, four representative buildings (two in Gorizia St. and two in Redipuglia St.) were selected on the basis of the homogeneity of construction material and the absence of obstacles (balconies, eave, etc.), metal or glass. IR thermal images were taken every 3 hours on Campaigns 1, 2 and 3 through a high performance FLIR T620 ThermalCAM, with a 640×480 pixels resolution and an image acquisition frequency of 50/60Hz (Figure 2). Air temperature and humidity were also recorded with an Extech Instruments MO297 moisture psychrometer. Air temperature was also measured every five minutes using a PT100 sensor assembled with Tinytag TGP-0073 by Gemini data loggers during the Main Campaign. The sensor was positioned at the first floor of the same building where the anemometers were installed. Images were analysed using an emissivity value of 0.96 for

asphalt and 0.94 for brick-limestone (building façade) (FLIR 2010 User's manual. FLIR reporter professional edition 8.5).

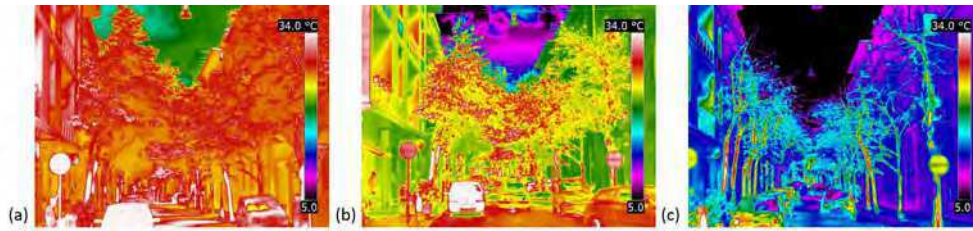


Figure 2. Example of cross-section thermal images of Redipuglia St. during Campaigns 1 (a), 2 (b) and 3 (c)

Numerical simulations

3D isothermal CFD simulations were performed by means of the general purpose code Fluent (at the Dipartimento di Ingegneria dell'Innovazione - University of Salento). The analysis considered Redipuglia St. (with trees) and meteorological conditions recorded at 21:00 (when conditions in the canyon could be assumed isothermal) during Campaign 1, with a wind direction equal to 140° (i.e. from south-south/east direction). The same simulation was performed without trees (tree-free). The Reynolds Stress Model (RSM) (Launder, B.E., 1989) was used. The domain was built using about one million elements. Equilibrium profiles of wind speed, turbulent kinetic energy (TKE) and dissipation rate (ε) were specified at the inlet (Di Sabatino, S. et al., 2007). Symmetry boundary condition was specified at the top, while at the downwind boundary a pressure-outlet condition was used. The aerodynamic characteristics of trees were modelled adding a momentum sink in the governing momentum equations where the inertial term is parameterized using a pressure loss coefficient $\lambda=0.35\text{m}^{-1}$ (Buccolieri, R. et al., 2008) estimated though $C_d \times LAD$, where C_d is the leaf drag coefficient taken equal to 0.2 (Gromke, C. and B. Blocken, 2013).

RESULTS

Effects of trees on temperature

Figure 3 shows profiles of ground and air temperatures recorded within Gorizia St. (tree-free) and Redipuglia St. (with trees) during Campaign 1, 2 and 3. Data are normalized by air temperature recorded at roof level (Anemometer 3). The effect of trees during Campaign 1 (Figure 3a,d) was that of lowering air and ground temperatures during daytime. Specifically, Redipuglia St. experienced a reduction of 30% of ground temperature with respect to Gorizia St. due to trees shadowing in the streets which prevented the asphalt to get lit by direct solar radiation. On the contrary, slightly larger ground temperatures were recorded during nighttime until sunrise given that trees reduced radiative cooling of the ground. During Campaigns 2 and 3 (Figure 3b,c,e,f), the trees effect was less pronounced during daytime resulting in similar ground temperatures in the two streets. During nighttime, Redipuglia St. still experienced larger ground temperatures despite the LAI was low, suggesting possibly the role of trees' roots in reducing the radiative cooling of the ground. Air temperature in the two streets followed a similar trend of ground temperature although differences during the nights were more pronounced.

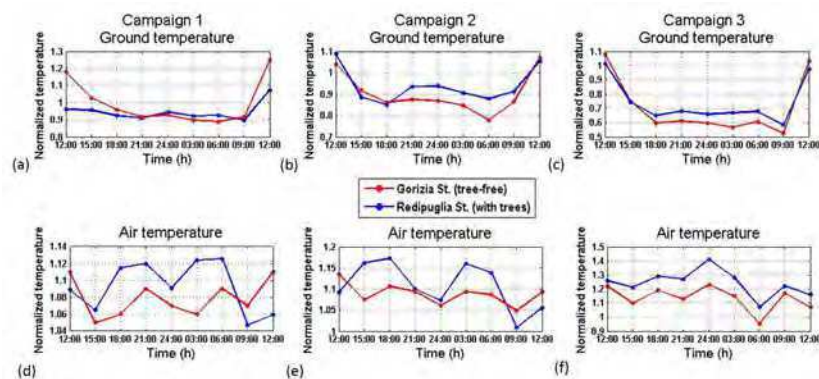


Figure 3. Normalized ground and air temperatures in Gorizia St. and Redipuglia St. during Campaigns 1, 2 and 3

The analysis of building façade temperatures further highlights the influence of trees on temperature distribution within the streets (Figure 4). During Campaign 1 (Figure 4a,d) surfaces directly exposed to east usually experienced maximum temperature at about 9am, while surfaces exposed to west reach their maximum temperature at about 3pm. The effect of trees was clearly different at the top and bottom of the façade, being trees lower than buildings. Overall, building façade temperatures in Gorizia St. were sometimes lower than air temperatures, while in Redipuglia St. this never occurred; this demonstrates that trees were effective in trapping heat close to the ground. As expected, during Campaigns 2 and 3 (Figure 4b,c,e,f) and 3 (Figure 4c,f) temperatures at the top of the façades were usually lower than those at the bottom within both streets; being trees characterized by low LAI, no inversion was found in Redipuglia St. as observed during Campaign 1. Air temperatures were considerably larger than façade temperatures. Measurements were in fact influenced by the presence of moisture on buildings façades.

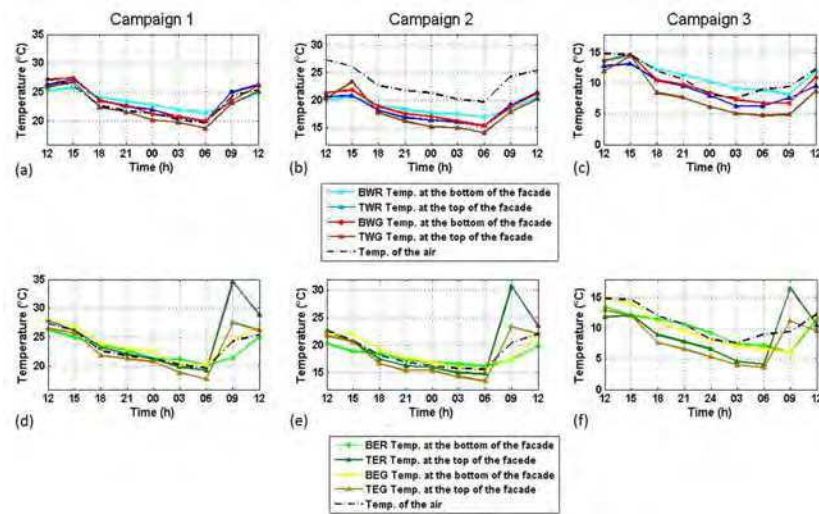


Figure 4. Mean temperatures at building façades in Redipuglia St. and Gorizia St.

Effects of trees on wind and turbulence

A windbreak effect and differences in wind direction were observed in the presence of trees (Campaign 1) with respect to leafless trees case (Campaign 3). In particular, during Campaign 1 (Figure 5a), despite the above roof wind blew from south (Anemometer 3), there was no wind channelling in the street since the interaction with trees induced wind direction oscillations below crowns. During Campaigns 2,3 (Figure 5b,c) the tree influence was smaller and the wind direction in the street similar to that above.

CFD simulations shows a typical wind channelling along Redipuglia St. in the tree-free case (Figure 6a), while in the presence of trees (Figure 6b) even though the main flow pattern within the street canyon was still maintained, wind speed at $z=8.5\text{m}$ (Anemometer 2 position) decreased of about 27% with respect to the tree-free case. *TKE* was also suppressed especially at the upstream entry of Redipuglia St. partially explaining higher observed temperatures (Figure 3). Further, trees enhanced the formation of a vortex leading to reverse flow at the downstream opening of Redipuglia St.

CONCLUSIONS AND FUTURE ANALYSES

The effects of trees on local meteorological variables in the inner core of a medium-size Mediterranean city were investigated through in situ measurements and CFD simulations. The analysis has shown that trees are effective in trapping heat close to the ground. This effect during nighttime was more important than the passive cooling through evapo-transpiration. Further, reduced wind speed, wind direction fluctuations and enhanced vortex size with reverse flow were observed within the street with trees.

Results well compare with our previous wind tunnel and CFD investigations (Buccolieri, R. et al., 2011) which showed that trees of similar crown porosity and stand density of those considered here reduce the air exchange rate at the canyon–roof interface and lateral sides of the street resulting in larger

concentrations. This was found to be mostly dependent on the approaching wind direction. From the present study we thus expect that the reduction of momentum exchange between the canyon with trees and the atmosphere above may lead to larger pollution street level concentration in Redipuglia St. than in Gorizia St. despite they are parallel and have a similar configuration. The analysis is in progress to explore consequences for ground level concentration in several tree-planting, wind direction and stability scenarios.

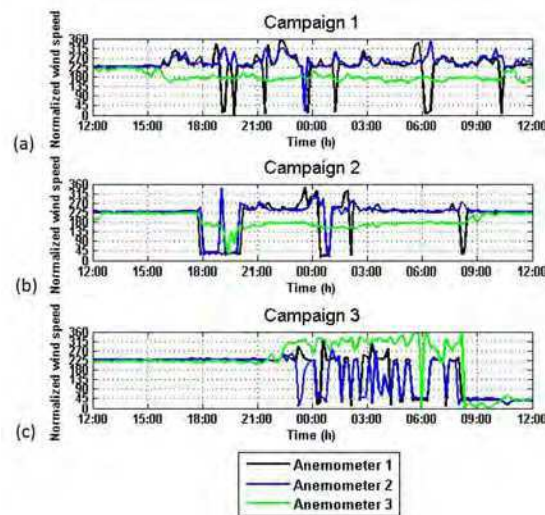


Figure 5. Wind direction recorded during Campaigns 1 (a), 2 (b) and 3 (c) in Redipuglia St.

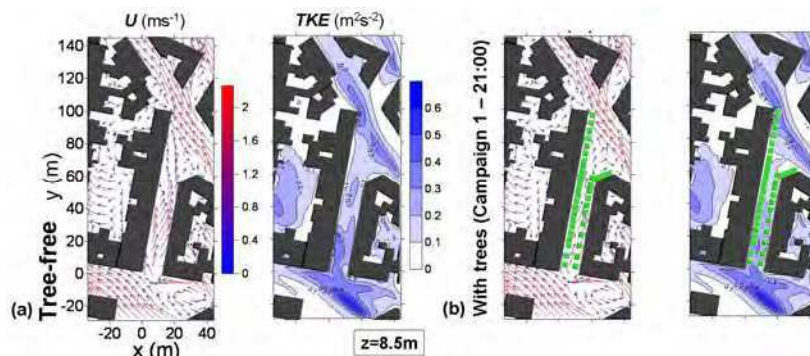


Figure 6. Wind speed and TKE from CFD simulations in Redipuglia St. for tree-free (a) and large LAI tree (b).

REFERENCES

- Buccolieri, R., S.M. Salim, L.S. Leo, S. Di Sabatino, A. Chan, P. Ielpo, G. de Gennaro, C. Gromke, 2011: Analysis of local scale tree-atmosphere interaction on pollutant concentration in idealized street canyons and application to a real urban junction. *Atmospheric Environment*, **45**, 1702-1713.
- Di Sabatino, S., R. Buccolieri, B. Pulvirenti and R. Britter, 2007: Simulations of pollutant dispersion within idealised urban-type geometries with CFD and integral models. *Atmospheric Environment*, **41**, 8316-8329.
- Gromke, C. and B. Blocken, 2013: On the relative importance of vegetation terms in computational fluid dynamics on flow and dispersion in the urban environment. 15th Int. Conf. on Harmonisation within Atmospheric Dispersion Modelling for Regulatory Purposes, Madrid, Spain.
- Launder, B.E., 1989: Second-moment closure: present and future? *International Journal of Heat Fluid Flow*, **10**, 282-300.
- McMillen, R.T., 1988: An eddy correlation technique with extended applicability to non-simple terrain. *Boundary-Layer Meteorology*, **43**, 231-245.

FEDSM2014-21566

**THE EFFECTS OF TREES ON MICROMETEOROLOGY IN A MEDIUM-SIZE
MEDITERRANEAN CITY: IN SITU EXPERIMENTS AND NUMERICAL SIMULATIONS**

Gianluca Pappaccogli

University of Salento
Dipartimento di Scienze e Tecnologie Biologiche
ed Ambientali
Lecce, Italy

Riccardo Buccolieri

University of Salento
Dipartimento di Scienze e Tecnologie Biologiche
ed Ambientali
Lecce, Italy

Giuseppe Maggiotto

University of Salento
Dipartimento di Scienze e Tecnologie Biologiche
ed Ambientali
Lecce, Italy

Laura S. Leo

University of Notre Dame
Department of Civil & Environmental Engineering
and Earth Sciences
Notre Dame, IN (USA)

Gennaro Rispoli

University of Salento
Dipartimento di Scienze e
Tecnologie Biologiche ed
Ambientali
Lecce, Italy

Francesco Micocci

University of Salento
Dipartimento di Scienze e
Tecnologie Biologiche ed
Ambientali
Lecce, Italy

Silvana Di Sabatino

University Of Salento
Dipartimento di Scienze e
Tecnologie Biologiche ed
Ambientali
Lecce, Italy

ABSTRACT

This study analyses the aerodynamic effects of trees on local meteorological variables through in situ measurements and Computational Fluid Dynamics (CFD) simulations. Measurements are taken in the inner core of a medium-size Mediterranean city (Lecce, IT) where two adjacent street canyons of aspect ratio $H/W \sim 1$ (where H is the average building height and W is the average width of the street) with and without trees are investigated. Building façades and ground temperatures are estimated from infrared (IR) images, while flow and turbulence are measured through three ultrasonic anemometers placed at different heights close to a building façade at half length of the canyon. Tree crown porosity is evaluated through the Leaf Area Index (LAI) measured by a ceptometer. Numerical simulations are made using a CFD code equipped with the Reynolds Stress Model (RSM) for the treatment of turbulence. Overall the analysis of measurements shows that trees considerably reduce the longitudinal wind speed up to 30%. Trees alter the typical diurnal cycle of surface and air temperature within the canyon, suggesting that in

nocturnal hours the trapping of heat is more important than the power of passive cooling through evapo-transpiration. Comparative numerical simulations provide further evidence that flow velocity reduces in presence of trees and although the typical wind channeling observed without trees is still maintained, trees enhance the formation of a corner vortex leading to reverse flow at the openings of the street. The reduction of the exchange of momentum between the canyon and the atmosphere above shown by the measurements in presence of trees is confirmed by numerical simulations.

INTRODUCTION

The constant increase of urbanization worldwide has posed increasing attention to augmented temperatures in the city and to the formation of urban heat island (UHI) [1]. This phenomenon became more evident as a consequence of the reduced density of green areas and the current trend in urban architecture towards high buildings with wide spacing among the built-up units.

Urban vegetation is considered a primary preventive measure to mitigate the UHI phenomenon by shading of buildings (sunlight is intercepted by trees before it warms a building) and ambient cooling (evapo-transpiration cools air). Compared to other mitigation strategies, the increase of vegetation cover induces a significant reduction of the sensible heat flux which is the most sensitive term in the surface energy balance [2,3]. However, when the focus is on pedestrian comfort at street scale, the capability of mitigating high temperatures must be set off against the obstruction effect to the wind, which reduces ventilation. The effect of buildings and trees on ventilation and air pollutant dispersion is scale dependent and still needs to be quantified. Field experiments combined with numerical investigations offer an excellent opportunity to analyze the problem in detail.

Several studies have been conducted with the aim of investigating the effects of trees on flow patterns, turbulent diffusion of airborne pollutants and temperature distribution by the evaporative cooling and shading effects [4,5]. From the first forest model constructed by wood pegs and plastic strips [6], to the recent extensive database on idealized street canyon with urban trees of varying permeability [7], it has been understood that for relatively small aspect ratios (such as those investigated in this paper), the effect of trees is more pronounced when the wind is perpendicular to the street axis, while for larger aspect ratios the effect is stronger for inclined wind directions. More recently vegetation canopy models have been evaluated using Computational Fluid Dynamics (CFD) models [8-12]. Overall, those studies confirm experimental findings that flow and dispersion at street scale strongly depend on the synergy between meteorological conditions, configuration of the street canyon and the presence of vegetation.

Within this context, the present paper is devoted to study the effects of trees on micrometeorology in a medium-size Mediterranean city through in situ experiments and CFD simulations. Two street canyons with and without trees of different Leaf Area Index (LAI [m^2m^{-2}]) were considered. Building façades and ground temperatures were inferred from infrared (IR) images, while flow and turbulence were measured through ultrasonic anemometers. The study period includes observations prior to and after to leaf-out of trees in order to quantify this effect on in-canyon air temperature, wind and turbulence.

METHODOLOGY

The study area

The study area is located in Lecce (UTM coordinates $40^{\circ}21'7.24''\text{N}$, $18^{\circ}10'8.9''\text{E}$), a medium size city of south Italy with about 100,000 inhabitants. Lecce is built on a flat land, approximately 40-50m above sea level and is characterized by a Mediterranean climate and a classical Mediterranean architectural design, consisting of 2-3 storey buildings and narrow street canyons (Fig. 1a). The study area is on the western side of the city where buildings despite the different

heights are distributed in a rather regular configuration (Fig. 1b).

The area size is 130m x 200m and comprises two main parallel street canyons (namely Redipuglia St. and Gorizia St.) running north-south with buildings heights ranging from 5m to 25m (Fig. 2a). Gorizia St. is a tree-free street canyon with aspect ratio H/W (where H is the average building height and W is the average width of the street) equal to 1.1, while Redipuglia St. aspect ratio is equal to 1.2 and is characterized by the presence of deciduous trees (Fig. 2b,c). A total of 36 trees (*Tilia Cordata* Mill.) are located along both sides of the street of which twenty-two along the left side and fourteen along the right side. The spacing between tree trunks is approximately 4m so that there is a leaf crown interference. The average height of the branch-free trunk is about 5m and the crown extends to about 8m in height (Fig. 2c). *Tilia Cordata* Mill. is widespread throughout Europe and is characterized by a dense pyramidal or oval crown which casts deep shade. It is commonly used in urban areas due to its predictable symmetrical shape, which makes it recommendable for shading sidewalks in residential streets.

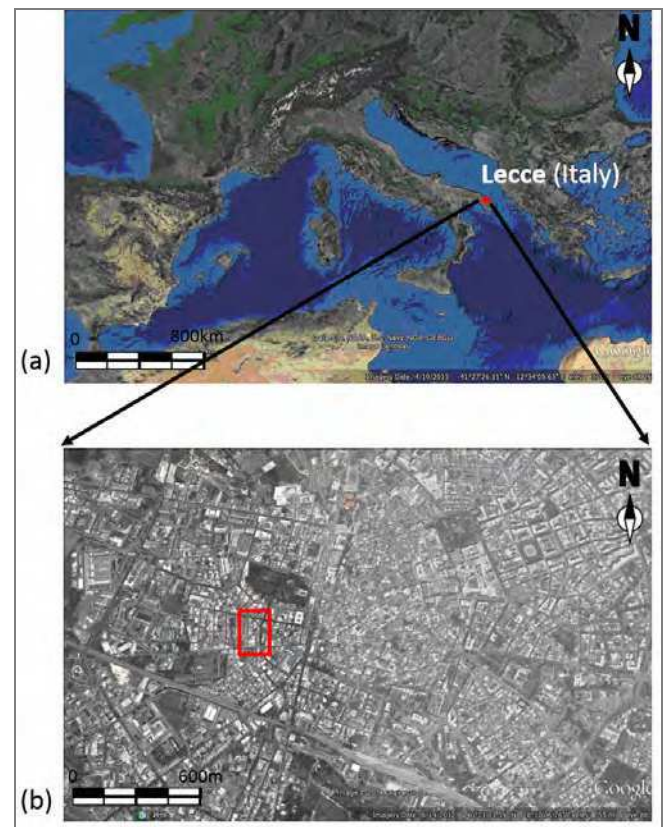


Figure 1. a) Position of Lecce city in south-east Italy; b) Position of the study area indicated by the red square (base maps from Google Earth).

Flow and air temperature measurements were carried out in Redipuglia St. in the period 11 October-7 December 2013

(Main Campaign hereinafter). This allowed us to capture the evolution of leaf fall. The Main Campaign included three intense measurements periods where LAI measurements, thermal imaging measurements of building façades, air temperature and relative humidity measurements were also conducted in Redipuglia St. and Gorizia St.; specifically from noon to noon of 11-12 October (Campaign 1 hereinafter), 8-9 November (Campaign 2 hereinafter) and 6-7 December 2013 (Campaign 3 hereinafter).

Flow and turbulence measurements

The three components of wind velocity and sonic temperature were measured at the acquisition sampling frequency of 50Hz by three GILL R3-50 sonic anemometers installed in Redipuglia St. (Fig. 3a,b). Measurements were taken at three different heights. Two anemometers were positioned inside the street canyon: the first (Anemometer 1) was just below the tree crown at $z=4.5\text{m}$ a.g.l. (above ground level) and the second (Anemometer 2) was just above the tree crown at $z=8.5\text{m}$ a.g.l. (Fig. 3b). Both anemometers were positioned on banisters of two balconies at the first and second floors of a 15m high building. The third anemometer (Anemometer 3), together with a Vaisala HMP45C thermo-hygrometer, were positioned on the roof of the same building at 18m a.g.l. (Fig. 3a). Collected data were analyzed using the Matlab © software to calculate 10mins averages of wind direction and wind speed and 5mins averages of turbulent fluxes, following standard techniques for the treatment of high frequency flow data in real scenarios (e.g. [13]).

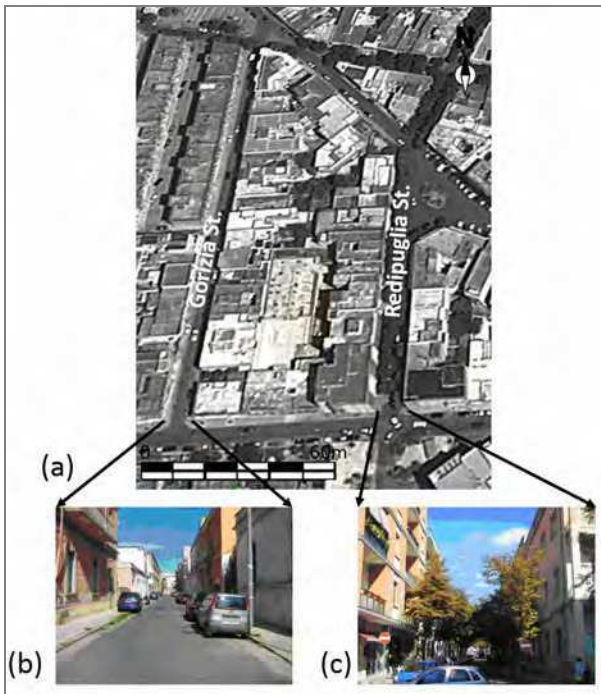


Figure 2. a) 3D view of the study area; b) Cross section of Gorizia St. without trees; c) Cross section of Redipuglia St. with trees.

Leaf area index measurements

The Leaf Area Index (LAI) of *Tillia Cordata* Mill. tree crowns was estimated from measurements of the photo-synthetically active radiation (PAR) (light in the 400-700nm waveband) acquired by an Accu-PAR LP80 ceptometer. Specifically, the LAI estimation was based on PAR measurements along with other variables related to the crown structure and position of the sun, such as the zenith angle, a fractional beam measurement value and a leaf area distribution parameter (indicated by x). The ceptometer automatically calculates both the zenith angle and the fractional beam, while it required the user to input a value for x . This parameter does not strongly affect the estimation of LAI, thus the default value $x=1$ which assumes a spherical crown distribution, was used.

All measurements were taken parallel to the ground and perpendicularly to the orientation of Redipuglia St. (281°). Five replicas were done at the same measurement point just near the crown (where the sensor measured unobstructed PAR) and at its base (where it was supposed that the LAI was maximum). A simple vertical profile was assumed for the distribution of the Leaf Area Density (LAD [m^2m^{-3}]) as follows:

$$LAD = \begin{cases} 0 & \text{if } 0 \leq h \leq h_c \\ LAD & \text{if } h_c \leq h \leq h_t \end{cases} \quad (1)$$

where h is the height above the ground, h_c is the lower average height of the crown, and h_t is the maximum average height of the tree [10]. LAD was thus roughly estimated dividing LAI by the depth of tree crown (3m) (Fig. 3c,d,e). We will refer to large LAI for trees for Campaign 1, intermediate LAI for Campaign 2 and low LAI (which corresponds to leafless trees) for Campaign 3 (Tab. 1).



Figure 3. Sonic anemometers in Redipuglia St. at a) roof level and b) within the street above the tree crown. Texture of tree during c) Campaign 1 (large LAI, LAD); d) Campaign 2 (intermediate LAI, LAD); e) Campaign 3 (low LAI, LAD).

	Campaign 1 (Large)	Campaign 2 (Intermediate)	Campaign 3 (Low)
LAI (m ² m ⁻²)	5.21	0.97	0.37
LAD (m ² m ⁻³)	1.74	0.32	0.12

Table 1. Leaf Area Index (LAI) measurements and Leaf Area Density (LAD) estimates during the three campaigns.

Thermal imaging measurements

To analyze temperature distribution of building façades, four representative buildings (two in Gorizia St. and two in Redipuglia St.) were selected on the basis of the homogeneity of construction material and the absence of obstacles (balconies, eave, etc.), metal or glass.

IR thermal images of building façades and streets (ground) were taken through a high performance FLIR T620 ThermalCAM, with a 640 x 480 pixels resolution and an image acquisition frequency of 50/60Hz. Air temperature and humidity were also recorded with a Extech Instruments MO297 moisture psychrometer. Images were acquired every three hours on Campaigns 1, 2 and 3. This choice allowed us to collect images at 12:00 (close to the maximum surface temperature), 15:00 (close to when maximum air was temperature), 21:00 (when the UHI intensity was maximum) and before sunrise (close to when air temperature was minimum).

Images were analysed using the FLIR QuickReport software. Different values of emissivity α (which is defined as the ratio of the energy radiated from a material's surface to that radiated from a blackbody ($\alpha=1$) at the same temperature) were chosen depending on the material. In particular, $\alpha = 0.96$ was used for asphalt and $\alpha = 0.94$ for brick-limestone (building façade). These values are those recommended by FLIR [14] and are consistent with values proposed by several authors (e.g. Carnielo and Zinzi's asphalt emissivity investigation [15] and Danov et al.'s study on limestone [16]). For the estimation of mean temperatures, cars and pedestrian were neglected to minimize errors on the estimation of the average temperature on facades and surfaces.

Air temperature was also measured every five minutes using a PT100 sensor assembled with Tinytag TGP-0073 by Gemini data loggers during the Main Campaign period. The sensor was positioned at the first floor of the same building where the anemometers were installed.

Numerical simulations

3D steady-state isothermal Computational Fluid Dynamics (CFD) simulations were performed by means of the general purpose code ANSYS Fluent. The aim is to aid interpretation of field measurements by providing information about the flow structure in the vicinity of the measurements points. A preliminary analysis considered meteorological conditions recorded at 21:00 (when conditions inside the canyon could be assumed to be isothermal) during Campaign 1. The study area includes Redipuglia St. (with trees, large LAI). To match recorded conditions, an approaching flow was taken to be equal to the mean hourly value (2.3ms⁻¹) observed at a meteorological station located outside the urban area (at z=20m), with a wind

direction equal to 140° (i.e. from south-south/east direction) which corresponds to an inclination of 40° with respect to the y axis (Fig. 4, top). The same simulation was performed without trees (tree-free) allowing us to isolate the effects of trees from the meteorological conditions (particularly wind direction) observed from field measurements (see the Results section).

The Reynolds Stress Model (RSM) [17] was used to calculate the individual Reynolds stresses using differential transport equations and, therefore, accounting for the differences in horizontal and vertical turbulent fluctuations. The inlet wind speed was assumed to follow a logarithmic law profile:

$$U(z) = \frac{u_*}{\kappa} \ln \left(\frac{z + z_0}{z_0} \right) \quad (2)$$

where $u_* = 0.17 \text{ms}^{-1}$ is the friction velocity estimated from log-law curve fitting of the observed wind velocity at the meteorological station located outside the urban area (at 20m); $z_0 = 0.1 \text{m}$ is the aerodynamic roughness length and κ is the von Kàrmàn constant (0.40). Equilibrium profiles of turbulent kinetic energy (TKE) [m²s⁻²] and dissipation rate (ε) [m²s⁻³] were specified to get a fully developed flow under neutral stratification conditions [18]:

$$TKE = \frac{u_*^2}{\sqrt{C_\mu}} \left(1 - \frac{z}{\delta} \right) \quad (3a)$$

$$\varepsilon = \frac{u_*^3}{\kappa z} \left(1 - \frac{z}{\delta} \right) \quad (3b)$$

where $\delta = 150 \text{m}$ (5 times the maximum height of the buildings in the study area) is the computational domain height and $C_\mu = 0.09$. When applying the RSM, turbulence quantities specified in Eqs. (3) are used to derive the Reynolds stresses at the inlet from the assumption of isotropy of turbulence. Symmetry boundary condition, required to enforce a parallel flow, was specified at the top of the domain. At the boundary downwind of the obstacles a pressure-outlet boundary condition was used. No-slip wall boundary conditions were used at all solid surfaces. Following the state-of-art requirements [19], the computational domain was built using about one million elements, with a finer resolution within the entire building area (the expansion ratio between two consecutive cells was below 1.3). The smallest dimension of the elements in the x, y and z directions was 0.25m (Fig. 4, bottom). The influence on the predictions of the choice of mesh size, using several refined meshes, was verified until overall velocity and TKE differences of no more than 5% were achieved within the street canyon.

The aerodynamic characteristics of trees were modeled using the methodology developed by Gromke et al. [20], i.e. adding a momentum sink in the governing momentum equations where the viscous term is neglected and the inertial term is parameterized using a pressure loss coefficient

$\lambda=0.35\text{m}^{-1}$. The latter is estimated though $C_d \times \text{LAD}$, where C_d is the leaf drag coefficient taken constant and equal to 0.2 as commonly assumed in the literature [e.g. 21,22].

A similar simulation approach for typical winter/spring days was used by Buccolieri et al. [23] in a real case scenario in which a complex urban junction formed by street canyons of similar aspect ratios and with trees were investigated.

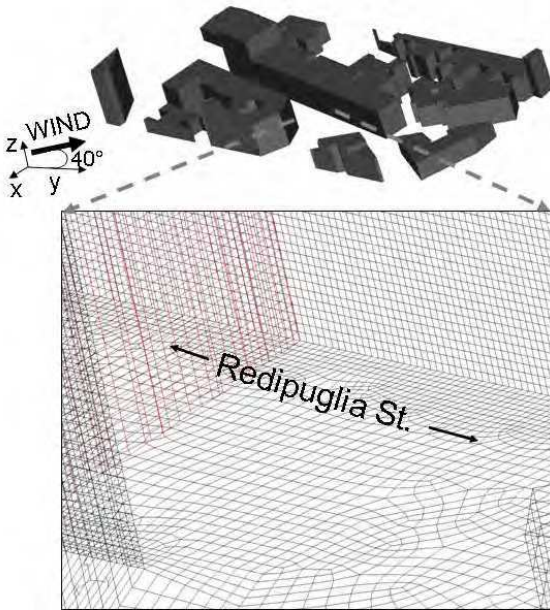


Figure 4. Sketch of geometry (top) and grid (bottom) used in CFD simulations.

RESULTS

Effects of trees on temperature

Figure 5 shows profiles of ground (a,b) and air temperatures (c,d) recorded within Gorizia St. (tree-free) and Redipuglia St. (with trees) during Campaign 1 (large LAI) and 3 (low LAI, i.e. leafless trees). Data were normalized by air temperature recorded at roof level (Anemometer 3). By looking at Fig. 5a,c it can be noted that the effect of trees during Campaign 1 was that of lowering air and ground temperatures during daytime. Specifically, Redipuglia St. during daytime experienced a reduction of 30% of ground temperature with respect to Gorizia St. This is due to trees shadowing in the streets which prevent the asphalt to get lit by direct solar radiation. On the contrary, slightly larger ground temperatures were recorded during nighttime until sunrise given that tree crowns reduce radiative cooling of the ground. During Campaign 3, the effect of trees was less pronounced during daytime resulting in similar ground temperatures in the two streets. During nighttime, Redipuglia St. still experienced larger ground temperatures (Fig. 5b,d) despite the LAI was low, suggesting possibly the role of trees' roots in reducing the radiative cooling of the ground. Air temperature in two streets follows a similar trend of ground temperature although differences during the nights are more pronounced.

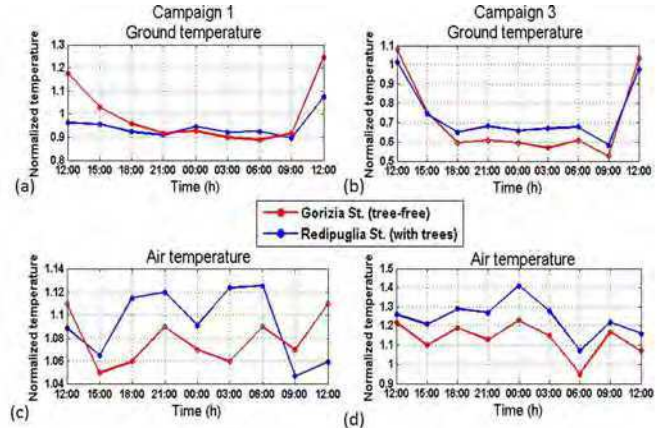


Figure 5. Normalized ground (a,b) and air temperatures (c,d) recorded in Gorizia St. (tree-free) and Redipuglia St. (with trees) during Campaigns 1 (large LAI) and 3 (low LAI).

The analysis of building façade temperatures further highlights the influence of trees on temperature distribution within the streets. Figure 6 shows profiles of mean surface and air temperature recorded during Campaign 1 (left) and Campaign 3 (right) at building façades exposed to east (denoted with E) and west (denoted with W) in Gorizia St. (denoted with G) and in Redipuglia St. (denoted with R). For example, the BWR profile indicates the temperature at the bottom (B) of the building façade exposed to west (W) in Redipuglia St. (R).

During Campaign 1 (Fig. 6, left), due to the north-south street orientation, buildings exposed to east experienced a high mean temperature at 9am until 3pm. Temperature in the afternoon until sunrise was instead slightly larger at buildings exposed to west. This results confirms previous findings [24,25] that surfaces directly exposed to east usually experience maximum temperature at about 9am, while surfaces exposed to west reach their maximum temperature at about 3pm. The effect of trees was clearly different at the top and bottom of the façade, being trees lower than buildings. Specifically, in Gorizia St. (tree-free) temperatures at the top of the buildings were always lower than those at the bottom, except that at 9am and 12am when façades exposed to east received direct solar radiation. On the contrary, in Redipuglia St. (with trees) the top experienced larger temperatures than the bottom due to trees shadow which prevented the solar radiation to reach the ground during daytime. During nighttime, the bottom became warmer than the top due to the trapping of heat by trees.

As expected, during Campaign 3 (Fig. 6, right) lower temperatures were registered during the day, except for building façades along the west side of the streets, i.e. those exposed to direct solar radiation after the dawn, and buildings characterized by strong heat loss from the indoor heating radiators. Similar to what found during Campaign 1, high temperatures were recorded at 9am and 12am for buildings exposed to east. Temperatures at the top of the façades were usually lower than those at the bottom within both the streets; being trees characterized by low LAI, no inversion was found in Redipuglia St. as observed during Campaign 1.

Finally, it is worth analysing differences between building façade and air temperatures. During Campaign 1 (Fig. 6, left), at 9am façade temperatures at the top of the buildings exposed to east were 3°C (Gorizia St.) and 10°C (Redipuglia St.) larger than air temperatures. These difference were due to the different building materials (brick-plaster) and color (white-red) between the two streets. For the buildings exposed to west, no substantial differences were found between the two streets. Overall, building façade temperatures in Gorizia St. were sometimes lower than air temperatures, while in Redipuglia St. this never occurred; this demonstrates that trees were effective in trapping heat close to the ground. On the contrary, during Campaign 3 (Fig. 6, right) air temperatures were considerably larger than façade temperatures. Measurements were in fact influenced by the presence of moisture on buildings façades. This effect is in fact accentuated in rainy days, especially on the oldest buildings. Specifically, due to the presence of thermal bridges, moisture accumulates within the walls (interstitial humidity) and due to the indoor-outdoor temperature differences it tends to evaporate and to subtract heat while passing from liquid to gaseous state [26]. In addition, measurements were influenced by larger wind velocities, which helped to further lower façade temperatures [27].

Summing up, during daytime the main effect of trees was to lower temperatures at the bottom of Redipuglia St. with respect to the tree-free Gorizia St., while after sunset they led to larger façade and air temperature.

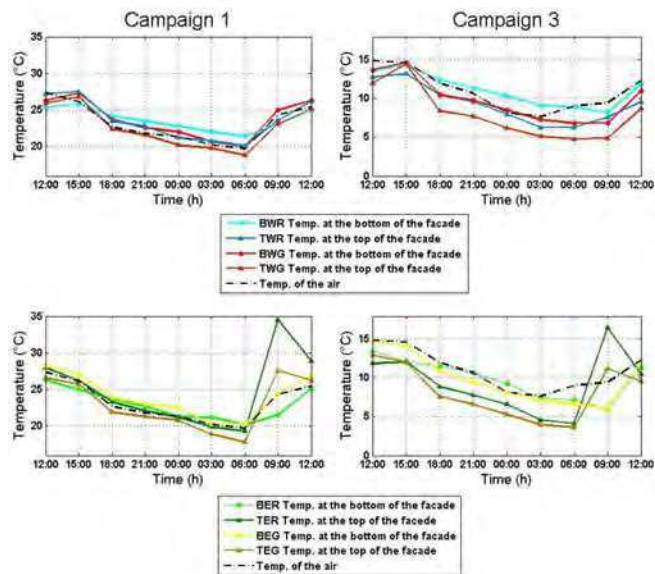


Figure 6. Mean temperatures recorded during Campaign 1 (large LAI) (left) and Campaign 3 (low LAI) (right) at the top (T) and bottom (B) of building façades exposed to west (W) and east (E) in Redipuglia St. (R) and Gorizia St. (G).

Effects of trees on wind and turbulence

The analysis of anemometric measurements allowed us to investigate the effects of trees on flow and turbulence within

Redipuglia St. and their dependence on tree crown density [23,28]. Figure 7 shows profiles of non-dimensional wind speed obtained from Anemometer 1 (at 4.5m, just below the tree crown) and Anemometer 2 (at 8.5m, just above the tree crown) normalized by wind speed at roof (at 18m, Anemometer 3 position) for Campaigns 1 (large LAI) and 3 (low LAI). As expected, a significant windbreak effect is observed in the presence of trees (Campaign 1) with respect to the situation with leafless trees (Campaign 3). In fact, during a daily cycle, average non-dimensional wind speeds reduction was up to 30% below tree crowns and 20% above. As observed by Dupont and Patton [28] this effect is due to “the canopy element induced dispersive contribution, namely a variation of the quantity with position due to biases in the observed flow imposed by the proximity of a physical canopy element”. Further, as shown by the scatter plots of normalized mean wind speed measured by Anemometer 2 vs Anemometer 1 (Fig. 8), in the presence of trees the flow below the tree crown is slightly decoupled from that above showing larger velocities at mid height of the canyon as a sort of speed-up effect. On the contrary, in the absence of leaves, the obstruction effect of trees is reduced and slightly larger velocities are found close to the ground due to the more frequent occurrence of the in-canyon vortex which in the tree case is less defined. Our findings are somehow in accordance with previous findings [e.g. 29] suggesting that trees may reduce wind speeds up to 54% in street canyons.

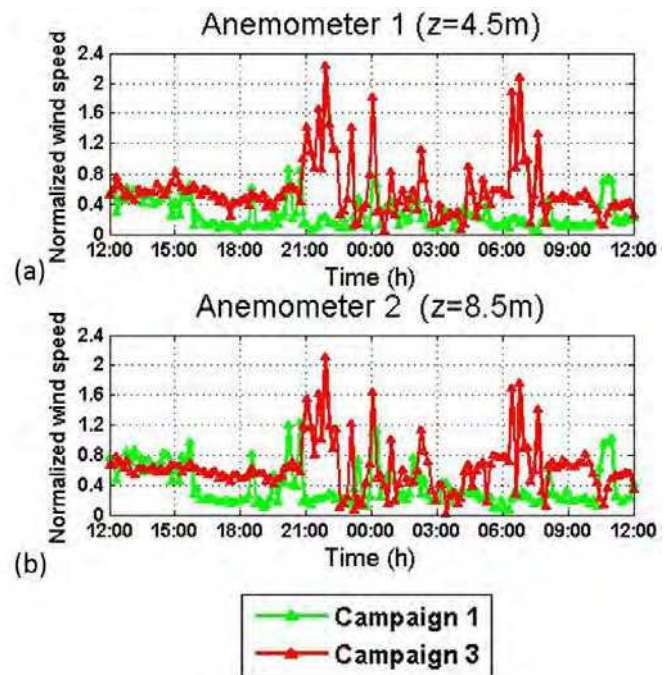


Figure 7. Normalized mean wind speed recorded at 4.5m just below the tree crown (a) and at 8.5m just above the tree crown (b) in Redipuglia St.

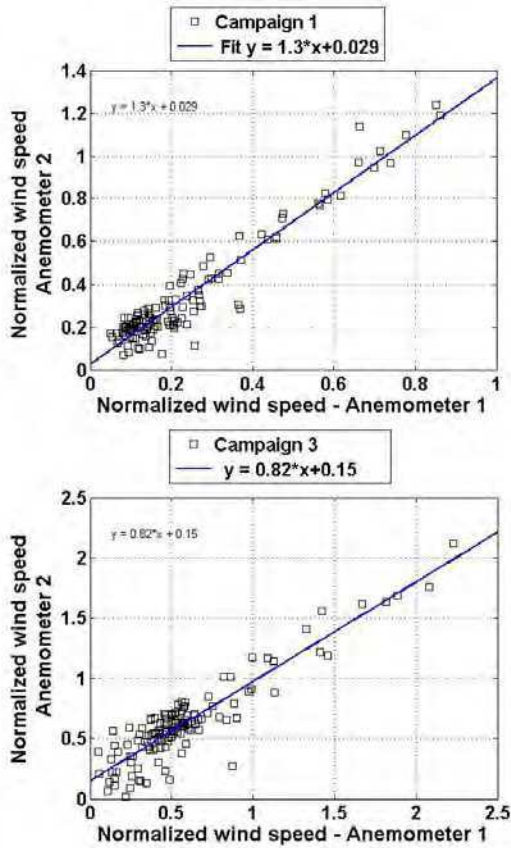


Figure 8. Scatter plots and linear fit of normalized mean wind speed at Anemometer 2 vs Anemometer 1 during Campaign 1 (top) and Campaign 3 (bottom) in Redipuglia St.

As shown in Fig. 9 wind directions were different during the two campaigns. During Campaign 1, despite the above roof wind blew approximately from south (Anemometer 3), no wind channelling is observed in the street since the interaction with trees induced wind direction oscillations below tree crowns (Fig. 9a). On the contrary, during Campaign 3 the influence of trees was smaller and the wind direction within the street is similar to that above the roof (Fig. 9b).

Figure 10 shows observed vertical profiles of TKE and momentum fluxes $\overline{u'w'}$ estimated at 15:00 and 21:00 at Anemometer 1, Anemometer 2 and Anemometer 3 (at 18m, above the roof level) for Campaigns 1 and 3. Both TKE and $\overline{u'w'}$ are normalized by u_*^2 evaluated at the Anemometer 3 position. The figure also shows profiles obtained from CFD simulations (with trees) at 21:00 of Campaign 1. We remind here that a CFD simulation without trees was also performed using the same meteorological conditions of Campaign 1, thus it does not correspond to Campaign 3 condition and for this reason it has not been reported in the figure. Even though we have not considered all possible cases in our CFD simulations, computed vertical profiles performed considering isothermal conditions are in agreement with measurements (Fig. 10). For example, both measurements and simulations show a TKE

increase with height. This is in accordance with previous studies (e.g. [30]) where the maximum TKE is found in the shear-layer region just about the roof-level. It can be further noted that TKE values within the canyon are larger during Campaign 3 (leafless trees) than those recorded during Campaign 1 due too overall smaller values of friction velocities during those hours. As reported by Baik et al. [11], in the absence of tree shading, for a street canyon with an aspect ratio equal to one with bottom heating (at 15:00 in our case), the thermally (positive-buoyancy) driven upward motion near the upwind building wall is constructively combined with the mechanically driven upward motion, enhancing the vortex and increasing the average TKE. During the night normalized TKE is even larger due to very small friction velocities in this case.

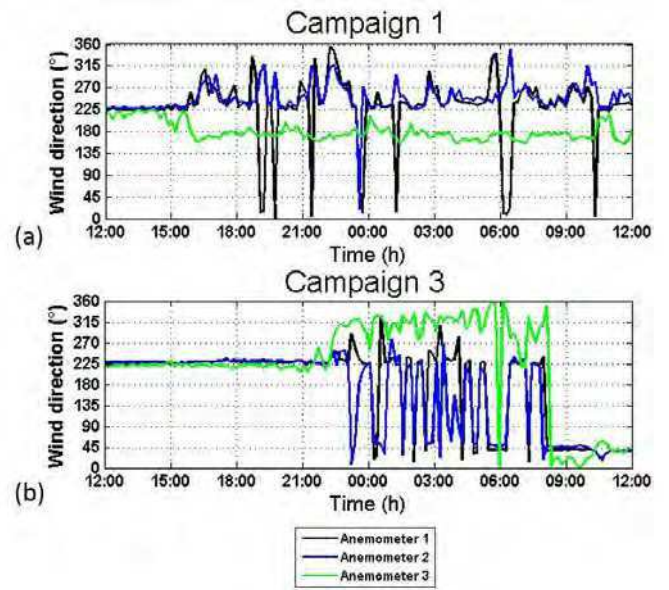


Figure 9. Wind direction recorded during a) Campaign 1 (large LAI) and b) Campaign 3 (low LAI) in Redipuglia St.

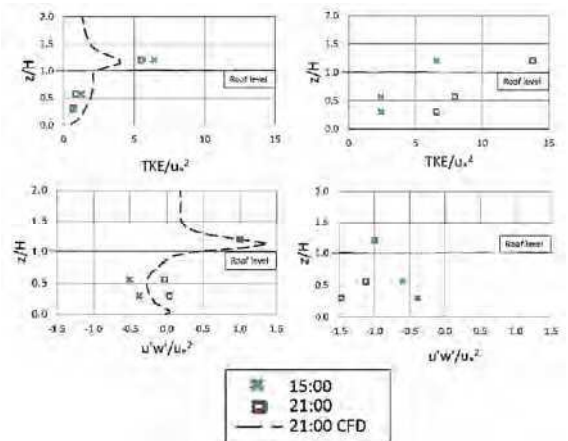


Figure 10. Vertical profiles of TKE (top) and momentum flux $\overline{u'w'}$ (bottom) during Campaigns 1 (left) and 3 (right) in Redipuglia St.

As far as momentum fluxes is concerned both measurements and numerical simulations show that in presence of trees they are typically small with small difference between day and night. This does not occur during the leafless case of Campaign 3 when diurnal and nocturnal conditions are much different.

The effects of trees discussed through the analysis of field data (Figs. 7-10) should thus be set against the dependence on wind direction. The simulation performed using the meteorological conditions of Campaign 1 but without trees allowed us to make the following observations. While in the tree-free case wind speed vectors show a typical wind channelling along Redipuglia St. (Fig. 11,top), in the presence of trees (Fig. 11, bottom) the main flow pattern within the street canyon is still maintained, but wind speed at $z=4.5\text{m}$ (Anemometer 1 position) decreases of about 8% with respect to the tree-free case. The TKE is also suppressed especially at the upstream entry of Redipuglia St. partially explaining higher temperatures found from field measurements (Fig. 5). Further, trees enhanced the formation of a vortex leading to reverse flow at the downstream opening of Redipuglia St. At Anemometer 2 position (not shown here) trees induced a wind speed reduction of 27%. Those findings are only partially in agreement with measurements considering that we found a larger reduction in wind speed in the middle height of the canyon rather than close to the ground. Nevertheless this can be seen as the solely effect of trees on flow rather than of its combination with changing meteorological conditions as in the real case. Our simulations need to be further refined to match closer meteorological conditions of the real cases and this left to future work.

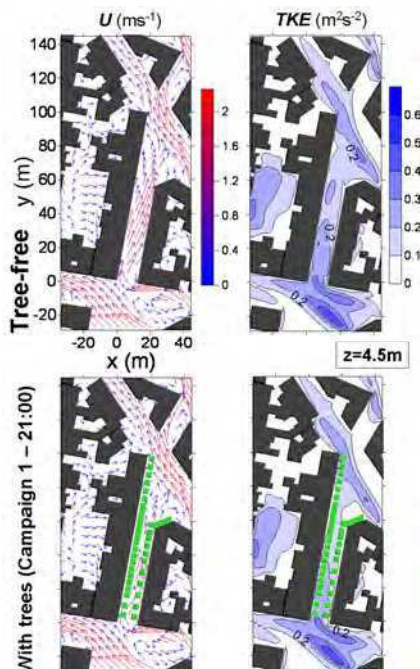


Figure 11. Wind speed (left) and TKE (right) at 4.5m from CFD simulations in Redipuglia St. for the tree-free case (top) and the large LAI tree case (bottom).

CONCLUSIONS

The aerodynamic effects of trees on local meteorological variables in the inner core of a medium-size Mediterranean city were investigated through in situ measurements and CFD simulations. The study was conducted for the period 11 October - 7 December 2013 using three ultrasonic anemometers, together with a thermo-hygrometer, a thermal imaging IR camera and a ceptometer. Several conclusions were achieved from this study.

Specifically, the use of IR thermal images and air temperature probes allowed us to investigate the temperature distribution within street canyons with and without trees. The analysis has shown that trees are effective in trapping heat close to the ground. This effect during nighttime is more important than the passive cooling through evapo-transpiration leading to increased temperatures with respect to the tree-free case. Using high-frequency flow data in combination with CFD simulations it has been possible to further appreciate the effect of trees on flow and turbulence within the street canyon. The wind channeling typical of the specific approaching wind directions was still maintained in the presence of trees, but with reduced wind speed and enhanced vortex size with reverse flow within the street.

The analysis of collected field data and CFD simulations is still in progress to further investigate the effect of trees on temperature distribution, flow and turbulence patterns under several stability conditions.

ACKNOWLEDGMENTS

The authors wish to thank the Dipartimento di Ingegneria dell'Innovazione - University of Salento for making available ANSYS Fluent.

REFERENCES

- [1] Oke, T.R., 1987, "Boundary Layer Climates", Routledge, London, UK.
- [2] Colombert, M., Diab, Y., Salagnac, J.-L., and Morand, D., 2009, "Effect and implementation of measures aiming at impacting urban climate," Proceedings of the 8th Workshop and Meeting CIB W108, Climate change and the Built Environment.
- [3] Desplat, J., Salagnac, J.-L., Kounkou-Arnaud, R., Lemonsu, A., Colombert, M., Lauffenburger, M., and Masson, V., 2009, EPICEA project 2008–2010 "Multidisciplinary study of the impacts of climate change on the scale of Paris", Proceedings of the 7th International Conference on Urban Climate, Yokohama, Japan.
- [4] Kikuchi, A., Hataya, N., Mochida, A., et al., 2007, "Field study of the influences of roadside trees and moving automobiles on turbulent diffusion of air pollutants and thermal environment in urban street canyons," Proceedings of the 6th International Conference on Indoor Air Quality, Ventilation and Energy Conservation in Buildings (IAQVEC 2007), pp. 137–144, Sendai, Japan.
- [5] Shashua-Bar, L., Pearlmutter D., and Erell, E., 2011, "The influence of trees and grass on outdoor thermal comfort in a

- hot-arid environment”, *International Journal of Climatology*, **31**(10), pp. 1498-1506.
- [6] Plate, E.J., and Quraishi, A.A., 1965, “Modeling of velocity distribution inside and above tall crops”, *Journal of Applied Meteorology*, **4**, pp. 400-408.
- [7] CODASC Database, 2008, Laboratory of Building- and Environmental Aerodynamics, IfH, Karlsruhe Institute of Technology.
- [8] Alexandri, E., and Jones, P., 2008, “Temperature decrease in an urban canyon due to green walls and green roofs in diverse climates”, *Building and Environment*, **43**(4), pp. 480-493.
- [9] Buccolieri, R., Gromke, C., Di Sabatino, S., and Ruck, B., 2009, “Aerodynamic effect of trees on pollutant concentration in street canyons”, *Science of the Total Environment*, **407**(19), pp. 5247-5256.
- [10] Vos, P.E.J., Maiheu, B., Vankerkom, J., and Janssen, S., 2013, “Improving local air quality in cities: To tree or not to tree?”, *Environmental Pollution*, **183**, pp. 113-122.
- [11] Baik, J.J., Kwak, K.H., Park, S.B., and Ryu, Y.H., 2012, “Effects of building roof greening on air quality in street canyons”, *Atmospheric Environment*, **61**, pp. 48-55.
- [12] Amorim, J.H., Rodrigues, V., Tavares, R., Valente, J., and Borrego, C., 2012, “CFD modelling of the aerodynamic effect of trees on urban air pollution dispersion,” *Science of the Total Environment*, **461-462**, pp. 541-551.
- [13] McMillen, R.T., 1988, “An Eddy Correlation Technique with Extended Applicability to Non-Simple Terrain”, *Boundary-Layer Meteorology*, **43**, pp. 231-245.
- [14] FLIR, 2010. User’s manual. FLIR reporter professional edition 8.5.
- [15] Carnielo, E., and Zinzi, M., 2013, “Optical and thermal characterisation of cool asphalts to mitigate urban temperatures and building cooling demand”, *Building and Environment*, **60**, pp. 56-65.
- [16] Danov, M., Petkov, D., and Tsanev, V., 2007, “Investigation of thermal infrared emissivity spectra of mineral and rock samples”, *New Developments and Challenges in Remote Sensing*, Z. Bochenek (ed.), Millpress, Rotterdam, ISBN 978-90-5966-053-3.
- [17] Launder, B.E., 1989, “Second-moment closure: present and future?”, *International Journal of Heat Fluid Flow*, **10**(4), pp. 282-300.
- [18] Di Sabatino, S., Buccolieri, R., Pulvirenti, B., and Britter, R., 2007, “Simulations of pollutant dispersion within idealised urban-type geometries with CFD and integral models”, *Atmospheric Environment*, **41**(37), pp. 8316-8329.
- [19] Di Sabatino, S., Buccolieri, R. et al., 2011, “COST 732 in practice: the MUST model evaluation exercise”, *International Journal of Environment and Pollution*, **44**(1/2/3/4), pp. 403-418.
- [20] Gromke, C., Buccolieri, R., Di Sabatino, S., and Ruck, B., 2008, “Dispersion study in a street canyon with tree planting by means of wind tunnel and numerical investigations – Evaluation of CFD data with experimental data”, *Atmospheric Environment*, **42**(37), pp. 8640-8650.
- [21] Katul, G.G., Mahrt, L., Poggi, D., and Sanz, C., 2004, “One and two equation models for canopy turbulence”, *Boundary-Layer Meteorology*, **113**(1), pp. 81-109.
- [22] Gromke, C., and Blocken, B., 2013, “On the relative importance of vegetation terms in computational fluid dynamics on flow and dispersion in the urban environment”, *Proc. 15th Int. Conf. on Harmonisation within Atmospheric Dispersion Modelling for Regulatory Purposes*, Madrid, Spain.
- [23] Buccolieri, R., Salim, M. S., Leo, L. S., Di Sabatino, S., Chan, A., Ielpo, P., de Gennaro, G., and Gromke, C., 2011, “Analysis of local scale tree – atmosphere interaction on pollutant concentration in idealized street canyons and application to a real urban junction”, *Atmospheric Environment*, **45**(9), pp. 1702-1713.
- [24] Hoyano, A., Asano, K., and Kanamaru, T., 1999, “Analysis of the sensible heat flux from the exterior surface of buildings using time sequential thermography”, *Atmospheric Environment*, **33**(24-25), pp. 3941-3951.
- [25] Di Sabatino, S., Hedquist, B.C., Carter, W., Leo, L.S., Brazel, A.J., and Fernando, H.J.S., 2009, “Results from the Phoenix Urban Heat Island (UHI) experiment: effects at the local, neighborhood and urban scales”, *Proceedings of the European Geosciences Union General Assembly (EGU 2009)*, Vienna, Austria.
- [26] Roche, G., 2012, “La termografia per l’edilizia e l’industria”, Maggioli, Ravenna, 450pp.
- [27] Lazzoni, D., 2012, “Diagnosi e certificazione energetica prove strumentali sugli edifici”, Maggioli, Ravenna, 386pp.
- [28] Dupont, S., and Patton, E.G., 2012, “Influence of stability and seasonal canopy changes on micrometeorology within and above an orchard canopy: The CHATS experiment”, *Agricultural and Forest Meteorology*, **157**, pp. 11-29.
- [29] Park, M., Hagishima, A., Tanimoto, J., and Narita, K., 2012, “Effect of urban vegetation on outdoor thermal environment: Field measurement at a scale model site”, *Building and Environment*, **56**, pp. 38-46.
- [30] Louka, P., Belcher, S.E., and Harrison, S.G., 2000, “Coupling between air flow in streets and the well-developed boundary layer aloft”, *Atmospheric Environment*, **34**(16), pp. 2613-2621.